Proc.Symposium on Earth's Gravitational Field & Secular Variations in Position (1973),290.

TAPLEY, B.D.
Department of Aerospace Engineering & Engineering Mechanics
University of Texas at Austin
Austin, Texas 78710
United States of America

Chairman's Introduction to Session F - "Laser Ranging to Satellites"

The application of laser ranging to Earth satellites has opened up a number of new and interesting areas of study and has given rise to a potential for contributing to a number of problems in geodesy and geodynamics.

Position range measurements are routinely made to the order of 50 cm with the expectation that this accuracy can be improved to the order of 10 cm.

Such precision holds promise for contributing to the solution to such problems as the study of solid Earth tides, short term polar motion, gravitational field definition, geoid determinations, etc.

The session this morning has four papers dealing with problems in these areas.

The first paper deals with the problem of dynamic determination of position and has the advantage that the information obtained is referenced to the Earth's centre of gravity (SMITH ET AL).

The second paper (by ONG) considers the role of geometrical determinations and has the advantage of being free from gravitation and other model errors, but has the associated disadvantage of requiring a large number of stations simultaneously tracking the vehicle if a solution is to be obtained.

The third paper (by PLOTKIN) will give some insight into the potential for achieving a range measuring accuracy in the 10 cm range, while the fourth paper (by PAQUET & DEJAIFFE) will discuss the Doppler measuring systems.

SMITH, D.E.
KOLENKIEWICZ, R.
AGREEN, R.W.
NASA Goddard Space Flight Center
Greenbelt Md 20771
United States of America

DUNN, P.J.
Wolf Research & Development Corporation
Riverdale Md
United States of America

Proc.Symposium on Earth's Gravitational Field & Secular Variations in Position (1973),291-314.

DYNAMIC TECHNIQUES FOR STUDIES OF SECULAR VARIATIONS IN POSITION FROM RANGING TO SATELLITES

ABSTRACT

During the last few years NASA Goddard Space Flight Center has been applying satellite laser range measurements to problems in Earth and ocean physics. Primary attention has been directed towards the measurement of the variation of latitude arising from polar motion and to the determination of the solid-Earth and ocean tidal distortion of the Earth's gravity field. These investigations have been successfully conducted using data obtained by a single laser station tracking a single satellite. It has further been demonstrated that these data can also be used to monitor the height or radial distance of the station and can contribute substantially to our knowledge of the gravity field.

Experiments involving two stations have also been conducted. Simultaneous range measurements to a satellite from two stations several hundred km apart have been used to determine the relative location of one station with respect to the other. This technique is now being used in an experiment (SAFE) to measure the motion between points 900 km apart on opposite sides of the San Andreas fault system in California. A simulation of this experiment for a seven year observing period has indicated that it should be possible to determine the average relative motion of the two sides of the fault to an accuracy of about 5 mm per year.

At the present time, all spacecraft equipped with laser retroreflectors are in relatively low orbits of 500 to 2000 km but in the next few years it is anticipated that geodynamic satellites at much greater altitude will be launched. At these greater altitudes of several thousand km, the perturbing effects of the Earth's gravity field will be much smaller and should permit an improvement of at least an order of magnitude in the determination of the product of the Earth's mass and gravitational constant.

In a few years it is anticipated that laser ranging measurements to high altitude satellites from a single site will permit the station to monitor its own latitude and height variations at the 5 to 10 cm level on a daily basis and determine the length of day to about 0.2 milliseconds. Multiple station experiments should enable crustal and tectonic motions to be measured to an accuracy of a few mm per year over a few years from which large scale strain fields could be derived. Observations of lower altitude satellites will yield information on the gravity field, the elastic response of the solid-Earth to tidal forces and the amplitudes and phases of certain components of the ocean tides.

1. Introduction

The successful development of high precision laser tracking systems over the last decade is now beginning to to permit the investigation of geophysical parameters of considerable interest and importance. At Goddard Space Flight Center the accuracy of laser ranging has improved nearly two orders of magnitude since 1964, and toward the end of 1973, reached a level of about 10 cm. With this quality, it can reasonably be expected that laser ranging to satellites will be able to contribute significantly to the measurement of the motions of the Earth, such as tectonic, polar, tidal and crustal, and to the determination of the Earth's gravitational field in both space and time. However, until very recently, the quality of the range measurements was of the order of 50 cm, a capability

achieved in 1970, and it is upon data of this quality that all our experience so far has been based. In this paper we attempt to review the major aspects of the analysis of satellite laser range measurements conducted at Goddard Space Flight Center since 1970 for ultimate application to geodesy and geodynamics.

The investigations at Goddard Space Flight Center (GSFC) have been restricted so far to those that can be achieved with one or two tracking systems. Until late 1973, GSFC possessed one fixed laser system sited at its optical facility in Greenbelt, Maryland and one mobile tracking system that could be driven, or shipped, almost anywhere. Both these systems were one joule ruby lasers with a pulse rate of one-per-second.

A major factor that influenced the analyses was the limited knowledge of the perturbing forces affecting the motion of the satellite. In 1970, our long wavelength knowledge of the gravitational field was almost entirely derived from optical satellite tracking data accurate to about two seconds of arc (10 m at about 1000 km range) (GAPOSCHKIN & LAMBECK 1970). Thus, the laser observations were about an order of magnitude better than the data used to derive the field and thus any analysis might ultimately be limited by errors in force field rather than the data. The position is hardly any different in 1973 than in 1970, and in none of the investigations conducted at GSFC in the last few years has any real evidence been uncovered which suggests that we have been limited by the quality of the data; even at the 50 cm level. Consequently, any modest achievements that can be established in the present environment should be well exceeded (even with the same data) when improved force models are available. It is therefore essential that research continue in the area of improving the Earth's gravity field and in the modeling of other perturbing influences of satellite orbits for the full potential of the orbit dynamic technique to be fully realized.

Because of the difficulty of assessing the full value of the range data already available, predictions of future capabilities, such as detecting plate motion, are almost entirely dependent on simulations or error analyses; which are themselves based on assumed error models. In the absence of any other technique this approach has been used at GSFC for projecting future capabilities with future satellites. It is from these simulations and error analyses, as well as from our own work over the last few years, that much of our optimism for the future is drawn.

In the following sections the major results obtained at GSFC over the last three years from the analysis of laser range data are described and discussed; followed by a brief description of some of our own ideas and plans for the future.

2. Laser Data

There are seven satellites presently in orbit carrying laser retroreflectors, Beacon Explorers B and C, and GEOS 1 and 2 launched by the United States, and three satellites launched by France, D1-C, D1-D and PEOLE. At GSFC most of our tracking operations have been on the U.S. satellites, particularly Beacon Explorer C (BE-C), and it is the analyses of tracking data on this spacecraft that is described here.

The orbit of BE-C is nearly circular at an altitude of about 1000 km with an orbital inclination of 41°. A typical pass of BE-C near a ground station lasts about 8 to 10 minutes and can be tracked by the laser station down to elevations of 20° or less fairly routinely (weather permitting) and some-

times below 10°; thus, with a pulse rate of one-per-second, 500 or more range measurements are obtained on a "good" pass of the satellite. Less than 100 measurements are considered "poor" passes but this does not necessarily imply that the data or the pass is any less valuable than a "good" pass. The average number of measurements per pass over nearly 18 months of tracking of BE-C by the fixed laser at GSFC was about 150.

The basic measurement of the laser system is the round-trip travel time of the laser pulse from the transmitter to the satellite and back down to the receiver (JOHNSON ET AL 1967). This time interval is corrected for system delays (calibration constants), for variation in the pulse shape and height, converted to a range, and corrected for atmospheric effects and for spacecraft size and attitude. The whole system is calibrated by ranging to a calibration target at a known distance from the tracking system before and after every satellite pass. The tropospheric correction amounts to about 2.5 m at zenith and is applied to each individual range measurement according to the elevation (E), pressure (P), temperature (T), and the station height above mean sea level (H), as shown below:

$$\delta\rho = \frac{2.238 + 0.0414\, P\, T^{-1} - 0.238\, H}{\sin E + 10^{-3} \cot E} \qquad (1).$$

The above formula is believed to provide the correction accurate to about 5 cm at 20° elevation.

A correction for spacecraft attitude and size is also made before the data are analyzed. The laser pulse is reflected from the surface of the spacecraft and yet the orbital dynamics are concerned with the motion of the spacecraft centre of mass. Thus, a range correction from the spacecraft surface to the centre of mass is made to each measurement. For BE-C, which is magnetically stabilized, this correction is on the average about 20 cm and varies slowly during a pass observed at GSFC between 15 cm and 27 cm.

After all corrections are applied, the final range measurements are checked for internal consistency by fitting an orbit or a polynomial through each pass of data for each station. This procedure provides the rms noise level of the data and identifies and measurements that are obvious errors. Further, the noise level can be used as an initial check that the system appears to be working correctly. For example, a sudden increase in the noise level from 50 cm to 100 cm between two consecutive passes probably indicates a change in performance of the system that needs to be investigated.

Figure 1 shows the range residuals to an orbit fitted to each of four passes of data obtained by the fixed Goddard laser (GODLAS). These four passes were obtained by the fixed Goddard laser (GODLAS) on September 2, 1970. The rms fits of the data about these orbits varies between 48 cm and 53 cm. The noise levels associated with each pass only indicate the internal consistency of the data and say nothing about possible biases that could exist. It will be seen in later sections, that if these pass-to-pass biases exist, they are extremely constant or probably no larger than the noise level. The quality of the data shown in figure 1 is typical of that collected during the Summer and Fall of 1970. During the latter part of 1971 the noise level of the data was generally higher at about 80 cm and is believed to have been the result of an unintentional increase in the length of the ruby pulse from about 20 to nearly 40 nanoseconds.

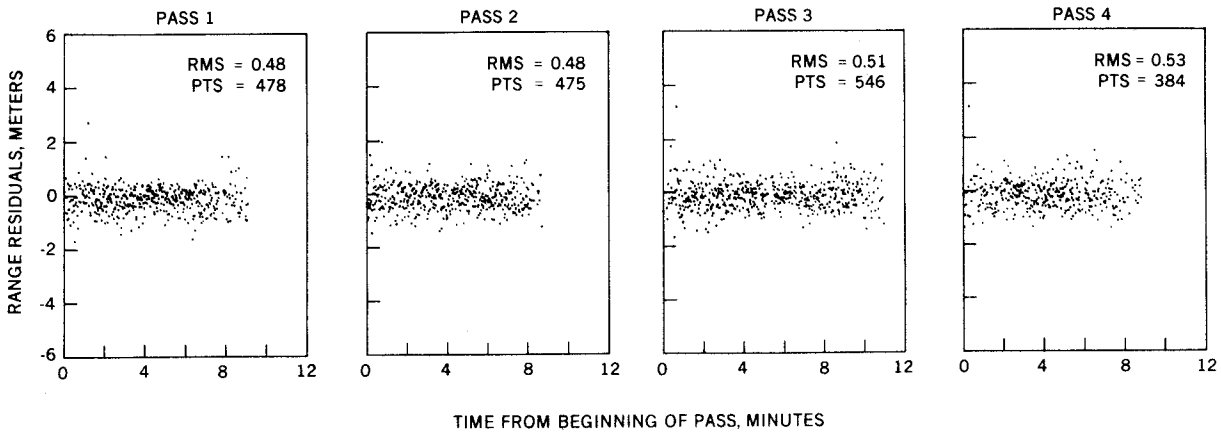

Figure 1. Laser Range Residuals to Four Beacon Explorer C Passes on September 2, 1970

The laser systems also output the direction of the receiving telescope at the time of each return pulse but we have never used these data in any of our investigations because of their relatively low accuracy and high probability of biases. The angular field of the receiving telescope is about one minute of arc and the return pulse could come from anywhere in the field of view. Further, the telescope is computer driven to follow a predicted path across the sky and if the satellite is acquired in one segment of the field of the receiving telescope, it may well remain in that "off-centre" position throughout the pass. The angle measurements would then be biased by anything up to about 30 arcseconds. On a number of occasions the quality of the angle data has been estimated by comparing the position of the satellite computed from a large number of range measurements, with the angle data. This comparison suggested the rms noise of the angle data was about 30 arcseconds with biases of the order of 15 arcseconds.

3. Orbit Determination

The latitude of the GSFC Optical Site is approximately 39°N and because this is comparable to the orbital inclination of BE-C (41°), the apparent motion of the satellite from the site is predominantly west to east. In addition, the site sees four consecutive passes of BE-C spanning about 6 hours each day (when the weather permits). In the analysis, an orbit has been determined for BE-C from laser

data on every occasion that four consecutive passes were observed at the GSFC site (GODLAS). Thirty-six sets of orbital elements have been determined in a five-hundred day period between July 1970 and November 1971. In order to assess the quality of these BE-C orbits, a simple analysis of the variations in the orbit parameters was conducted. For this test, 28 sets of orbital elements obtained for the Summer and Fall of 1970 were used in a short arc minus long arc analysis.

The short minus long arc approach involves comparing orbit parameters obtained from short arcs (for example, four passes) with the same parameters obtained from a long arc (several weeks or months) and is basically equivalent to comparing observations (short arcs) with theory (long arcs). In situations, such as at GSFC, where numerical integration is used in the orbit determination programs, no "theory" exists and must be replaced with a numerical computation. This computation must provide the best orbit available and be equally representative of the true orbit at each of the observation points (short-arc orbits). The way this "theoretical" orbit can be produced is by fitting one single orbit to all the data covered by the short arcs. If this long-arc is sufficiently long, it will average through perturbations that are not accounted for in the integration of the orbit and it then becomes equivalent to the theoretical orbit. The short arcs, on the other hand, are unable to average through any unmodeled perturbation that has a periodicity longer than the time span of the short arc. The short arc therefore (in contrast to the long arc) absorbs the perturbations into the orbit parameters. Subtracting the orbit parameters of the long arc from the parameters of the short arcs therefore reveals perturbations that are not computed in the long arc as well as errors, or deficiencies, in the modeling of forces that are included. Figure 2 shows residuals in semi-major axis, argument of perigee, right ascension of the node, eccentricity and mean anomaly obtained from a short minus long arc analysis of the BE-C data. The residuals in inclination are not shown in figure 2 bacause they are described and discussed in considerable detail in later sections of this paper. It will be seen in these sections that the orbital inclination is the best determined parameter.

Figure 2 shows the variation in semi-major axis is bounded by about plus and minus 3 m with the suggestion of a 70 to 80 day oscillation. This oscillation is probably more evident in the orgument of perigee and mean anomaly, and to a lesser extent in the eccentricity. There is no evidence, however, of an oscillation in the nodal residuals which are dominated by a linear acceleration of about 1.5×10^{-5} degrees/day, equivalent to an error of about 3 parts in 10^6 in the precession of the node. In terms of satellite position, the residuals in mean anomaly and semi-major axis indicate a maximum difference between the short arc and long arc positions of less than 1 km. A fact to be noticed in figure 2 is that the eccentricity and argument of perigee are negatively biased. The cause of these, and other trends and patterns in figure 2 are at present unknown. The connection between these residuals and a possible error in **GM**, the product of the gravitational constant and the Earth's mass, is being investigated. It should also be noted from figure 2 that each of the elements appears to have high internal consistency suggesting that the patterns and trends clearly visible are caused by errors in the Earth parameters (gravity, station position, etc.) rather than the data.

In general, the fit of the orbit to the laser data in a four-pass orbit never equals the quality of the data. Typically, the rms of fit of the laser data in a four-pass orbit is between 1 and 3 m (in contrast to 40 to 60 cm on a single pass) and we have found that the fit is very dependent on the gravitational field being used in the orbit analysis. For the Goddard Earth Model 1 (GEM 1), the average rms of fit over 36 four-pass orbits containing nearly 36,000 laser range measurements is

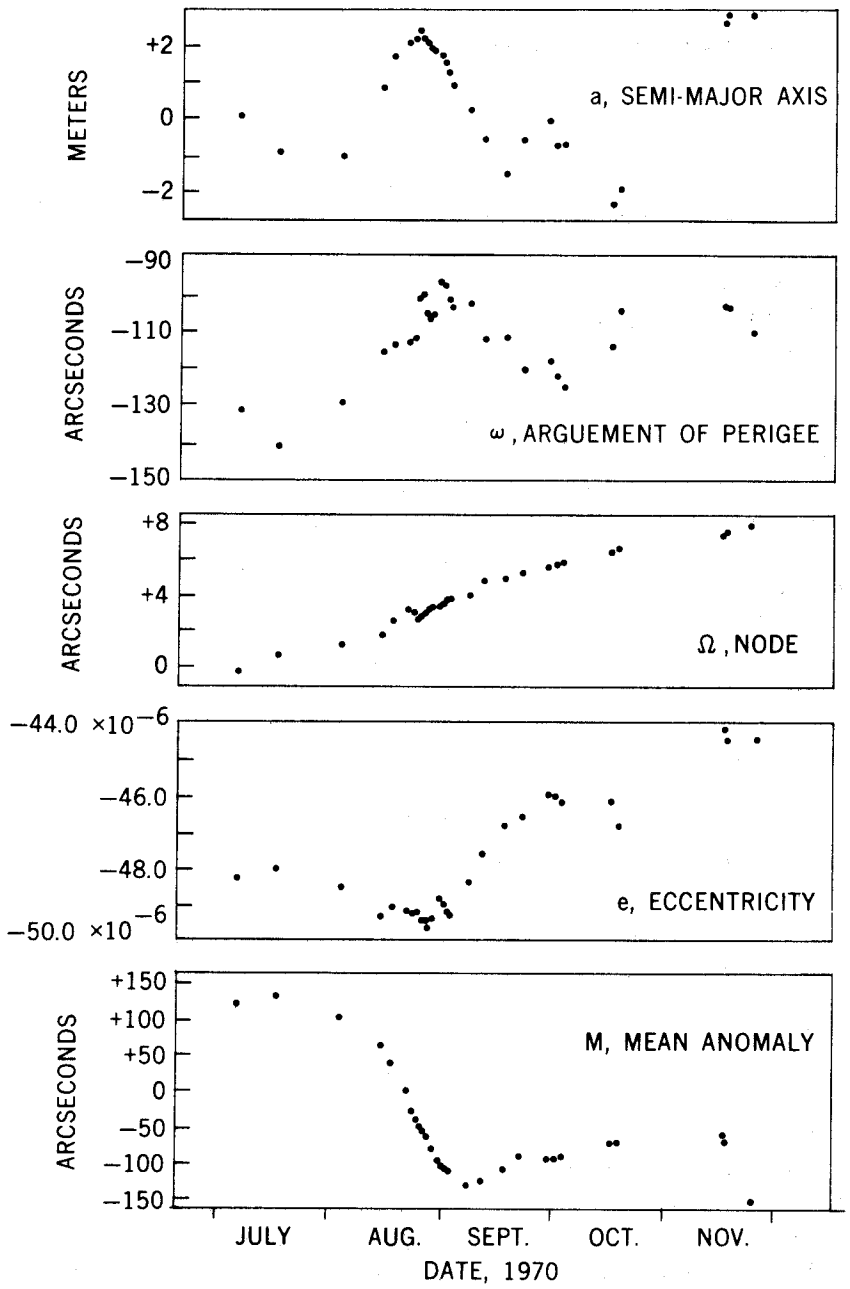

Figure 2. Beacon Explorer C Orbital Element Residuals

1.32 m. There appears to be no correlation between the number of measurements and the rms of the fit. Further, we have found no evidence of poor data in the orbital arcs with the larger rms deviations.

Table 1

Results of the Determination of the Position of the Seneca Laser and the Baseline Between Goddard and Seneca

TIME OF FIRST PASS Y – M – D	RANGE MEAS. GODDARD	RANGE MEAS. SENECA	R.M.S. FIT TO ORBIT GODDARD (cm.)	R.M.S. FIT TO ORBIT SENECA (cm.)	ADJUSTED SENECA POSITION LAT. 42° 42'	ADJUSTED SENECA POSITION LONG. 283° 10'	ADJUSTED SENECA POSITION HEIGHT	BASELINE DEVIATION FROM MEAN
70–08–22	1792	580	153	135	4.900"	17.278"	191.48 m.	+96 cm. (max.)
70–09–01	2002	817	105	106	4.845	17.334	189.16	–80 cm. (min.)
70–09–02	1883	1522	128	134	4.874	17.282	190.95	+14 cm.
70–09–07	1351	1399	147	145	4.848	17.253	189.81	–69 cm.
70–09–11	778	917	82	202	4.879	17.218	193.48	+38 cm.

MEAN BASELINE	408,701.92 m.	INDIVIDUAL BASELINE SIGMA	74 cm.
BASELINE SPREAD	176 cm.	MEAN BASELINE SIGMA	33 cm.

An inspection of the residuals on a 4-pass arc shows that they are far from random. Periodic trends are clearly evident in the residuals, of which a good example is shown in figure 3a. This pattern reflects the errors or deficiencies in the gravitational field model (in this case GEM 1) and changes with the field. Thus the residual pattern for the Standard Earth II field is quite different from that for GEM 1 although the pattern is still quasi-sinusoidal. The possibility that these patterns are a result of other errors, such as the position of the tracking station, has been explored but this has been rejected because another tracking station only a few hundred km away has the same pattern when the same gravitational field is used. It is not difficult to show that modifying the solar radiation pressure perturbation model has no effect on the residual patterns of the short four-pass orbits. It should be further mentioned that all four-pass orbits derived from data collected at the same station exhibit almost identical patterns.

It is interesting to note that if orbits are fitted to only two or three consecutive passes (instead

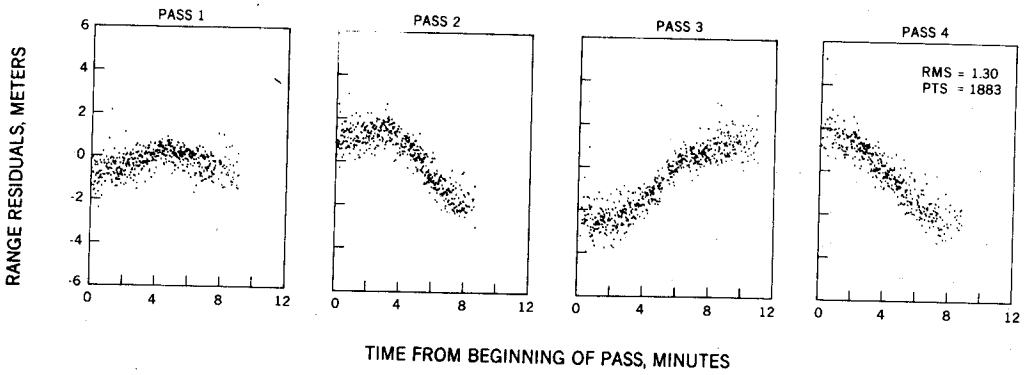

Figure 3a. Laser Range Residuals to Beacon Explorer C - Four Pass Orbit

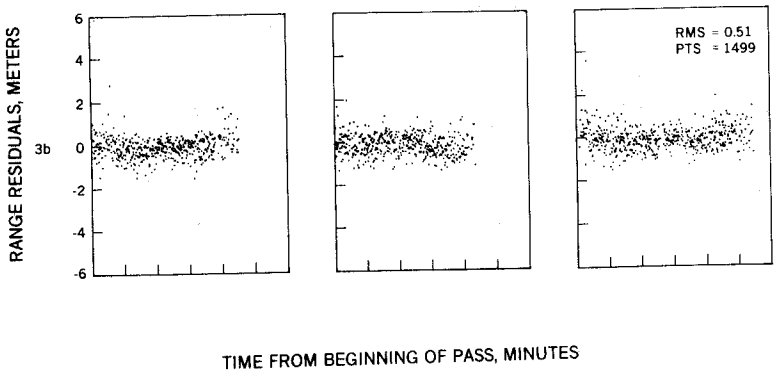

Figure 3b. Laser Range Residuals to Beacon Explorer C - A Three-Pass Orbit

of four), the rms fits of the observations about the orbits are significantly improved and the patterns less pronounced. Indeed, on two pass orbits, the patterns are no longer evident. Figures 3b and 3c show a three-pass and a two-pass orbit. The data in figures 3b and 3c are subsets of that shown in figure 3a.

The average range residual on a four pass orbit is usually a few cm but in our initial investigations we usually found this average to be a few decimetres and we postulated that it was caused by an error in the height of the station. Consequently, we made a determination of the station height from each four pass orbit in a simultaneous solution with the six orbit parameters. In all 36 cases, the average residual was less than 10 cm in in most cases only a few cm. The values of the height recovered from each four-pass orbital arc are shown in figure 4. They range over nearly 20 m about a weighted mean of 9.29 m with a rms deviation of 3.85 m. The mean height is only a few metres larger than the *a priori* value and was adopted as the "true" height of the station. The results shown in figure 4 were obtained with the GEM 1 gravity field and from earlier experiments employing different gravity models we know that the distribution of the points is almost completely dependent on the gravity field used in the analysis. For example, one might reasonably suspect some of the outlying points in figure 4 to be a result of poor data but this is not the case. The analysis of these data with other gravity fields has shown other points to be outliers and convinced the authors that figure 4 is unable to shed any light on the general quality of the data but rather on the

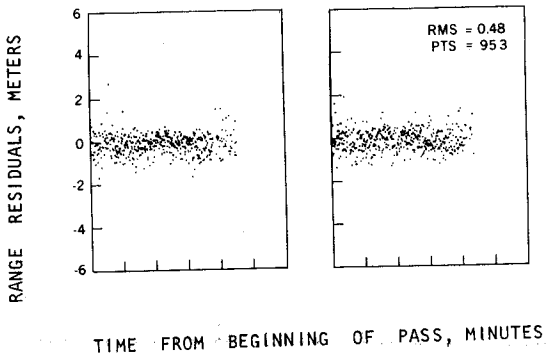

Figure 3c. Laser Range Residuals to Beacon Explorer C - A Two-Pass Orbit

quality of the gravity field.

In order to aid in the interpretation of figure 4, a kind of spectral analysis of the 36 heights has been performed by fitting a large number of sine curves through the data and by determining the least squares amplitude and phase for different frequencies. The results of this analysis are shown in figure 5 in which the square of the amplitude is plotted against frequency. A proper spectral analysis of the data could not be performed because of its sparcity and the irregular intervals between the measurements. If data had been obtained on all possible occasions, the interval between the measurements would (on average) have been about 23 hours 39 minutes (determined by the precession of the orbit with respect to the sun). Thus the highest frequency that was removed was one cycle/day; the lowest was 0.01 cycles/day.

Figure 5 is essentially noisy throughout the whole frequency range. One peak around 0.032 cycles/day (31.2 days) might be significant but those near 0.31 (3.2 days) are almost certainly noise. The 31 day period is difficult to explain. It is close to a month and therefore one is tempted to ask if it is indirectly caused by the moon. This is unlikely, however, because most lunar effects have periods determined primarily by the motion of the moon with respect to the orbit, which for BE-C are around 11 and 85 days.

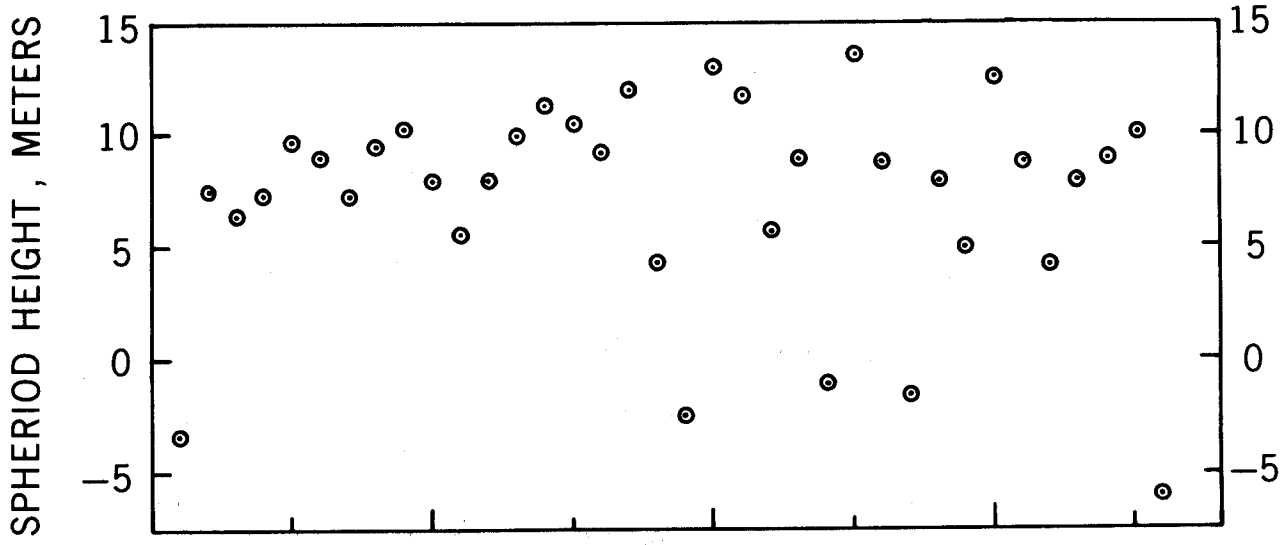

Figure 4. Height of Goddard Laser Obtained from Thirty-Six Four-Pass Orbital Arcs of Beacon Explorer C. The rms Deviation of a Single Height Measurement is 3.85 m

4. Solid Earth and Ocean Tides

One of the major aims of this analysis was the detection of the perturbations of the orbit by the solid-Earth and ocean tides. Since the latitude of the Goddard tracking station (GODLAS) was within a few degrees of the apex of the Beacon Explorer C orbit, most of the observations were obtained when the satellite had a predominant motion from west to east. Thus, during a four-pass observing period, the observations were clustered around the position of maximum latitude attained by the satellite and hence the orbital inclination was a well determined parameter. The variations in orbital inclination obtained from the 36 four-pass orbits have been analyzed using the "short-arc minus long-arc" technique in order to isolate the tidal perturbations.

The largest perturbations of the orbital inclination result from the non-sphericity of the Earth, which causes both short and long period effects. The largest short period term is caused by the Earth's oblateness, given by (MERSON 1961)

$$\delta i = -\frac{3}{2} J_2 \left(\frac{R}{p}\right)^2 \sin 2i \left[\left\{\frac{1}{2}\sin^2 u + \frac{1}{3} e \cos\omega\right\} + \left\{\frac{1}{3} e \sin^2 u \cos\nu - \frac{1}{3} e \cos u \cos\omega\right\}\right] +$$

$$\text{terms of order } J_2 \text{ squared} \qquad (2),$$

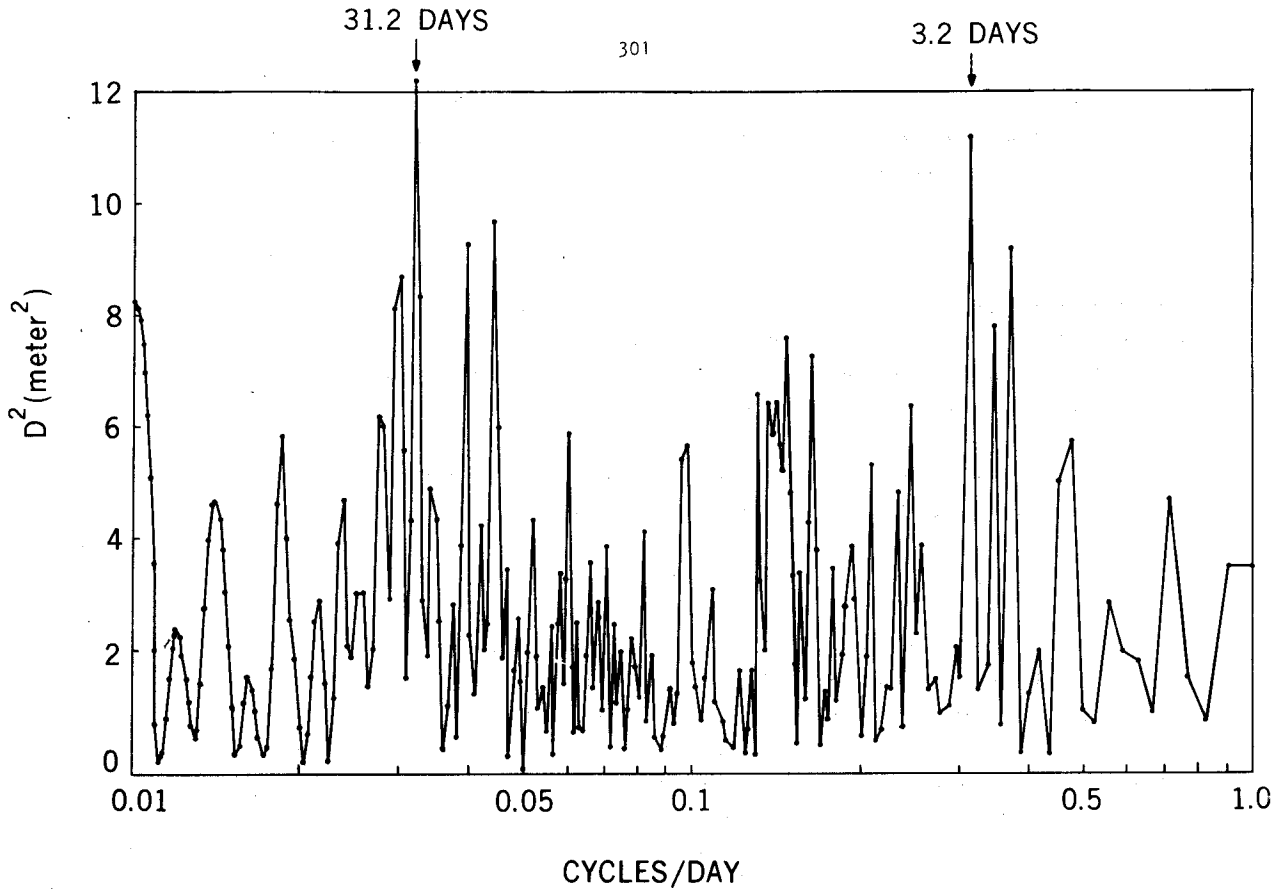

Figure 5. Frequency Analysis of the Height Determinations of the Goddard Laser

where δi is the perturbation in inclination, J_2 is the second degree zonal harmonic coefficient, R is the Earth's equatorial radius, p is the semi-latus rectum, i is the orbital inclination, u is the argument of latitude, e is the eccentricity and ω is the argument of perigee. Since $J_2 \sim 1.1 \times 10^{-3}$, the amplitude of δi is about 60 arcseconds, or about 2 km projected onto the Earth's surface. An important aspect of the perturbation given by equation 2 is that the major term ($\frac{1}{2} \sin^2 u$) is only a function of the projected motion of the satellite on the Earth's surface and consequently can be ignored if the orbital inclination is determined for the same argument of latitude (u). For example, suppose the orbit of the satellite is determined at the position of maximum northerly latitude ($u=\frac{1}{2}\pi$) then the terms inside the brackets in equation 2 reduce to

$$\frac{1}{2} + \frac{2}{3} e \sin \{\tfrac{1}{2}(\omega - \nu)\}$$

which has an amplitude of about 120 m for BE-C. Thus, the short period perturbations of the inclination by the gravity field can be kept to a minimum by determining the orbit at the maximum latitude position.

The J_2^2 terms and other geopotential coefficients cause short period perturbations (in the inclination) of about 10 m. Slightly longer period terms, the so-called M-daily terms of low order (M), can cause perturbations equivalent to a few tens of metres in the orbital inclination with periods of 24 hours,

12 hours, 8 hours, etc. The next largest period is that of the primary resonance which is about 5.5 days for Beacon Explorer C and associated with terms of order 13. The argument of the primary thirteenth-order resonance is

$$\omega + M + 13(\Omega - \theta),$$

where M is the mean anomaly, Ω is the right ascension of the node, and θ is the sidereal time. After approximately $5\frac{1}{2}$ days the ground track of the satellite repeats itself, that is, when the argument of the primary resonance has moved through 2π. The amplitude of this resonance (for BE-C) is about 0.35 arcseconds in the inclination (11 m).

There are also long-period perturbations in the inclination that are associated with the odd zonal harmonics in the gravity field. The principal terms take the form (MERSON 1961)

$$\delta i = (A J_3 + B J_5 + C J_7 + \ldots) \sin \omega \qquad (3),$$

where A, B, C .. are functions of the orbit parameters, and J_3, J_5, J_7, .. are the odd zonal harmonics. The perigee rotation period, and therefore the period of the perturbation, for BE-C is 70 days, and the amplitude of the perturbation is about 2 arcseconds and is equivalent to about 60 m projected onto the Earth's surface. Other long period perturbations are caused by the gravitational attraction of the sun and moon, and contain several periods ranging from 10 days to 85 days. In addition, there are very long period terms with periods up to about 19 years, but all these luni-solar perturbations can be computed with adequate accuracy from a knowledge of the positions of the sun and moon.

The major unknown perturbations of long period are those associated with the solid-Earth and ocean tides and are effectively indirect luni-solar perturbations. The sun and moon raise ocean and body tides that involve sufficient mass that they perturb the motion of the satellite. These tidal disturbances of the gravity field can be largely represented by a second degree spherical harmonic with axial symmetry in the approximate direction of the tide rising body. With this representation, the major terms in the tidal perturbation of inclination can be written (KOZAI 1965; FISHER & FELSENTREGER 1966; MUSEN & FELSENTREGER 1973)

$$\delta i = \frac{3}{4} m_D \frac{n_D^2}{n} \left(\frac{R}{a} \right)^5 \frac{k_2}{(1-e^2)^2} \cos^2(\tfrac{1}{2} i_D) \left\{ \frac{\sin i \cos^2(\frac{1}{2} i_D)}{2(\dot{L} - \dot{\Omega})} \cos 2(L-\Omega) - \frac{2 \cos i \tan(\frac{1}{2} i_D) \cos i_D}{(\dot{\Omega} - \dot{\Omega}_D)} \cos(\Omega - \Omega_D) - \right.$$

$$\left. \frac{\cos i \sin i_D}{(2\dot{L} - \dot{\Omega})} \cos(2L - \Omega) \right\} \qquad (4),$$

where m_D is the ratio of the mass of the tide raising body to the mass of the Earth, n_D is the mean motion of the disturbing body, n the mean motion of the satellite and a the semi-major axis. k_2 is Love's number of second degree, i_D is the orbit of the disturbing body to the Earth's equator, L is the longitude of the disturbing body and Ω and Ω_D are the right ascensions of the ascending nodes of the orbits of the satellite and disturbing body. The dot quantities refer to time derivatives. The Love number is defined as the ratio of the tidal potential to the tide raising potential.

The amplitudes of these perturbations (of BE-C) amount to a few tenths of an arcsecond for each of the terms in equation 4 for both the sun and moon. Their periods are about 10, 12 and 85 days for the moon and 35 days, 58 days and 85 days for the sun. For Beacon Explorer C the expected total perturbations has a peak-to-peak variation of about 2.1 arcseconds, or about 70 m projected onto the Earth's surface.

The initial step in isolating the tidal perturbations was to determine the maximum latitude reached by the satellite on each pass of the 36 four-pass orbits. This was accomplished with the aid of an ephemeris which was generated for each orbital arc from a least squares fit to the data. The second step was to derive the maximum latitude on each pass from the long-arc orbit described in section 3. Finally, the long-arc maximum latitudes were subtracted from the short-arc maximum latitudes and the "max-lat" residuals showed very clearly the effects of the tide on the orbit. From these residuals we made an estimation of the Love number k_2 (amplitude) and the phase of the tides. Initially this estimate was only made from the first five months of data (SMITH ET AL 1973) and subsequently extended through the following year (KOLENKIEWICZ ET AL 1973). The observed max-lat residuals are shown in figure 6, together with the best fit theoretical curve for $k_2 = 0.245$ and ϕ (phase) $= 3.2°$. The precision with which the data fit the curve indicates a standard deviation of 0.005 for k_2 and $0.5°$ for ϕ.

The actual procedure for deriving the values of k_2 and ϕ extended over several months (DUNN ET AL 1973). In the initial analysis of the tides, the differences between the laser data and the theory shown in figure 6, contained an oscillation of amplitude about 2 m and period 5.5 days. This pattern is characteristic of an error in the resonance terms (order 13 for BE-C) in the gravity field and consequently an adjustment was made to two coefficients. An approximately 19% decrease in $C_{19}{}^{13}$ and approximately 18% increase in $S_{19}{}^{13}$, with respect to the GEM 1 values, removed the sinusoidal residual pattern (KOLENKIEWICZ ET AL 1973). At this stage the analysis was restarted from the beginning with this new gravity field which we referred to as GEM 1*. Having re-analyzed the orbits and redetermined the station heights (with GEM 1*) we found almost no change from out original analysis with GEM 1 with the exception of removing the patterns in the residuals in inclination (maximum latitude) in the tide analysis. It is with the GEM 1* field that the laser points in figure 6 have been computed and from which the Love number and phase already given were derived.

Because the determination of k_2 and ϕ was obtained from a separate analysis of the residuals in inclination rather than from a large least squares adjustment from the raw laser data, it was neccesary to undertake a second re-analysis of all the observational data with the tides modeled (using the recovered values of k_2 and ϕ) in order to check that the tidal solution had converged. Only insignificantly small changes in the recovered heights for the Goddard laser were obtained and there was no change from the original best fit values for k_2 and ϕ.

The most important single result evident from figure 6 is that the amplitude of the perturbation is significantly smaller than expected. From seismic data we know that k_2 should be around 0.30 and therefore that there must be some additional perturbations of the BE-C orbit that are tending to compensate for the solid-Earth tides. Since the agreement between the theoretical curve and the data is so good in figure 6, it must be concluded that the functional form of the perturbation must be very similar to that of the solid-Earth tide, that is, a second degree spherical harmonic. Thus, it has been suggested that the additional perturbation is caused from the global ocean tides (LAMBECK

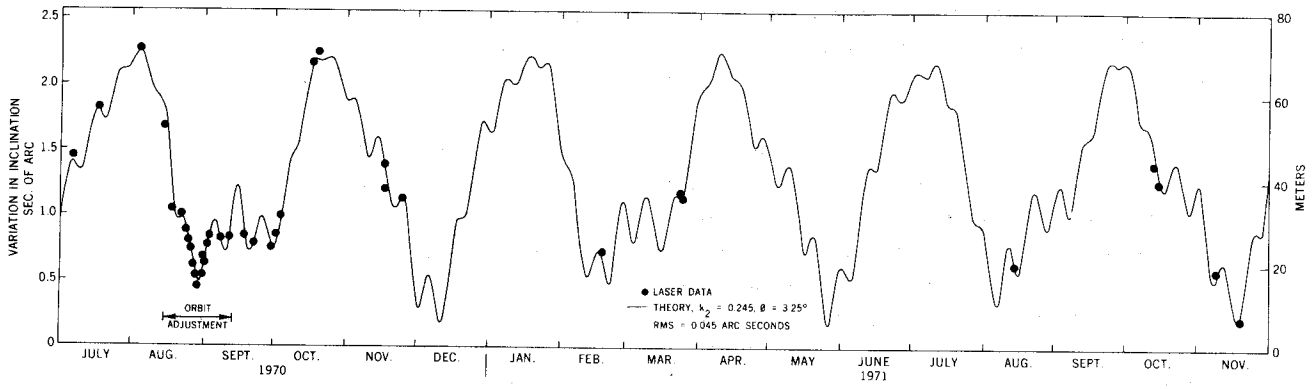

Figure 6. Tidal Perturbations of the Orbital Inclination of Beacon Explorer C

& CAZENAVE 1973). The ocean tides, however, contain many components which can be represented in spherical harmonic form but it is only those of second order, and principally second and fourth degree, that actually perturb the spacecraft to any significant extent (MUSEN 1973). We may therefore argue that this tidal analysis has identified a perturbation equivalent

$$(k_2)_{ocean} = 0.30 - 0.245 = 0.055$$

from the ocean tides.

The solution for the phase of the tidal perturbations (ϕ=3.2°) is more difficult to interpret. The phase of the solid-Earth tide is believed to be small, of the order of a degree or less, and the difference with the result here suggests a larger phase lag for the ocean tides. This is not inconsistent with observations of the tides except that each tidal component is believed to have a different phase and thus a single observation of the phase lag of the tidal gravitational field (of even degree and order two) must be a composite value and hence difficult to interpret. We must await further observations of the ocean tidal perturbations of other satellites before the contributions and phase lags from each tidal component can be identified.

5. Variation of Latitude

In the analysis previously described it was necessary to include polar motion which has the effect of

changing the latitude, and to a small extent longitude, of the laser tracking station. The magnitude of the variation in latitude (MUNK & MACDONALD 1960) amounts to about 0.3 arcseconds in a year (10 m on the Earth's surface) and is monitored routinely by the Bureau International de l'Heure (BIH). In our computations the 5-day smoothed mean position of the pole published by the BIH has been used. The accuracy of the BIH data is probably about 0.02 arcseconds but because these values are averaged over 5 days it is possible for real departures of several hundredths of an arcsecond to exist with respect to a continuous smooth curve.

During the 17 months of laser data, the latitude of the Goddard station varied by approximately 15 m due to the combined effects of the annual and Chandlerian motions of the pole. In order to determine our sensitivity to these motions we suppressed the modeling of polar motion in the 36 short orbital arcs so that the variation of latitude of the tracking station would be forced into the orbital inclination and hence into the values of maximum latitude. Subtracting the long arc maximum latitudes from the short-arc maximum latitudes revealed, as expected, the variations in latitudes of the tracking site (SMITH ET AL 1972b;KOLENKIEWICZ ET AL 1973) shown in figure 7. In analyzing this variation it was essential to include the tidal effects and use the improved resonant gravity terms described in the previous section. The BIH smoothed variation of latitude is also shown in figure 7 and the rms fit of the laser data about the BIH curve is 1.38 m (0.045 arcseconds). At the present time it is probably correct to assume that the differences between the laser and BIH results of figure 7 are primarily due to errors in the laser values rather than in the BIH and that the scatter reflects errors in the gravitational field model used in the orbit computations. As our knowledge of the gravity field improves over the next few years, the scatter in the latitude variation (from the laser data) of figure 7 should decrease correspondingly.

In order to better understand the causes of the scatter of residuals in figure 7, an attempt was made to determine any major periodicities within the residuals to the BIH curve. The same method as used in analyzing the station heights of section 3 (figure 5) was employed. A set of sinusoidal oscillations was fitted through the residuals with frequencies between 1 cycle/day and 0.01 cycles/day. The square of the amplitudes (D) of the recovered oscillations are shown against frequency in figure 8. As might be expected, the variation of D^2 with frequency is largely noise but there may be one or two peaks that are significant. There is a peak near 0.165 cycles/day (6.0 day period) which is one of the resonant periods for the odd degree thirteenth order geopotential terms, and another unidentified peak at about 0.035 cycles/day (28.2 day period). A comparison of figures 5 and 8 is important in their interpretation since the laser data are the source of both the height and latitude measurements. The only difference in technique used to generate these figures is that figure 8 is an analysis of residuals obtained from differencing short and long orbit arcs, while figure 5 is based purely on short arc analysis. Hence errors in the short-arc orbit computation will appear in both figures while errors in the long arc only affect figure 8. There is probably only one significant peak in the height analysis of figure 5, at about 0.032 cycles/day (31.2 day period). This frequency is reasonably close to the peak at 0.035 cycles/day seen in figure 8, but a frequency this low in the orbit perturbations is difficult to explain. Further, the amplitudes of these oscillations (if they exist) are so large, 3.5 m in height and 0.034 arcseconds (1 m) in latitude, that their origin cannot be geophysical. However, it is possible that the orbit is resonant with terms of very high degree and order, say 27, and this possibility is being investigated.

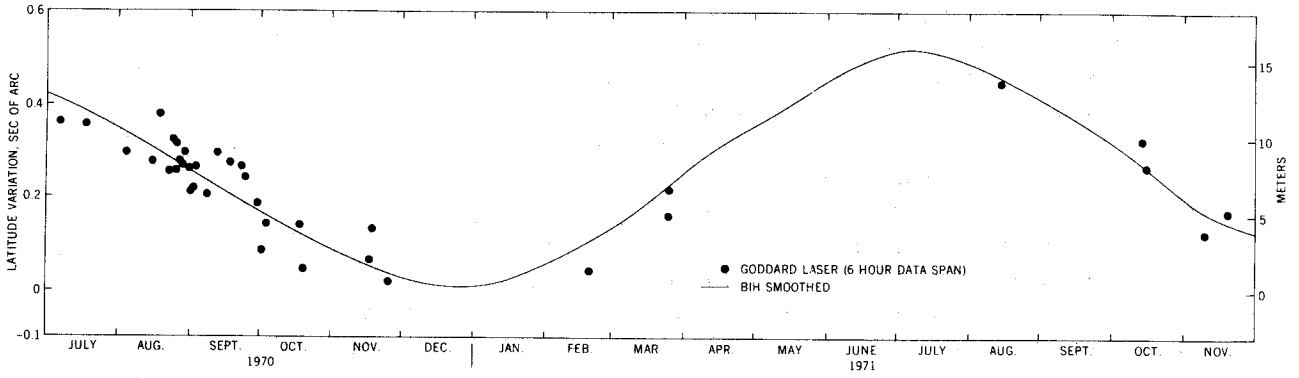

Figure 7. Variation of Latitude of the Goddard Laser

6. Two Station Experiments

The results described in the previous sections were obtained with a single laser tracking system and the fundamental objective of that work was to try and develop techniques that will permit a laser tracking system to monitor its own latitude and height variation at a geophysically useful level. In this section we describe some of our experiments using two laser systems in which the fundamental objective is the measurement of phenomena, such as tectonic and fault motion by the precise determination of the position of one of the tracking systems with respect to the other.

During August and September 1970 a second GSFC laser tracking system was operating from a site near Seneca Lake, New York (SMITH ET AL 1972a). This station was 408 km due north of the laser system at the GSFC Optical Site with which the polar motion and tidal data were obtained. The original purpose of establishing the Seneca station was to determine polar motion in a joint experiment with the Goddard laser. However, it was subsequently found that the second station was not essential for polar motion studies but that with two stations tracking the same satellite on the same passes, it was possible to determine the distance between the lasers very precisely.

There were 5 occasions when the Seneca station observed four consecutive passes of BE-C simultaneously with the Goddard station. From these data, during August and September 1970, the position of the

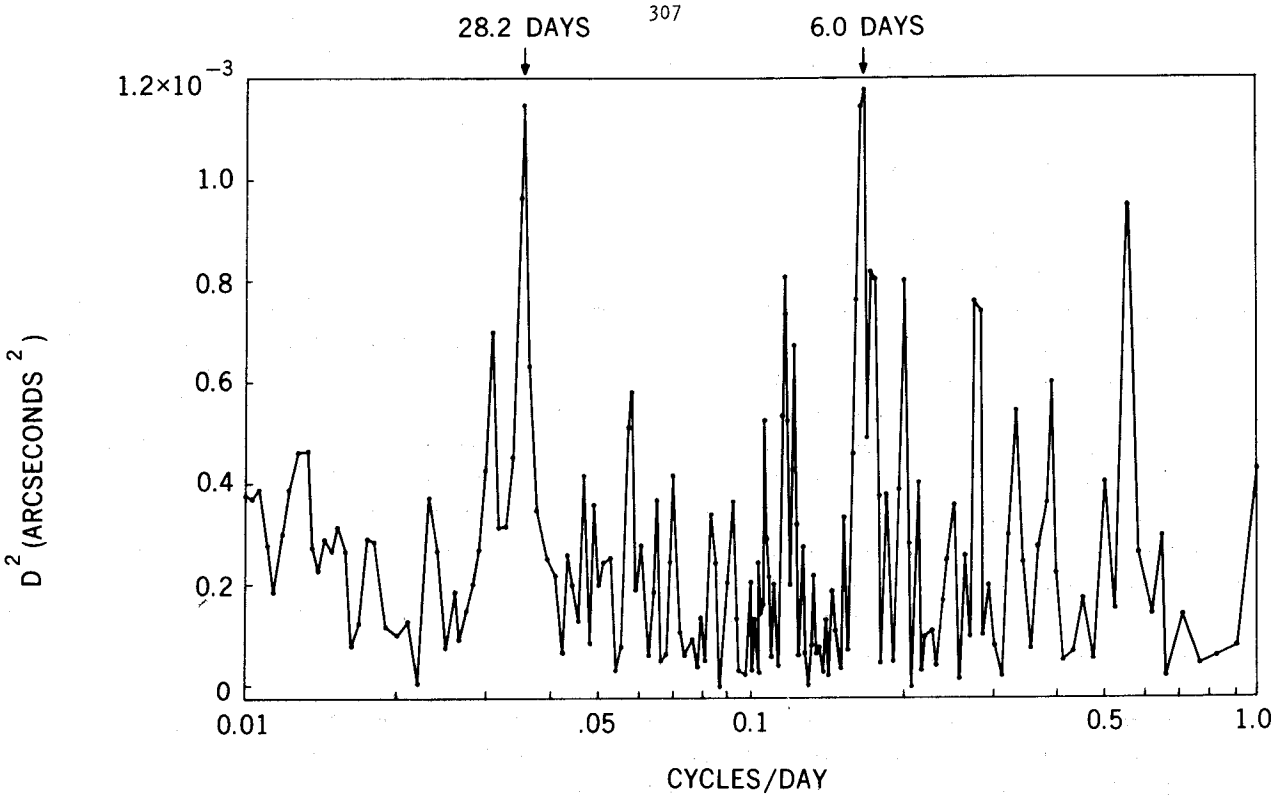

Figure 8. Frequency Analysis of the Variation in Latitude of the Goddard Laser

Seneca station has been determined. In these calculations the position of the Goddard station has been assumed known with the following co-ordinates:

Goddard: Latitude 39° 01' 13.88" N; Longitude 283° 10' 18.50" E; Height 9.29 m.

The values of the latitude and longitude were adopted from early work at GSFC on tracking station positions and are not crucial in the analysis. The height value is a dynamic average of the values in figure 4, derived by simultaneously adjusting the orbital parameters on each of the 36 orbital arcs together with the station height (a single least squares value for all 36 arcs). The numerical value of the height is dependent on the latitude adopted for the station (as above), the product of the gravitational constant (G) and the mass of the Earth (M), the gravitational field (GEM 1*, see section 4) and the mean equatorial radius (R_E) of the Earth. Throughout these analyses we have used the following values:

$$GM = 3.986\,013 \times 10^{20}\ cm^3/sec^2 \quad ; \quad R_E = 6\,378\,155\ m.$$

The results of our determination of the Seneca position are shown in table 1.† The position of Seneca has been determined from each four-pass orbital arc and table 1 shows the range of values of latitude is 0.055 arcseconds (1.7 m), of longitude is 0.116 arcseconds (2.7 m at the latitude of Seneca) and 4.32 m in height. Because Seneca is due north of Goddard, the baseline values have the same range as the latitude values. The baseline length according to survey is 408,698.77 m which is about 3 m less than the value obtained from the co-ordinates given in table 1; the accuracy of the survey is about ± 2 m.

†p.297

The major sources of error in the satellite solution for the Goddard-Seneca baseline are estimated to be:

gravity	2.5 m;
GM (1 part in 10^6)	0.2 m;
range biases (1 m)	0.3 m;
refraction (5%)	0.1 m; and
Goddard height (10 m)	1.6 m,

where the gravity error model (MARTIN & ROY 1972) is taken as one quarter the difference between the Smithsonian Astrophysical Observatory's Standard Earth I field (LUNDQUIST & VEIS 1966) and the Applied Physics Laboratory's 3.5 Model (GUIER & NEWTON 1965). There is of course considerable uncertainty in the above estimates for the accuracy of the parameters used in the analysis but a total accuracy of 2 to 3 m appears reasonable. Gravity errors dominate the solution but because of the technique that has been employed, all the orbital arcs (4 passes) have very similar geometric distribution with respect to the tracking stations. Hence, the errors on one 4-pass orbit are very similar to the errors on any other 4-pass orbit so that the repeatability of the baseline measurement can be expected to be considerably better than the accuracy. This situation is supported by table 1 in which the standard deviation of an individual baseline measurement is probably better than 1 m even though our best estimate of the accuracy is, perhaps, 3 m.

The internal accuracies (noise standard deviation) of the Goddard-Seneca experiment are of particular interest because they represent the ultimate capability of the technique if our knowledge of everything affecting the motion of the spacecraft were known perfectly. Based on laser range measurements of 1 m noise (no biases), the standard deviation of latitude would be about 15 cm, longitude about 8 cm, and height 9 cm. Thus, the technique has the capability of reaching the 1 cm level in all co-ordinates with laser systems of the 5-10 cm noise level, which are projected to be available in 1974.

With the introduction of radar altimeters, satellite-to-satellite tracking techniques and more accurate laser data in greater quantities, significant improvements in the gravity field, GM and station co-ordinates can be projected such that 10 cm precision relative positioning should be a realizable objective from a single four-pass orbital arc. In 1972, a plan was formulated for applying this technique to the measurement of motion along the San Andreas fault in California, which is the boundary between the tectonic plates of the Pacific and North America. In its simplest concept, one laser tracking station would be established on the western side of the fault, that is, on the Pacific plate, near San Diego and a second station on the eastern side of the fault, the North American plate, near Quincy in northern California (see figure 9). The distance between the two stations is nearly 900 km and the angle between the baseline and the fault is about 15° so that the change in baseline length over several years will be very similar to the gross fault motion across the plate boundary. Present estimates of the fault motion are between 3 and 5 cm/yr.

A simulation of this experiment (AGREEN & SMITH 1973), the San Andreas Fault Experiment (SAFE), has been completed and is summarized in table 2. The experiment has been simulated to last for 8 years, using the BE-C satellite and stations at San Diego and Quincy. Table 2 shows the effects of various errors on the baseline between the two stations when each year of measurements is composed of 16 simultaneous short-arcs of three consecutive passes. (Three passes were used because the

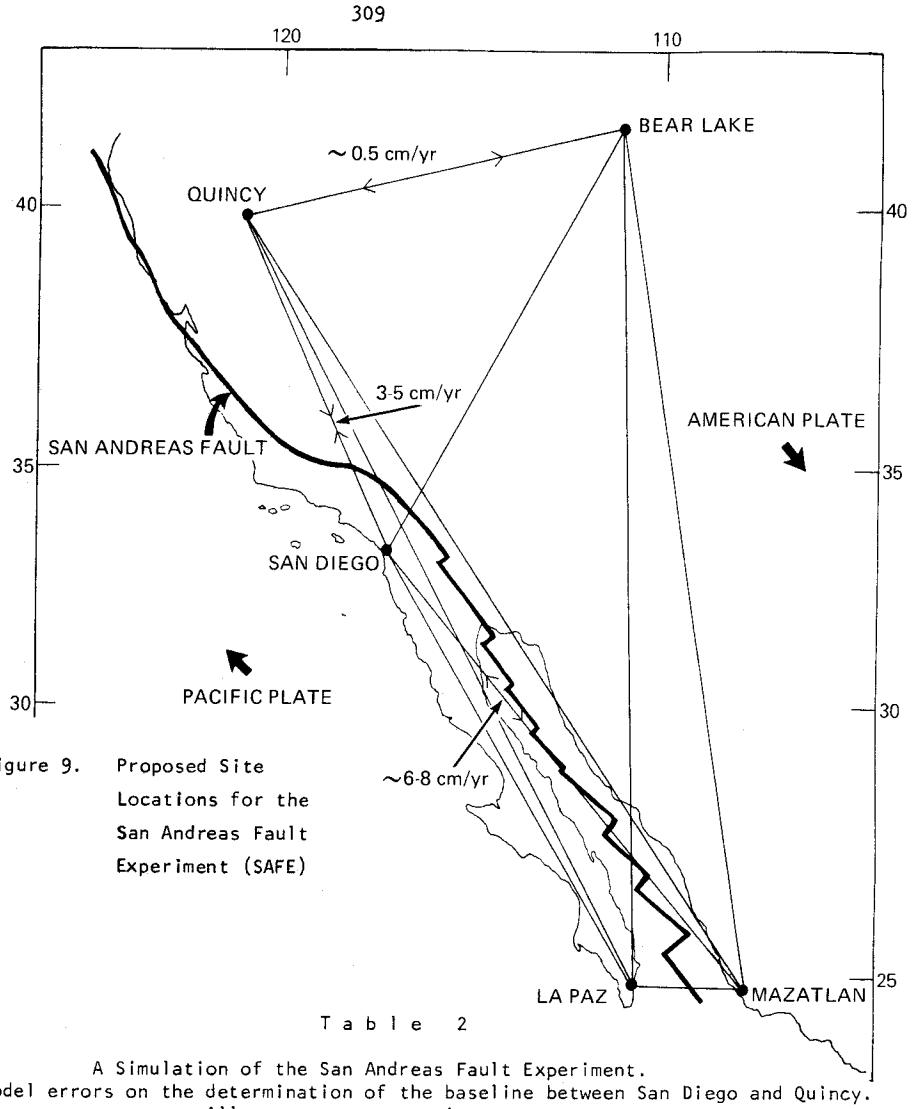

Figure 9. Proposed Site Locations for the San Andreas Fault Experiment (SAFE)

Table 2

A Simulation of the San Andreas Fault Experiment.
Effects of model errors on the determination of the baseline between San Diego and Quincy.
All measurements are in cm.

Year	GM	Gravity Model	Quincy Bias	San Diego Bias	Solar Radiation	Atmospheric Drag	C 19,13	S 19,13	San Diego Longitude	San Diego Latitude	San Diego Height
1970	102	-62	-2	7	-1	-1	1	1	0	-14	-110
1971	95	-68	-2	8	-2	-1	0	0	0	0	-99
1972	109	-53	-3	7	0	-1	1	0	0	-2	-113
1973	102	-66	-2	7	0	-1	0	0	0	-9	-107
1974	102	-57	-2	7	0	-1	1	0	0	-8	-108
1975	98	-61	-2	7	1	-1	0	0	0	-4	-103
1976	102	-75	-3	7	1	-1	1	0	0	-9	-107
1977	99	-64	-3	7	0	-1	0	0	0	-5	-104
Average	101	-63	-2.4	7.1	-0.1	-0.5	0.5	0	0	-6.4	-106
RMS	3.8	6.3	0.3	0.3	0.9	0	0.5	0	0	4.2	4.1

simulation suggested that three passes gave a greater precision than four passes). The error sources in the simulation were 1 part in 10^6 for GM, ½(SAO Standard Earth 1 - APL 3.5) for gravity, 10 cm range biases, 10% error in solar radiation and air drag models, ½ nominal values of the 19th degree, 13th order resonant terms in the geopotential, and 5 m in each co-ordinate at San Diego.

From table 2 we obtain the root-sum-squares as ±9.5 cm for the baseline precision based on the *a priori* magnitudes of the error sources already given. These *a priori* estimates are believed to reflect our knowledge in 1972-73 and can be expected to improve considerably during the present decade. If we postulate that there will be the following improvements in our knowledge by 1980 (over 1972-73 values)

GM	by a factor	20	(to 5 parts in 10^8);
Gravity	by a factor	7;	
San Diego Position	by a factor	20	(to 25 cm); and
Laser Systems	by a factor	5	(to 2 cm),

the precision of the baseline measurement will be 1 to 2 cm with an accuracy of about 10 to 15 cm. This will permit the determination of the change in baseline (plate motion) to better than 0.5 cm/yr over a 7 year period.

The full plans for SAFE include the establishment of a third laser site near Bear Lake, Utah and proposals for two sites in Mexico, on either side of the Gulf of California. These additional sites will enable the gross plate motion and crustal deformation to be measured along a 2000 km stretch of the western United States and Mexico. Motions along the fault in the Gulf of California are estimated to be much larger than those in southern California, with estimates generally in the 6 to 8 cm/year range. The site in Utah will enable the spreading rate across northern California and Nevada to be estimated, although this motion is probably only of the order of 0.5 cm/year and consequently very difficult to measure.

The SAFE experiment is planned to begin in the Spring of 1974 but a preliminary tracking experiment was conducted in September 1972 between the San Diego and Quincy sites (SMITH & VONBUN 1973). In this test experiment, both sites successfully tracked four consecutive passes of BE-C on four simultaneous occasions from which estimates of the position of Quincy with respect to San Diego have been obtained. During this period the laser systems were performing at about the 60 to 80 cm noise level, implying biases of this order could be in the data. Essentially the same techniques were used in this analysis as had been used in the Goddard-Seneca experiment. From all the four-pass orbital arcs obtained at San Diego, the height of the station was derived. The latitude, longitude and recovered height of the station used in the subsequent analysis were

San Diego: Latitude 32° 36' 02.53" N; Longitude 243° 09' 32.87" E; Height 989.5 m.

Based on the above co-ordinates, the results shown in table 3 were obtained with the GEM 1* gravity field. Unfortunately, there are only four determinations and any statistics concerning the solutions must, therefore, be treated with caution. However, the four solutions do agree at least as well as might be expected from our knowledge of the data and the models. Further, there is a very obvious correlation among the recovered latitudes and longitudes in table 3. In addition, this linear variation is approximately perpendicular to the direction of the San Diego-Quincy baseline, showing that there is a tendency for the Quincy solutions to lie on an arc centered on the primary station

Table 3

Results of the Determination of the Position of the Quincy Laser and the Baseline Between San Diego and Quincy

TIME OF FIRST PASS Y – M – D	RANGE MEAS. QUINCY	SANDIE	R.M.S. FIT TO ORBIT QUINCY (cm.)	SANDIE (cm.)	ADJUSTED QUINCY POSITION LAT.	LONG.	HEIGHT	BASELINE DEVIATION FROM MEAN
					39° 58'	239° 03'		
72–09–17	623	1047	299	357	24.447"	37.787"	1062.76 m.	+35 cm. (max.)
72–09–18	327	920	205	250	24.411	37.732	1061.42	–19 cm.
72–09–30	649	926	190	153	24.402	37.686	1062.24	+15 cm.
72–10–03	439	578	127	98	24.373	37.659	1064.24	–30 cm. (min.)

MEAN BASELINE	896,275.17 m.	INDIVIDUAL BASELINE SIGMA	30 cm.
BASELINE SPREAD	65 cm.	MEAN BASELINE SIGMA	15 cm.

(San Diego) thereby giving a better determination of the baseline length than of the individual co-ordinates of the second station (Quincy).

7. Future Satellites and Investigations

In the course of the investigations described in the previous sections it became increasingly obvious that the full potential of the techniques could not be achieved without significant improvements in many geophysical parameters, including GM and the gravity field. The major problem area has probably been the gravity field so far, partly because our experience has been with relatively low altitude spacecraft like BE-C . However, this may change if the planned high altitude satellites such as TIMATION III and LAGEOS are launched. TIMATION, expected to be at an altitude of about 14,000 km, will be much less affected by a lack of knowledge of the higher harmonic coefficients of the gravity field and therefore, in principle, a much better spacecraft to use for satellite geodynamic research.

In order to assess the impact of TIMATION III on an experiment, such as SAFE, a series of simulations of the determination of the San Diego-Quincy baseline have been completed. In summary, the major error sources are now only GM and the position of San Diego. Further, results of the same accuracy and precision can be obtained from a few days of TIMATION tracking compared to about 2 months of BE-C tracking and because the gravity perturbations are very small, high altitude spacecraft offer the possibility of determining GM. Simulations of a small world-wide network of laser stations indicate that an improvement in GM by about two orders of magnitude (to 1 part in 10^8) should be realizable in the next five years (CARPENTER ET AL 1972). Thus, the TIMATION and LAGEOS type spacecraft are expected to have a major impact on this type of investigation.

Projecting the type of techniques used on Beacon Explorer C into the future with more advanced spacecraft and better orbits, and further realizing that there will be substantial improvements in our knowledge of the gravity field through the application of newer tracking techniques, such as satellite-to-satellite tracking and altimetry, we anticipate that geophysically useful measurements of fault motion, tectonic plate motions and polar motions will be obtained within the next five years.

The accuracies which will be achievable from about one week of data will probably be of the order of 5 to 10 cm in distance measuring for distances up to about 10,000 km, and about 5 to 10 cm in the variation of latitude and 10 to 20 cm in the variation in height of a station from 6 to 12 hours of tracking. In addition, it should also be possible to determine the variations in the length of day (LOD) to a few tenths of a millisecond on a daily basis, although other techniques, such as very long baseline interferometry, may be better suited to this measurement. In the laser technique for LOD studies, the essential requirement is a suitable satellite in a highly inclined orbit to the equator so that a station, or stations, can measure the time and longitude of the satellite crossing a given latitude. Daily measurements of this type permit the rotation of the Earth with respect to the plane of the orbit of the satellite to be derived.

8. References

AGREEN, R.W. & SMITH, D.E. 1973. A Simulation of the San Andreas Fault Experiment. *Rep. X*-592-73-216,Goddard Space Flight Center,Greenbelt Md.

CARPENTER, L. (ed.) 1972. Preliminary Study of the Application of the TIMATION III Satellite to Earth Physics. *Rep. X*-553-72-50,Goddard Space Flight Center,Greenbelt Md.

DUNN, P.J., SMITH, D.E. & KOLENKIEWICZ, R. 1973. Techniques for the Analyses of Geodynamic Effects Using Laser Data. *First International Symposium, Use of Artificial Satellites for Geodesy & Geodynamics*,Athens.

FISHER, D. & FELSENTREGER, T. 1966. Effects of the Solar and Lunar Tides on the Motion of an Artificial Earth Satellite. *Rep. X*-547-66-560,Goddard Space Flight Center,Greenbelt Md.

GAPOSCHKIN, E.M. & LAMBECK, K. 1970. 1969 Smithsonian Standard Earth II. *Spec.Rep.* 315, Smithsonian Astrophysical Observatory,Cambridge Mass.

GUIER, W.H. & NEWTON, R.R. 1965. The Earth's Gravitational Field Deduced from the Doppler Tracking of Five Satellites. *J.geophys.Res.* 70(18),4613-4626.

JOHNSON, T.S., PLOTKIN, H.H. & SPADIN, P.L. 1967. A Laser Satellite Ranging System, 1, Experiment Description. *IEEE J.Quantum Electron.* QE-3(11),435-439.

KOLENKIEWICZ, R., SMITH, D.E. & DUNN, P.J. 1973. Polar Motion and Earth Tides from Beacon Explorer C. *First International Symposium,Artificial Satellites for Geodesy & Geodynamics*,Athens.

KOZAI, Y. 1965. Effects of the Tidal Deformation of the Earth on the Motion of Close Earth Satellites. *Publ.astron.Soc.Japan* 17,395-402.

LAMBECK, K. & CAZENAVE, A. 1973. Fluid Tidal Effects on Satellite Orbits and Other Temporal Variations in the Geopotential. *Bull.* 7,Groupe Recherches de Geodesie Spatiale,Paris.

LUNDQUIST, C.A. & VEIS, G. (Ed.) 1966. Geodetic Parameters for a 1966 Smithsonian Institution Standard Earth, Vol. 1. *Spec.Rep.* 200,Smithsonian Astrophysical Observatory, Cambridge Mass.

MARTIN, C.F. & ROY, N.A. 1972. An Error Model for the SAO 1969 Standard Earth. In HENRIKSEN, S.W., MANCINI, A & CHOVITZ, B.H. (ed.). "The Use of Artificial Satellites for Geodesy". *Geophys.Monograph* 15,American Geophysical Union,Washington DC,161-167.

MERSON, R.H. 1961. The Motion of a Satellite in an Axi-Symmetric Gravitational Field. *Geophys.J. R.astr.Soc.* 4,17-52.

MUNK, W.H. & MACDONALD, G.J.F. 1960. *The Rotation of the Earth.* Cambridge University Press,London.

MUSEN, P. 1973. A Semi-Analytical Method of Computation of Oceanic Tidal Perturbations in the Motion of Artificial Satellites. *Rep. X*-590-73-190,Goddard Space Flight Center,Greenbelt Md.

MUSEN, P. & FELSENTREGER, T. 1973. On the Determination of the Long Period Tidal Perturbations in the Elements of Artificial Earth Satellites. *Celestial Mechanics* 7,256-279.

SMITH, D.E., KOLENKIEWICZ, R. & DUNN, P.J. 1972a. Geodetic Studies by Laser Ranging to Satellites. In HENRIKSEN, S.W., MANCINI, A. & CHOVITZ, B.H. (ed.). "The Use of Artificial Satellites for Geodesy". *Geophys.Monograph* 15,American Geophysical Union,Washington DC,187-196.

SMITH, D.E., KOLENKIEWICZ, R., DUNN, P.J., PLOTKIN, H.H. & JOHNSON, T.S. 1972b. Polar Motion from Laser Tracking of Artificial Satellites. *Science* 178,405-6.

SMITH, D.E., KOLENKIEWICZ, R. & DUNN, P.J. 1973. A Determination of the Earth Tidal Amplitude and Phase from the Orbital Perturbations of the Beacon Explorer C Spacecraft. *Nature* 244, 498.

SMITH, D.E. & VONBUN, F.O. 1973. The San Andreas Fault Experiment. *24th Congress,International Astronautical Federation*,Baku.

9. Discussion *

GUBBAY: You have listed the longitude of the adjusted stations to a thousandth of an arcsecond. I wonder how well you know systematic errors and how well you can hold down the measurement errors to astronomical position?

DUNN: The expression of the results to 0.001 arcseconds may be optimistic. Your question regarding this is interesting. We claim that the absolute time co-ordinate is irrelevant to baseline consistency monitoring and we are happy to have incestuous time reference systems common to both lasers, in order to monitor baselines on a regular basis. There are other ways of getting absolute values of errors in the rotation rate of the Earth. I haven't addressed these problems in this particular presentation because our attempts to do so would have been frustrated by lack of data. The paper itself addresses the problem of monitoring the Earth's rotation rate.

WALCOTT: What is the future of satellite laser ranging in view of the sensitivity to weather, the very high cost of installation as compared with electronic distancing?

DUNN: Among the electronic systems, the most competetive is VLBI. One advantage of the laser system is that the results are obtained very quickly. To obtain a range from a laser return is a relatively simple technique, and we can obtain a 6 hour orbit just a few minutes after the last results have come in, which makes the technique very useful for quasi-real time observations for polar motion and earthquake prediction. So one practical advantage of laser ranging is very quick measurement capability compared with the more complex technique of VLBI which requires complicated software for searching for fringes and producing the time delay and fringe rate measurements.

WALCOTT: It seems to me to be very unreliable. How many days was the Seneca-Goddard experiment washed out by the weather?

DUNN: Too many. The returns in the California experiment are much better. During the SAFE experiment, we plan to return to the same location every year to monitor the change in the baseline length. We will try to get started earlier in the fall to use the better weather.

MUELLER: Referring to the slide on the Earth tide effect; does the solid line represent the values for some model and the dots the observations?

DUNN: Yes; the solid curve represents the simple second degree model of the disturbing potential of the sun and the moon through its effect on the inclination of BE-C as an Earth tide. The values fitted were the amplitude of the curve and indirectly, the phase of the curve, as we concentrated the effect into two parameters.

MUELLER: The distribution of the dots is poor.

DUNN: Yes; although there are two peaks and three well defined valleys, and though areas are sparse, in the critical areas of the peaks and the valleys, good agreement was obtained.

RAPP: Did you run the baseline experiment with different gravity models and if so what was the difference of baseline lengths with different models?

DUNN: I do not have exact figures; but up to week before last, there was no model that gave better results than GEM 1. We find that different GEM models give different fits up to ±3 m.

RAPP: I don't understand your statement that you are not concerned about length.

DUNN: Absolute length is tied to GM; we are concerned with relative length measurements.

RAPP: I'd like to know how the gravity model affects the length.

DUNN: We'd like to know ourselves. The gravity model adopted influences the consistency of the results in the precision to which one can monitor changes in baselines. We usually obtain worse consistency in the baselines with gravity models generated outside Goddard (Space Flight Center).

STOLZ: Why do you calculate only changes in latitude? Can you be sure that you have removed the effects of the other parameters?

DUNN: We claim to have solved for the tidal parameters and geopotential resonance terms which can affect our latitude measurements.

STOLZ: You assume the values obtained are error free?

DUNN: We assume the form of the tidal model is error free. The value of the Love number k_2 is an adjusted parameter and is quite controversial. We have claimed for k a precision which is related to the value of the sigma in amplitude of the Earth tide perturbation to inclination. As the noise level of our data about the BIH polar motion curve is 138 cm over 18 months, it does suggest that our modeling is adequate.

---

* Paper presented by P.J. DUNN

ONG, K. M.
Tracking and Orbit Determination Section
Jet Propulsion Laboratory
California Institute of Technology
Pasadena, California
UNITED STATES OF AMERICA

Proc.Symposium on Earth's Gravitational Field & Secular Variations in Position (1973),315-327.

3-D MULTILATERATION FOR MEASUREMENT OF EARTH CRUSTAL DEFORMATION AND NETWORK DENSIFICATION*

ABSTRACT

This paper presents a discussion of how range and range-difference data types can enable precise three dimensional measurement of ground station positions and the position of an artificial signal source, without explicit dependence upon the signal source trajectory.

Previous analysis of range only multilateration has shown a capability of determining relative station locations with 1 cm accuracy given ranging accuracy of a few centimeters. Such ranging accuracy could be obtained by either laser or possibly by radio methods. Because all-weather operation is so desirable, a radio implementation is the preferred mode.

Another possible radio approach is range-difference multilateration. Very Long Baseline Interferometry (VLBI) has demonstrated few cm range-difference measurements using cross correlation techniques. The analysis of VLBI multilateration is not yet as well developed as the range only multilateration; however, preliminary results indicate comparable few cm performance potential.

Although a multilateration system is capable of stand-alone operation, the need for intercontinental geodetic measurements would require a high flying earth orbiting satellite with its associated disadvantage of substantial costs, particularly when data are needed over many years.

A more effective strategy is to combine the multilateration approach with a VLBI system using natural radio sources. The VLBI methods would provide a coarse grid of three dimensional benchmark locations on a regional and global scale. Multilateration stations would then occupy these coarse grid locations and provide a means for highly portable, relatively low cost units to then densify networks on a regional and local scale.

Because a multilateration approach can make use of strong artificial radio sources, it makes possible the use of relatively low cost, highly mobile stations. Such mobile stations are virtually essential for three dimensional surveying in heavily urbanized areas or in rugged terrain. Accurate three dimensional station location determinations on a fine scale are likely to play an important role in the search for earthquake premonitory phenomena. For example, Southern California (like many other regions of the world) is tectonically very complex with faulting and possible earthquake premonitory crustal uplift occurring over regions of a few km. Therefore, there is an obvious need for dense three dimensional network establishment for which multilateration techniques offer great promise.

This paper presents the results of one phase of research carried out at the Jet Propulsion Laboratory, California Institute of Technology, under Contract No.NAS 7-100, sponsored by the National Aeronautics and Space Administration.

1. Introduction

It is of great worldwide geophysical interest to develop a global tectonic monitoring system which can accurately measure secular variations in three-dimensional position on the earth's crust. Such a monitoring system, if accurate to the centimetre level, will no doubt revolutionalise the field of geodesy, with no less dramatic impact on geodynamic and seismological research such as the search for earthquake premonitory phenomena, the test of continental drift and plate tectonic theories etc.

Through the advent of new aerospace and electronic technology, together with the new concepts of systems approach to large-scale problems, it is now believed that setting up such a global tectonic monitoring system is a distinct possibility. Specifically, in this paper, geometric techniques (multilateration) will be outlined which will enable the relative three-dimensional coordinates of a group of ground stations to be determined using electronic techniques for slant range or range-difference measurements to an artificial satellite or signal bearing vehicle in space. Another technique (Very Long Baseline Interferometry or VLBI) which employs natural radio sources is described by MacDORAN (1973). Both of these techniques have the potential of determining station coordinates to a few centimeters.

Even though historically the techniques of multilateration and of VLBI have been pursued separately, it has recently been realised that the two techniques can be combined into a network densification system in a cost-effective manner. Such a system, which may be called VLBI Multilateration, will operate with a high flying aircraft emitting artificial radio sources, simultaneously received at several ground stations. The processing of these signals will then determine the relative station coordinates in a combined solution. These coordinates may then be tied to the inertial coordinates determined from VLBI measurements established on a global scale. It is the merging of these two techniques which will make the establishment of a global tectonic monitoring system a practical possibility.

In the following sections, range-only and range-difference multilateration concepts will be discussed. Justification of the required accuracy will be provided for a range-only system using laser ranging stations. The same system can of course be operated in a radio ranging mode implementation, at the sacrifice of some precision, but with the advantage of all-weather operation.

The other radio mode implementation, namely, range-difference multilateration, makes use of differential time of arrival measurements or interferometrically derived values for the range-difference. Such a system to date is not as well developed as the range-only system, but preliminary analysis shows that it also has promise for centimeter level position determination if properly designed.

2. Range-Only Multilateration

A laser ranging multilateration system based on range-only multilateration has been designed at the Jet Propulsion Laboratory and reported in ESCOBAL et al (1973a). This section reviews the systems analysis and section 3 the hardware implementation aspects of that work.

Suppose we are given a number of ground stations simultaneously ranging to an earth orbiting satellite. It proves to be convenient to work in a relative coordinate system as indicated in figure 1, where station coordinates are denoted by $(0, 0, 0)$, $(X_2, 0, 0)$, $(X_3, Y_3, 0)$ and (X_j, Y_j, Z_j), $j = 4, 5, \ldots 1$, and the vehicle trajectory coordinates are denoted by (x_n, y_n, z_n),

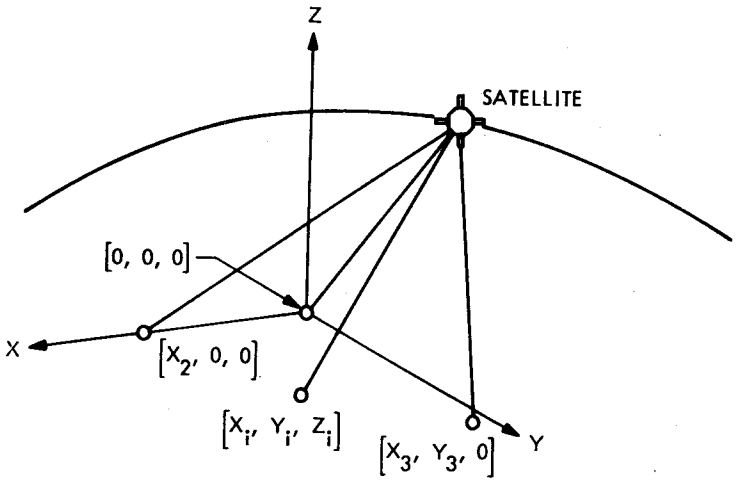

Figure 1. Adopted geometric coordinate system.

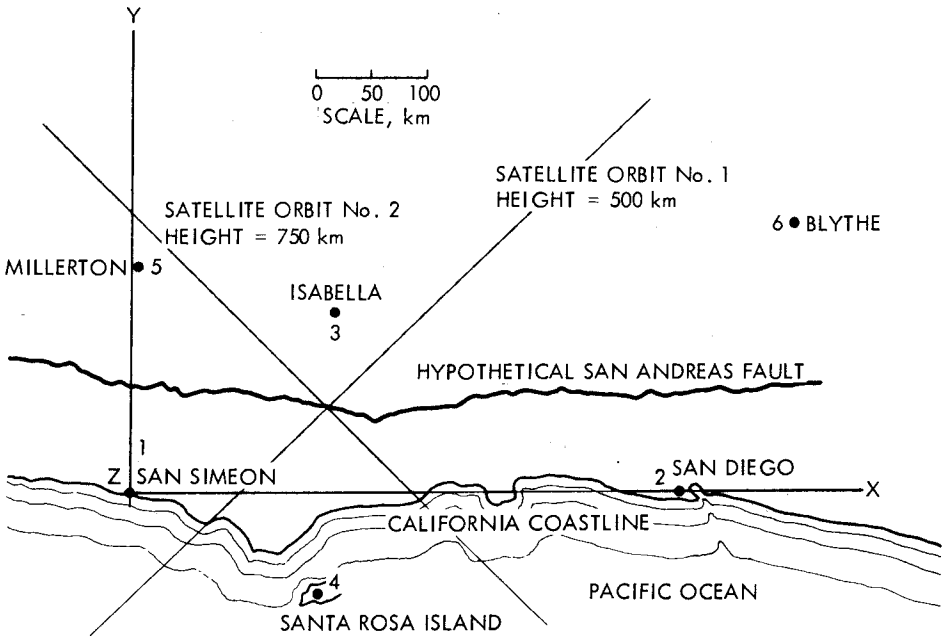

Figure 2. A six station multilateration network along the San Andreas Fault in Southern California.

$n = 1, 2, \ldots N$. Let ρ_{in} be the slant range from the i-th station to the n-th trajectory point. Furthermore, let all the non-vanishing station coordinates be collectively denoted by the vector $\vec{S}$:

$$\vec{S} \equiv (X_2, X_3, Y_3, X_4, Y_4, Z_4, \ldots Z_1)$$

and all the measurement date ρ_{in} be denoted by the data vector $\vec{\rho}$

$$\vec{\rho} \equiv \left\{ \rho_{in} \mid i = 1, 2, \ldots 1; \quad n = 1, 2, \ldots N \right\}$$

It is shown in ESCOBAL et al (1973) that the following "multilateration equations" can be formulated for the determination of $\vec{S}$ from the observed ranges:

$$F_{jn}(\vec{S}, \vec{\rho}) = X_j^2 + Y_j^2 + Z_j^2 - 2x_n X_j - 2y_n Y_j - 2z_n Z_j - \delta_{jn} = 0 \qquad (1)$$

$$j = 4, 5, 6, \ldots 1, \qquad n = 1, 2, 3, \ldots N$$

where the satellite coordinates (x_n, y_n, z_n) can be expressed in terms of station locations and the data by the following equations:

$$x_n = (X_2^2 - \delta_{2n})/(2X_2)$$

$$Y_n = \left(X_3^2 + Y_3^2 - \delta_{3n} - \frac{X_3}{X_2}(X_2^2 - \delta_{2n})\right)/(2Y_3) \qquad (2)$$

$$z_n = \left(\rho_{1n}^2 - x_n^2 - y_n^2\right)^{\frac{1}{2}}$$

and

$$\delta_{in} \equiv \rho_{in}^2 - \rho_{1n}^2$$

Solution of equation system 1 in the appropriate least squares sense will then yield the required station coordinates which will in turn determine the satellite positions through equations 2.

The minimum number of stations required in a range only multilateration system is four for which at least six range points must be taken. If the four stations lie on the same plane, it turns out that the solution to the multilateration equations is degenerate; i.e. a unique set of station coordinates cannot be obtained no matter how many range points are taken. Although in a real-world situation, stations will not exactly lie on a plane, however, a nearly coplanar configuration will lead to high sensitivity of station coordinate errors with respect to ranging errors. Such difficulties associated with station coplanarity can be overcome only if 6 or more stations are used. In addition to degeneracies due to the placement of stations, there is also the class of degeneracies due to orbit selections. The general mathematical problems of singularities encountered in ranging systems has been discussed by ESCOBAL et al (1973b), BLAHA (1971) and ONG & ESCOBAL, (1972).

To ascertain the accuracy of the range only multilateration system under measurement uncertanties, a number of hypothetical configurations involving baselines of local to intercontinental magnitudes have been simulated. Figure 2 shows the location of six hypothetical stations placed along a region of great tectonic interest, i.e. the Southern California portion of the San Andreas fault. Two

circular-orbit satellite passes, whose projections on the XY plane of the adopted coordinate system are as indicated, were used in the simulation. The altitudes of the two satellites are approximately 500 km and 750 km respectively. Fifty points from each orbital arc were generated with X-coordinates varying from San Simeon to San Diego. Assuming ranging errors to be Gaussian distributed with zero mean and 1 cm (1σ), the standard deviations of the computed station coordinates from solving the multilateration equations are displayed in table 1.

TABLE 1

Errors in Station Coordinates for
Southern California Stations Assuming
1 cm Normal Random Errors in Ranging

Station	σ_x (cm)	σ_y (cm)	σ_z (cm)
1. San Simeon	/	/	/
2. San Diego	2.06	/	/
3. Isabella	1.11	3.56	/
4. Santa Rosa I	1.31	1.76	0.99
5. Millerton	1.14	4.16	0.71
6. Blythe	2.64	4.74	1.18

Another hypothetical configuration suitable for the study of continental drift and global plate tectonics is depicted in figure 2. Again a total of 100 points from two satellites at altitudes of 6000 and 10000 km were employed. With ranging errors again assumed to be Gaussian distributed with zero mean and 1 cm (1σ), the errors in calculated station coordinates are given in Table 2.

TABLE 2

Errors in Station Coordinates for the
Intercontinental Configuration Assuming
1 cm Normal Random Error in Ranging

Station	σ_x (cm)	σ_y (cm)	σ_z (cm)
1. Mexico City	/	/	/
2. London	1.87	/	/
3. New York	1.43	1.20	/
4. Freetown	2.08	2.81	1.45
5. Reykjavik	2.01	1.00	1.33
6. Caracas	0.09	1.64	0.51

3. Laser Implementation of 3-D Multilateration

The 3-D Multilateration technique can be implemented through use of a number of ground stations which simultaneously transmit laser pulses to compact reflectors on a moving vehicle, e.g. an airplane or a satellite. Each station evaluates station-to-vehicle range by measuring the time interval between transmission of the original pulse and reception of the reflected pulse. Simultaneous range measurements are then processed so as to yield relative station locations in three dimensions.

The hardware subsystem for measuring station-vehicle ranges is identical for all station configurations. In order to attain high accuracy range measurements, the subsystem utilises a new type of pulsed laser. This laser is a mode-locked, Q-spoiled ruby laser, and has the capability of emitting light pulses of very short duration (0.1 ns or less). The subsystem employs a tracking mount to aim transmitting and receiving telescopes at the vehicle. A measurement is made of the time required for a laser pulse to make a round-trip flight from the station to the vehicle-borne retroreflector. This time, measured with a resolution of 0.1 ns, is used in conjunction with an atmospheric model to calculate the range to the vehicle.

Each ground station also contains an X-Y tracking mount for steering the two telescopes, a small computer to direct the tracking mount toward the satellite, timing ciruitry, recording equipment, and power supplies. In order to satisfy the requirement for "simultaneous" ranging, the clocks at each station must be synchronised to 3 μs; such synchronisation is easily achievable using low-cost components. Synchronisation of laser firing to 1 ms is adequate and well within the state of the art; variations of laser firing within this range are compensated for by time-tagging range measurements, and interpolating between successive measurements so as to obtain effective simultaneity among stations.

It is emphasised that the system errors caused by the satellite, Earth constants, and orbital perturbations do *not* enter into the process. In fact, since the proposed techniques are independent of the location of the retroreflector, the only error sources which enter into the range measurement are:

1) Bias error due to atmospheric delay
2) Random error due to atmospheric turbulence
3) Random equipment measurement error
4) Equipment bias error

A demonstration ranging system was assembled using commercially available components in order to evaluate the measurement errors produced by current hardware. This system simulated a long distance ranging system over short path lengths by using attenuated return signals. The results obtained with this system show that hardware-related errors in range measurement can be made acceptably small, typically less than 3 cm. Future systems can be expected to operate at satellite distances with 1-cm ranging accuracy.

Figure 4 indicates the schematic of hardware components in the system. These can be assembled from commercially available components, packaged compactly, and placed in a transportable van as indicated in figure 5.

4. Range Difference Multilateration

The laser ranging multilateration system discussed in section 3 suffers from one great drawback in

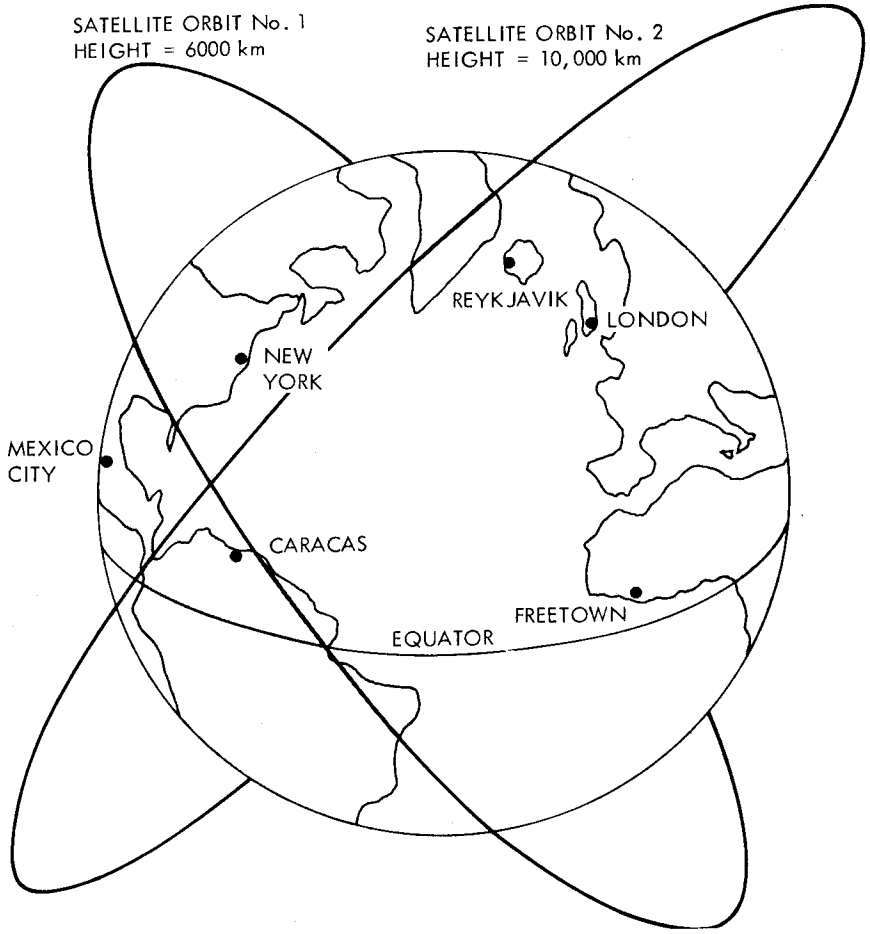

Figure 3. A global multilateration system

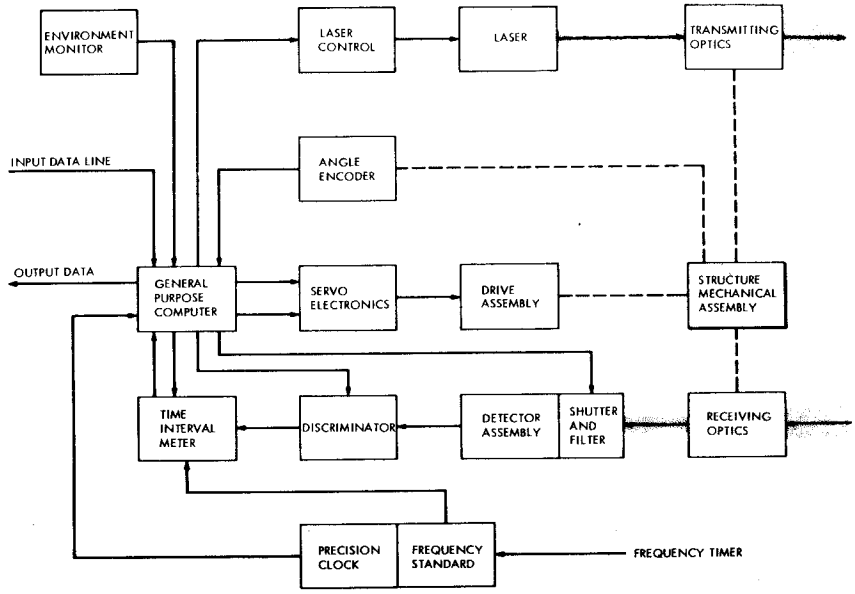

Figure 4. Schematic of laser ranging station hardware

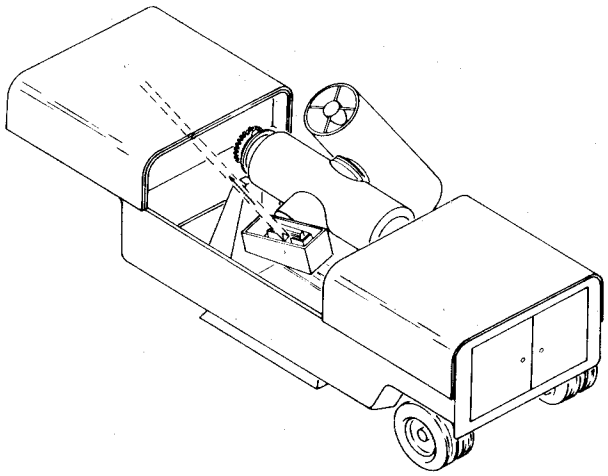

Figure 5. Artist's conception of laser tracking station

that simultaneous observation from 4 to 6 stations to an orbiting vehicle may be easily weathered out. On the other hand, a radio (radar) implementation of range only multilateration, while it has the distinct advantage of all-weather operation capability, can not be expected to yield the same degree of accuracy as laser ranging insofar as present-day technology is concerned. There is, however, another kind of data type, i.e. range differences, which can be measured via radio interferometric techniques and yet has the potential of centimeter-level accuracy comparable to the laser range data type. For a discussion of the instrumentation and methodology for measuring range differences via radio interferometry, the reader is referred to THOMAS (1973). In the present section, only the theoretical foundation relative to such a "range-difference multilateration" technique is discussed. A complete systems study of this problem comparable to the laser ranging technique is presently under way.

The standard relative, station-based coordinate system of figure 1 is again adopted for this analysis. The observables of the system are the differences in slant ranges between station 1 (the origin) and another (say the i-th) station to the vehicle:

$$\varepsilon_{in} \equiv \rho_{in} - \rho_{1n}$$

The problem is to determine the (3I - 6) - component station coordinate vector:

$$\vec{S} = (X_2, X_3, Y_3, X_4, Y_4, Z_4, \ldots X_I, Y_I, Z_I)$$

in terms of the data vector $\vec{\varepsilon}$:

$$\vec{\varepsilon} = \left\{ \varepsilon_{in} \mid i = 2, 3, 4, \ldots I; \quad n = 1, 2, \ldots N \right\}$$

This mathematical problem has been solved in ESCOBAL et al (1973), where it was shown that at least 5 stations are needed for unique determination of $\vec{S}$, and that at least 6 stations will be required in the case of coplanar configurations. The components of $\vec{S}$ are determined by solving the following

systems of equations:

$$F_{jn}(\vec{S}, \vec{\varepsilon}) = X_j^2 + Y_j^2 + Z_j^2 - 2x_n X_j - 2y_n Y_j - 2z_n Z_j - \varepsilon_{jn}^2 - 2\varepsilon_{jn} u_n = 0$$

$$j = 5, 6, \ldots J \qquad (3)$$

$$n = 1, 2, \ldots N$$

where x_n, y_n, z_n can be expressed as functions of the station coordinates and the data vector $\vec{\varepsilon}$ by means of the following equations:

$$x_n = A_{1n} + B_{1n} u_n,$$

$$y_n = A_{2n} + B_{2n} u_n,$$

$$z_n = \left(u_n^2 - x_n^2 - y_n^2\right)^{\frac{1}{2}}, \text{ always positive by definition,}$$

$$A_{1n} = \left(X_2^2 - \varepsilon_{2n}^2\right) / \left(2X_2\right)$$

$$B_{1n} = -\varepsilon_{2n}/X_2$$

$$A_2 = \left(X_3^2 + Y_3^2 - \varepsilon_{3n}^2 - 2X_3 A_{1n}\right) / \left(2Y_3\right)$$

$$B_{2n} = -\left(X_3 B_{1n} + \varepsilon_{3n}\right) / Y_3$$

The quantities u_n are the ranges from station 1 to each of the vehicle trajectory points. They are determined from the coordinates of the first 4 stations by the following equations:

$$\Gamma_{1n} u_n^2 + \Gamma_{2n} u_n + \Gamma_{3n} = 0 \qquad (4)$$

where

$$\Gamma_{1n} = B_{3n}^2 - 4Z_4^2\left(1 - B_{1n}^2 - B_{2n}^2\right)$$

$$\Gamma_{2n} = 2\left[A_{3n} B_{3n} + 4Z_4^2\left(A_{1n} B_{1n} + A_{2n} B_{2n}\right)\right]$$

$$\Gamma_{3n} = A_{3n}^2 + 4Z_4^2\left(A_{1n}^2 + A_{2n}^2\right)$$

$$A_{3n} = X_4^2 + Y_4^2 + Z_4^2 - 2\left(A_{1n} X_4 + A_{2n} Y_4\right) - \varepsilon_{4n}^2$$

$$B_{3n} = -2\left(B_{1n} X_4 + B_{2n} Y_4 + \varepsilon_{4n}\right)$$

Note that u_n is determined from a quadratic equation. In the coplanar case ($Z_4 = 0$), the left-hand side of equation 4 turns out to be a perfect square and hence u_n is uniquely determined. In general when $Z_4 \neq 0$, there may exist two physically acceptable solutions to u_n. The choice between the 2 solutions can be made by using approximate, a-priori knowledge of the ranges u_n, or by bringing in

additional stations.

The above system of equations can be solved by means of Newton-Raphson iteration in the appropriate least-squares sense. Preliminary analysis indicates that error magnification factors, i.e., the ratio of the errors (standard deviations) occasioned in station coordinates to the error assumed for the data, for suitably chosen configurations are quite small. Since this study has not been completed at the time of writing, such results will be left for a future paper.

5. Network Densification by Means of VLBI Multilateration

The range only and range difference multilateration systems considered in the previous sections are capable of stand-alone operations, i.e., it is not necessary to provide additional information other than the fundamental data types (range or range difference). However, for intercontinental geodetic measurements, high flying earth-orbiting satellites with varying altitudes will be required in order to yield respectable accuracy in the solution. Such high flying satellites and their associated equipments will incur substantial costs since data will be required over many years for the tectonic monitoring program. It is thus not cost-effective to use multilateration for intercontinental measurements.

Another difficulty which may be encountered in the use of multilateration techniques for large scale tectonic monitoring may be traced to the relative nature of the coordinate system adopted for such analysis. It can be readily seen that the station coordinate vector $\vec{S}$ will remain invariant if the whole ensemble of multilateration stations undergoes *rigid* displacement or rotation. Geophysically this means that if all the stations lie on the same rigid tectonic plate, then motion of the plate itself with respect to the rest of the earth cannot be detected through multilateration. It is therefore advantageous to be able to tie these relative coordinates determined by multilateration to a more inertial frame of reference, perhaps independently established by other techniques. The technique of Very Long Baseline Interferometry (VLBI), which has the potential of determining accurately three-dimensional coordinates of baselines of arbitrary magnitudes in a coordinate reference frame defined by extragalactic radio sources, appears to satisfy these needs (MacDORAN 1973). However, because the radio flux density of natural sources (quasars) are of the order of magnitude of 10^{-26} watts/m^2/Hz when received at the surface of the earth, it takes highly sophisticated electronic equipments to receive and record such signals, making even a portable VLBI station difficult to be moved from place to place. (Conventional VLBI stations are usually permanent tracking stations such as the Goldstone and the Canberra Radio Tracking Stations.) It is, nevertheless, important to be able to determine 3-dimensional station locations on a fine scale in a tectonically complex region such as Southern California. It would therefore seem extremely desirable to have available a system making use of highly portable equipment for the purpose of regional and local tectonic monitoring augmenting the coarse-grid VLBI network. Range difference multilateration with low-flying vehicle-borne artificial signal sources appears to meet these requirements.

A simple calculation shows that a one-watt transmitter broadcasting random noise over a 100 MHz bandwidth received at a distance of 100 km will exhibit a radio flux density of approximately 10^{-19} watts/m^2/Hz. This improvement of 7 orders of magnitude relative to a natural radio source can be exploited in the form of a vast reduction in the sophistication of the radio interferometer stations and a corresponding increase in mobility. The range difference multilateration technique as discussed in the previous section can be used in conjunction with these small portable interferometers for densifying the regional or local geodetic networks.

Thus, conceptually, a global tectonic monitoring system works as following. First, intercontinental bechmarks are established via conventional (natural source) VLBI techniques such as Project ARIES presently carried out at the Jet Propulsion Laboratory. This will enable the establishment of a coarse grid network in a quasi-inertial reference frame defined by the extragalactic objects. Range difference multilateration stations (or laser ranging stations if applicable) will then occupy these sites. Each of these sites will then serve as the origin of a denser network of multi-lateration stations covering the local region. Low flying vehicles bearing laser retroflectors or radio noise transmitters are then used in conjunction with the multi-lateration stations. Simultaneous determination of the relative station and vehicle coordinates is then possible through the use of the developed analytic techniques. Such a network densification scheme is illustrated in figures 6a and 6b.

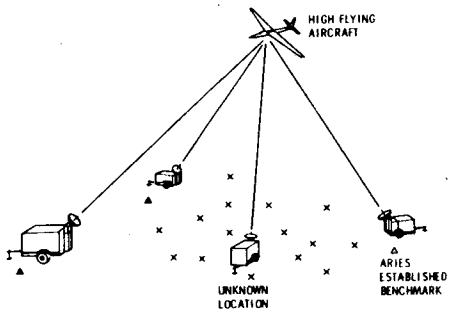

Figure 6(a). Network densification by 3-D Multilateration

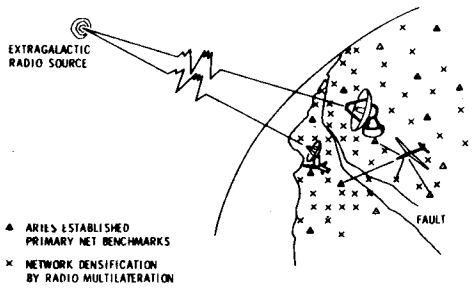

Figure 6(b). VLBI Multilateration Earthquake Monitoring System

6. Summary

In this paper, analytical methods of range only and range difference multilateration for relative 3-dimensional station location determination have been discussed. Implementation of range only multilateration through the use of laser ranging stations has also been outlined. Because of the desirability of all-weather operation capability, a radio mode implementation is preferred.

This can be accomplished through radio ranging, or through interferometric range difference multilateration. The latter technique makes use of low-flying artificial signal bearing vehicles and small diameter dish antennae for ground reception. This makes such a system highly mobile and thus suitable for network densification purposes in tectonically complex regions such as Southern California. Dense local networks, combined with a global, coarse-grid network established by natural source VLBI in a global reference frame will enable the worldwide monitoring of tectonic events and the detection of secular variations in position on earth.

7. Acknowledgment

The author wishes to thank P. R. Escobal, H. F. Fliegel, R. M. Jaffe, P. M. Muller, M. S. Shumate and O. H. von Roos for their contributions to the 3-D Multilateration project, and P. F. MacDoran and J. B. Thomas for their advice on the concepts of VLBI systems and network densigifcation.

8. References

BLAHA, G. 1971. "Investigation of Critical Configurations for Fundamental Range Networks", Ohio State University Dissertation, and references cited therein.

ESCOBAL, P.R., ONG, K.M., VON ROOS, O.H., SHUMATE, M.S., JAFFE, R.M., FLIEGEL, H.F. & MULLER, P.M. 1973a. "3-D Multilateration: A Precision Geodetic Measurement System". *NASA Technical Memorandum* 33-605, Jet Propulsion Laboratory, Pasadena California.

ESCOBAL, P.R., ONG, K.M. & VON ROOS, O.H. 1973b. "Range Difference Multilateration for Obtaining Precision Geodetic and Trajectory Measurements", submitted to *Astronautica Acta*.

MacDORAN, P.F. November 1973. "Very Long Baseline Interferometry (VLBI) Applications to Secular Geodynamics and Earth Strain Measurement", presented at the International Symposium on Earth's Gravitational Field and Secular Variations in Position, Sydney, Australia (This volume,380-395).

ONG, K.M. & ESCOBAL, P.R. 1972. "Multilateration: A Nondegenerate Method of Obtaining Station Coordinates and Satellite Ephemerides", submitted to *Journal of Astronautical Sciences*.

THOMAS, J.B. August 1973. "An Analysis of Long Baseline Radio Interferometry, Part III". *Jet Propulsion Laboratory Technical Report* 32-1526, Vol.XXVI.

9. Discussion

STOLZ: Do you see any application of your technique to lunar laser ranging?

ONG: We have not analyzed the multilateration geometry for lunar laser ranging. I think it is possible that the orbit of the moon could serve as the positions in space for multilateration. It might cause certain problems in that we have only one pass of a satellite (i.e., the moon). There might be an accuracy problem involved which could degrade the accuracy of the station locations. You should have sufficient separation in space co-ordinates to achieve an adequate accuracy.

MUELLER: The obvious problem is that of the weather; to obtain six station simultaneity is almost impossible. We have statistics now about this. For example the (US) National Geodetic Survey global satellite triangulation observed 2,200 events, and they always tried to co-ordinate observations between three, four and five stations if possible. From memory there were less than 25% of the three station events and less than 2% of the four station events.

ONG: Yes, this is a problem, but it should be possible to use the method over small areas with aeroplane type experiments.

MUELLER: In the case of the second method, the problem is one of range differences. I'd like to draw your attention to the work done with geoceivers, using them in an integrated mode and getting range differences. The whole geometry of the adjustment technique and the receiver configuration was thoroughly analyzed by several groups working with geoceivers, most of the work coming from Duane Brown Associates.

DUNN: With the Goddard lasers, very stringent precautions are taken to prevent aircraft flying into laser beams.

ONG: I think the safety precautions taken about laser beams have been over-emphasized. In a study reported in (*Laser Focus* 8,22-27,May 1972), and in our report (*NASA/JPL Technical Memorandum* TM 33-605) which studied the safety problem, it was shown that correct safety measures as to the use of lasers are not difficult to achieve.

ECKHARDT: I would like to answer the question as to whether the multilateration approach can be used with lunar ranging from different sites but not exactly simultaneously. You have the direction of the moon in space from which you can pick up the orbit of the moon.

GUBBAY: I've heard we are measuring position, and keep wondering what we are measuring with respect to; what the prevailing system of reference is. I know we are thinking in terms of complementary techniques but the reference systems are different. How do we fuse all these measurements together? They are liable to small errors. Can these errors be recovered?

ONG: No. The assumption is that VLBI uses an inertial co-ordinate system while multilateration could use a local system on a relative basis. By fine filtering or referencing multilateration networks together with VLBI, it will be possible to provide the global co-ordinates of all stations relative to an inertial reference system. The problem we are looking at now is a very difficult one and might include transformations which would introduce additional error sources. It does not appear likely that these errors can be recovered to the degree of accuracy we are talking about.

GUBBAY: Even with VLBI, you need one position to start with. Where can you start from?

ONG: In defining a co-ordinate system for geodetic applications we are not too interested where the dynamical centre of the Earth is. We are more interested in relative positions and relative motion and relative motion of stations with respect to one another. The search for an "absolute" reference frame is important, but for applications in monitoring changes in position, this is not important. We can therefore start from any convenient station.

PLOTKIN, H.H.
NASA Goddard Space Flight Center
Greenbelt Md 20771
United States of America

Proc.Symposium on Earth's Gravitational Field & Secular Variations in Position (1973),328-346.

LASER TECHNOLOGY FOR HIGH PRECISION SATELLITE TRACKING

ABSTRACT

Fixed and mobile laser ranging stations have been developed to track satellites equipped with retro-reflector arrays. These have operated consistently at data rates of once per second with range precision better than 50 cm, using Q-switched ruby lasers with pulse durations of 20 to 40 nanoseconds. Improvements are being incorporated to improve the precision to 10 cm, and to permit ranging to more distant satellites. These include improved reflector array designs, processing and analysis of the received reflection pulses, and use of sub-nanosecond pulse duration lasers.

1. Text

There are now 7 satellites in near Earth orbit fitted with retroreflectors, commencing with the first in the BE series (figure 1). There are two more such satellites scheduled for launch by the

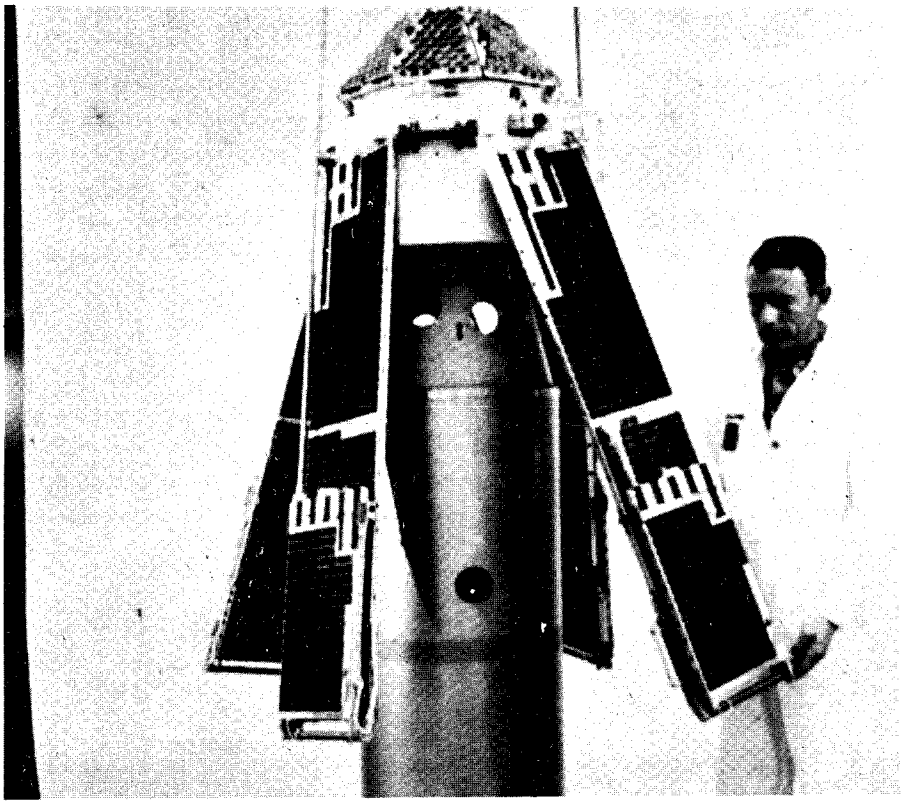

Figure 1. **Beacon-Explorer B. The First Satellite Orbited (October 1964) with Retroreflectors for Laser Tracking** *(Goddard Space Flight Center)*

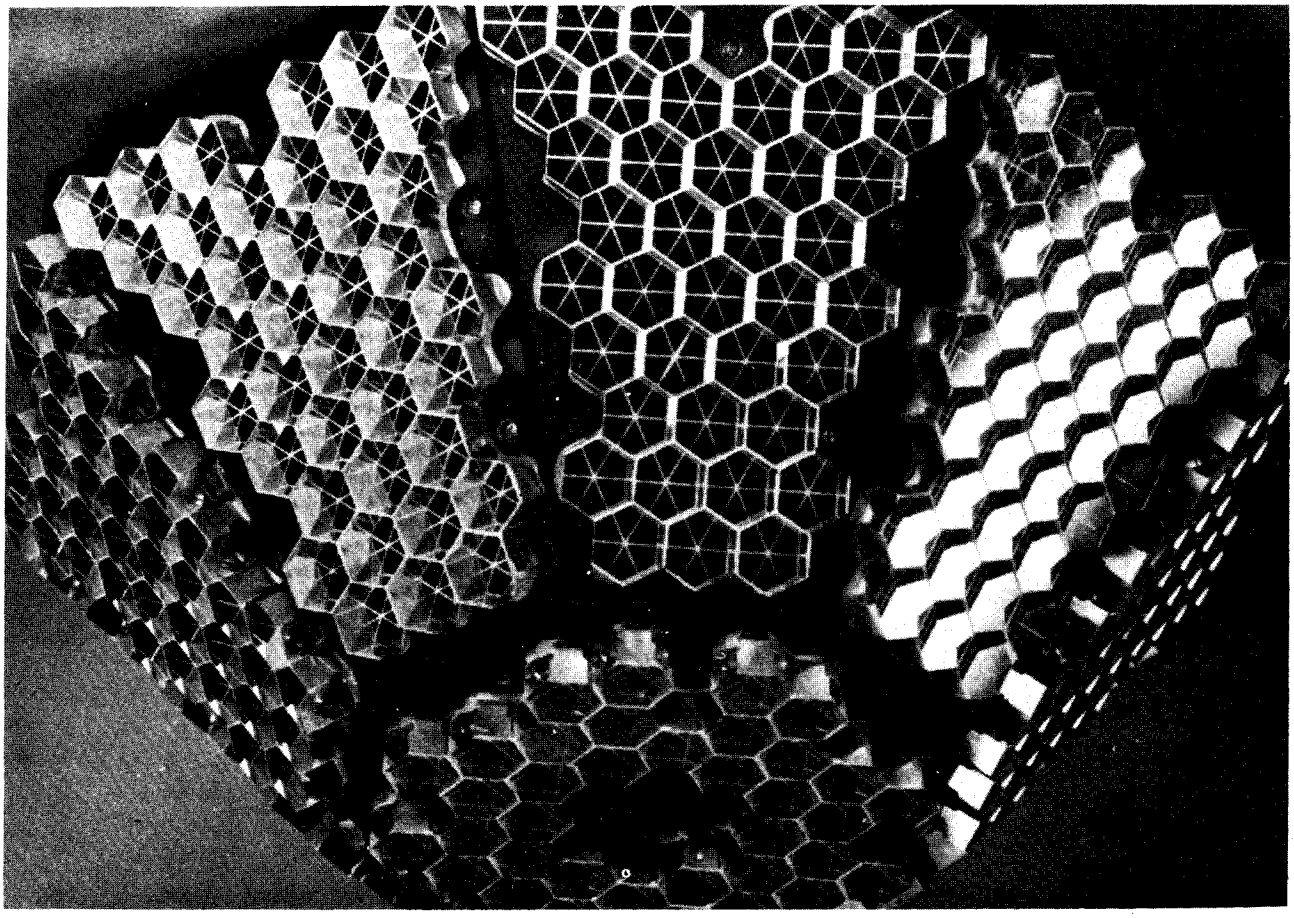

Figure 2. Retroreflector Array on Beacon-Explorer

United States in 1974, and another in 1976. There are large quantities of data that have been taken , with rms scatter in range measurement (and, presumably, accuracy) of ±50 cm.

We are now preparing a new generation of satellite laser trackers which have a precision of ±10 cm. Our plans are to further improve the precision to ±2 cm over several years. We think this can be done , but as users of this data you must understand the source of our confidence in the accuracy, and ultimately draw your own conclusions. The only way I can impart this degree of confidence is to describe the design features of our technique, in more detail than some would like and too rapidly for others.

The retro-reflector array (figure 2) is composed of a number of fused silica corner cubes; these

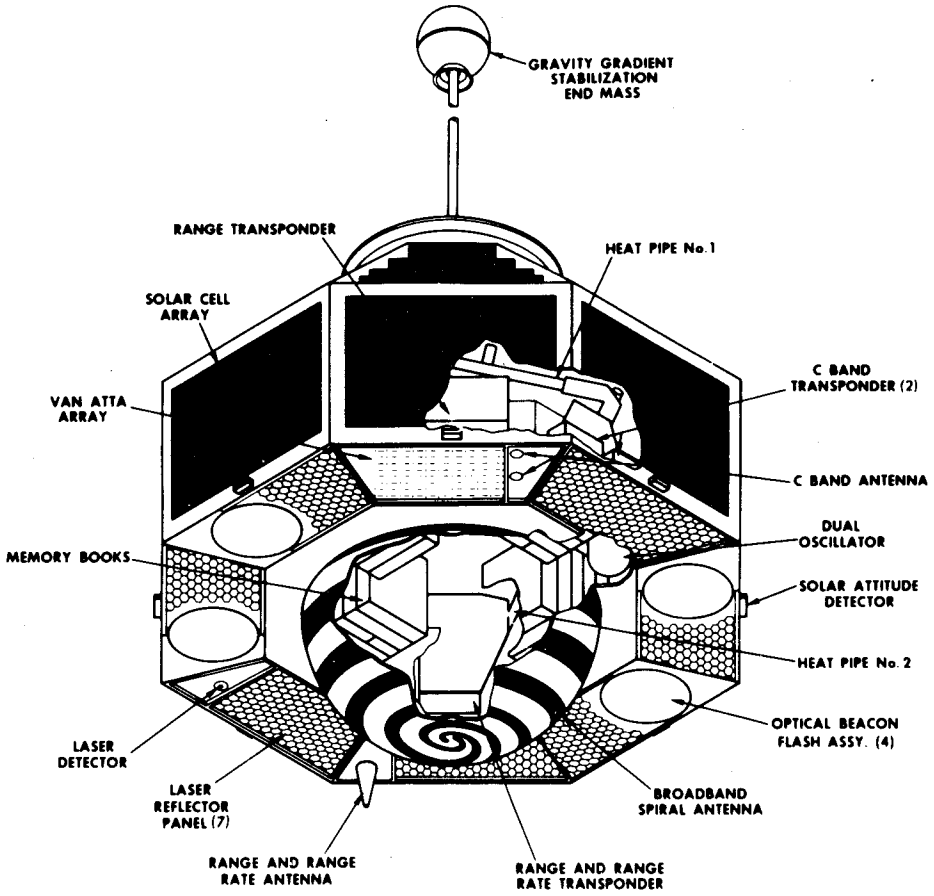

Figure 3. GEOS-B Spacecraft

corner cubes have the property that a beam of light incident on them is reflected directly back towards the transmitter. The Beacon-Explorer (BE) satellites are magnetically stabilized and a pyramid reflecting cap was placed on the north-seeking end of the spacecraft. I am embarrassed to say that this made it particularly useless for observations from Australia. But we have learned from our errors. The GEOS-A and GEOS-B spacecraft (figure 3) which are stabilized by the gravity field gradient, and all our future satellites, will *not* be useless for observations from Australia. In these cases, the retro-reflectors will be mounted on the Earth-viewing surface of the spacecraft, pointing down so that they can be seen from all hemispheres of the Earth.

The signal depends on three terms (figure 4). The *first* term is the incident energy on the reflectors and that depends on the energy which is transmitted, the number of reflectors, the area of the individual reflectors and the divergence of the transmitted beam. The *second* term depends on

CLASSICAL BISTATIC RADAR EQUATION

$$S = \underbrace{\frac{P_T G_T}{4\pi R^2}}_{\text{POWER DENSITY AT TARGET}} \times \underbrace{\frac{\sigma(\alpha)}{4\pi R^2}}_{\text{POWER DENSITY AT RECEIVER PER UNIT POWER AT TARGET}} \times \underbrace{\frac{G_R \lambda^2}{4\pi}}_{\text{EFFECTIVE ANTENNA RECEIVING AREA}}$$

$$G = \left(\frac{\pi D}{\lambda}\right)^2 \quad \text{ANTENNA GAIN}$$

$$\sigma(\alpha) = \frac{4\pi A^2}{\lambda^2} \quad \text{RADAR CROSS SECTION}$$

Figure 4. Classical Bistatic Radar Equation

the area or gain of the individual reflectors because they will determine the spot size of the downward reflected beam. The *third* term is the area of the receiving telescope.

In addition to these terms we also have to remember that when you look at the cube corner at an oblique angle (figure 5), the effective area will be less since there will be a tilt effect. There are also losses in the optics and losses in the atmosphere. Finally, there is also an effect due to the fact that the satellite is moving - a velocity aberration effect. All these effects will affect the design of a satellite.

For instance, we want to look at the satellite at a very low elevation angle so that we get maximum coverage. In order to do that, we have to mount the cube corners at an angle on the surface of a cone and tilt them outward so that we can see them even when the satellite is at a very low elevation angle. We must also mount the cube corner in such a way that the return pulse is spread

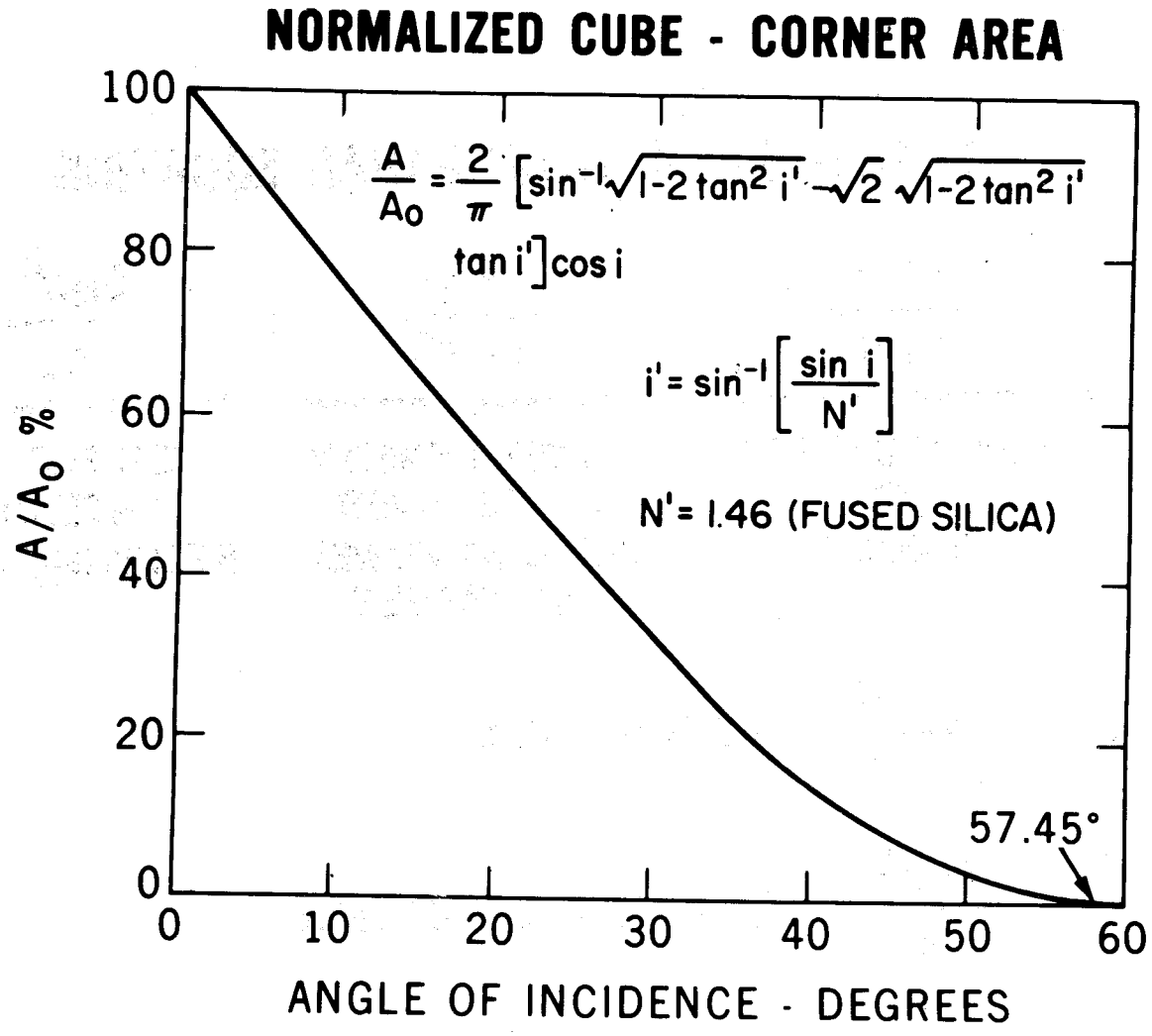

Figure 5. Normalized Cube-Corner Effective Area

in a very well defined manner so that we can measure the range with respect to the centre of mass of the spacecraft. Unless we can measure that range accurately with respect to the centre of gravity, the precision we are going to talk about will be senseless. For these reasons, the reflector arrays on GEOS-C (figure 6) has a well defined geometry and is tilted outward at an angle of 45°.

Now, how large shall the individual cube corners be? That will be decided upon by the velocity aberration. In figure 7, a ray of laser light hits the satellite and gets reflected. But because the satellite is moving with a velocity v, the reflected spot doesn't come back to the source but is displaced. The size of the spot will depend on the diffraction effect at the individual cube corners. The larger the cube corner is, the smaller the spot will be. If the spot is very small, it will miss the transmitter and you will get no signal. If the spot is very large, the energy is spread over a large area and you are making inefficient use of the return signal.

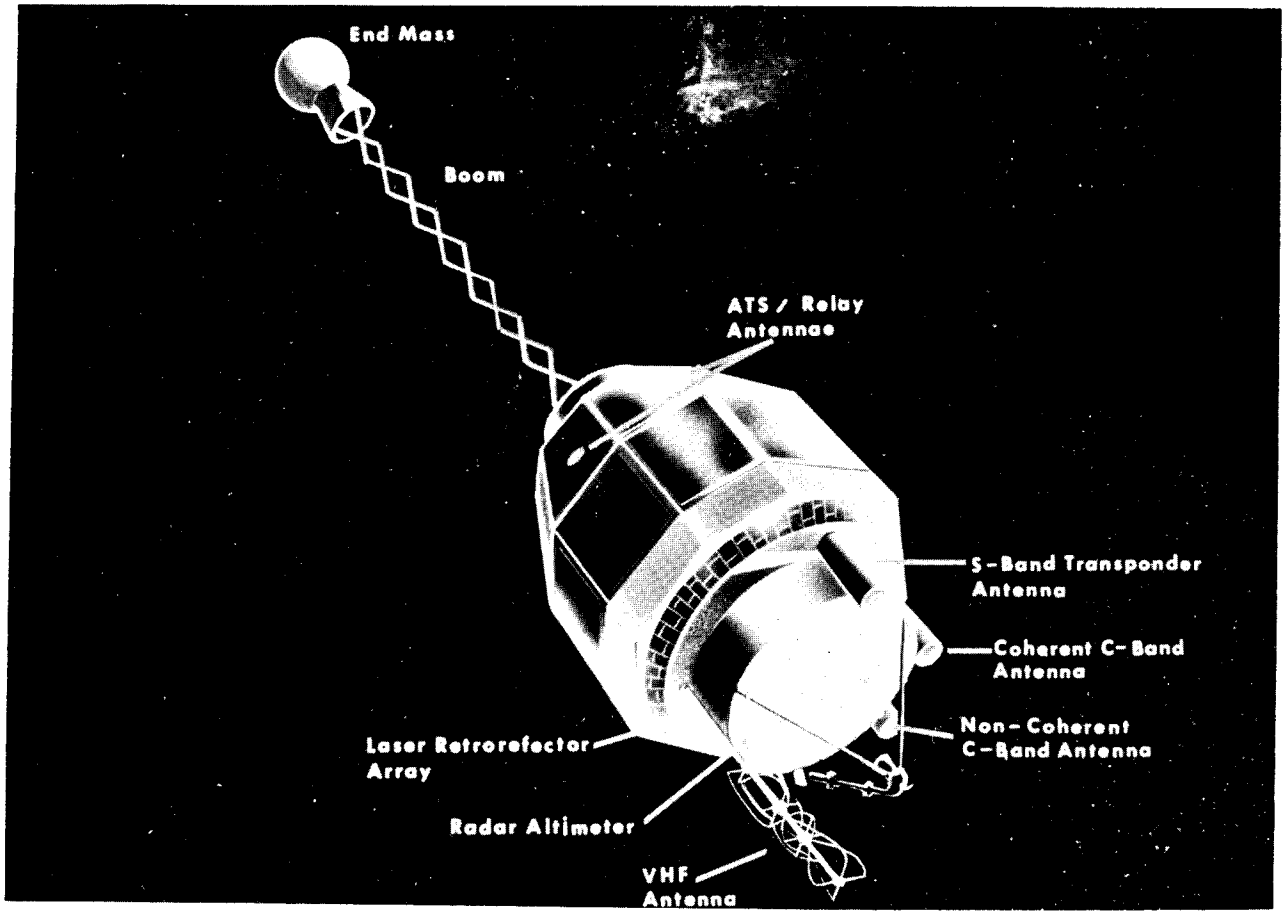

Figure 6. GEOS-C - To be Launched by NASA in 1974

If you look at the spot in detail, the intensity profile of the diffraction pattern is given by a Bessel function and the optimum value is a function of the velocity itself. But the velocity is a function of the satellite altitude (figure 8). For GEOS-C, the optimum cube corner size is about 4 mm in radius. On the other hand, TIMATION III is a satellite we also plan to launch in 1974 at an altitude of 14,000 km. Its reflectors should have an optimum diameter of about 7 mm. For the TIMATION satellite, we will indeed use the optimum diameter as given in figure 8. However, for GEOS-C, 4 mm is too small for convenience. In order to get the required total area, you would have to mount a great many such 4 mm reflectors, and it would be too expensive. Therefore, we essentially ignored figure 8 to design GEOS-C.

Instead we use 3½ cm diameter reflectors. This would ordinarily produce a very small spot which would miss the transmitter. What we did was to introduce errors into the angles of the cube corners and because of these errors, the returned ray split into 6 spots forming a toroidal distribution and the amount of the splitting was designed so that it compensated for the velocity

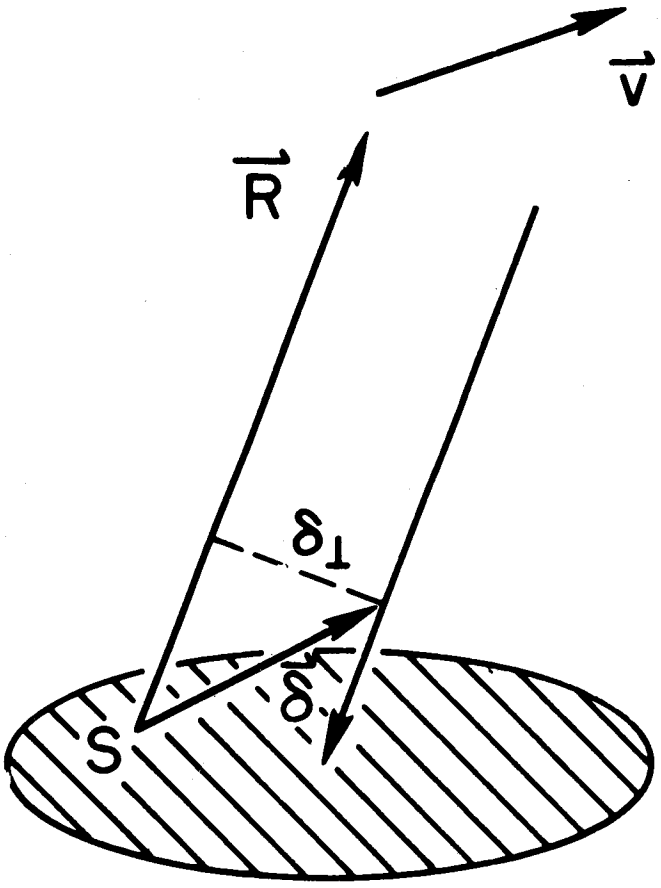

$$|\delta| = 2\frac{v}{c}R$$

$$\delta_\perp = \frac{(\vec{R}\cdot\vec{\delta})^2 - \delta^2 R^2}{R\,|\vec{R}\times\vec{\delta}|}$$

Figure 7. Displacement of Reflected Spot Due to Velocity Aberration

aberration. The receiving telescope will find itself out on the toroid ring, where the intensity has been optimized. This turns out to be a better design than the optimum small reflector.

Figure 9 is a quick summary of the returned signal we would expect if we were to assume we use a pulsed ruby laser with 1 J of energy per pulse, a transmitter divergence of 1 mrad, a 50 cm diameter receiver, and satellite reflectors which are 3½ cm in diameter. There will be 270 of these on GEOS-C. Here we can't use the diffraction formula for 3½ cm cube corners. We lose a factor of 36 which comes about because we have split the reflected beam into 6 spots. The range of GEOS-C will be approximately 1000 km.

The received signal, if all reflectors were facing downward, would be 2×10^5 photoelectrons. This is further reduced by a factor of 20 because we tilted them away from the zenith. The signal received is therefore 10^4 photoelectrons - a goodly number - one with which we should be very comfortable.

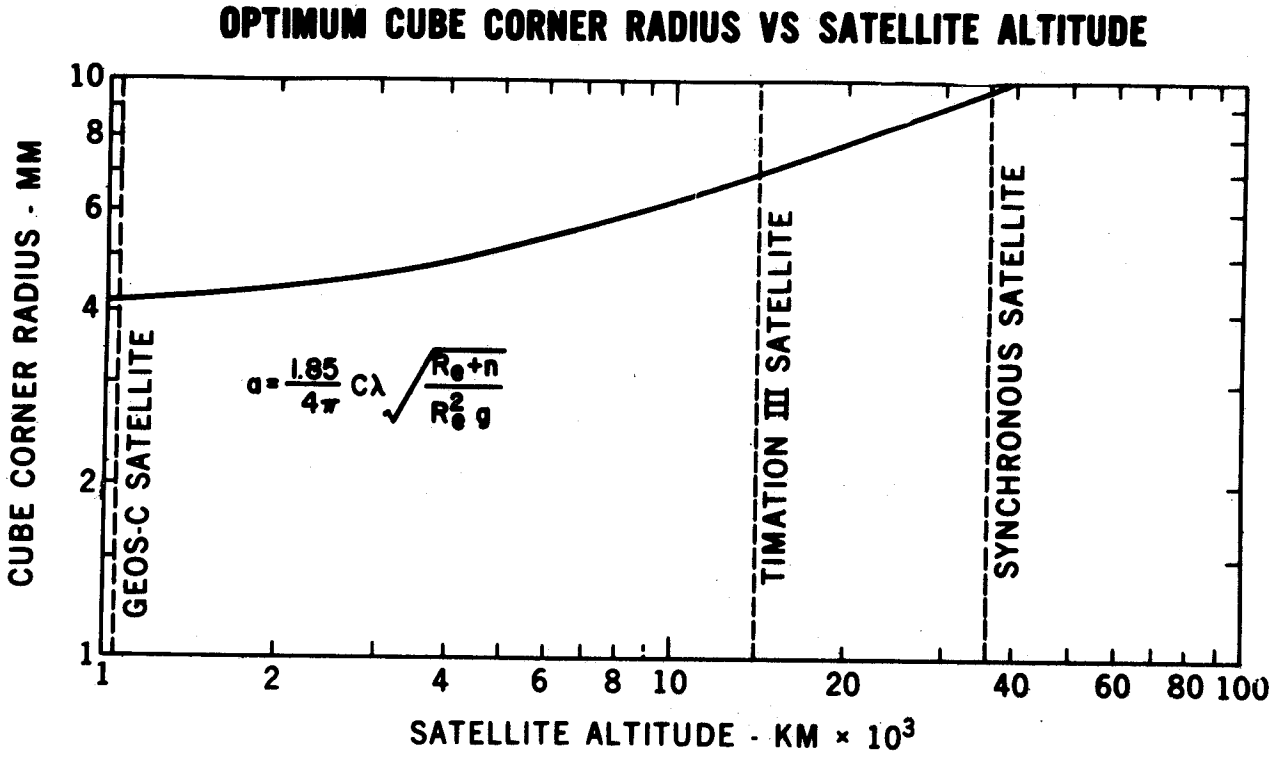

Figure 8. Optimum Cube-Corner Radius as a Function of Satellite Altitude. This optimization assumes perfect cube-corners with metallized reflecting surface.

Figure 10 is a picture of the mobile laser ranging station which is now reaching completion at the Goddard Space Flight Center. It is self-contained in its own van. The back closes up for road travel. The laser is mounted underneath the van and is accessible through a door. The laser light comes up through a smaller collimating telescope at the right. The reflected light is received by the larger telescope and is detected in the photo-multiplier mounted at the Cassegrain focus. The system is directed toward the satellite by a computer program which derives the expected satellite orbit, and all preliminary data processing and recording is done within the van.

I now want to come to the real reason for my talk. The question is :

How will we know what the accuracy of the measurement is?

The accuracy will depend on the degree to which we can calibrate the system and out ability to measure pulse position (figure 11). Up to now, the laser pulses we have used for satellite tracking have had a duration of about 20 nanoseconds. The laser at McDonald Observatory used for ranging

$$S_0 = \frac{P_T G_T G_R \lambda^2 \sigma L_S}{(4\pi)^3 R^4}$$

		dB	Value
P_T	Power Transmitted	0	1 J
G_T	Transmitter Gain	81.1	$\theta_T = 5 \times 10^{-4}$
G_R	Receiver Gain	127.1	$D_R = .5$ M
λ^2		-123.2	$\lambda = .6943$ um
σ	Radar Cross Section		
	$\sigma = N \frac{4}{36} \frac{A^2}{2}$	82.5	$D_C = 3.5$ cm $N = 270$
$(1/4\pi)^3$		-33.0	
$1/R^4$	Range	-238.7	$R = 9.27 \times 10^5$ M
L_S	System Losses	-11.1	$\rho = 7.8\%$
S_0	Received Signal	-115.3	2.95×10^{-12} J
	$N_S = \eta \frac{S_0}{H\nu}$		
η	Quantum Efficiency	-17.0	0.02
$(H\nu)^{-1}$	Photon Energy	185.4	
N_S	Received Photoelectrons (Flat Array)	53.1	2×10^5
N'_S	GEOS-C Array = .05 N_S		10^4 P.E.

Figure 9. GEOS-C Signal Calculation

to the moon has a pulse duration of 3 nanoseconds. We are now designing lasers which will have pulse durations of 0.2 nanoseconds. However, for the next few years, we are stuck with pulse durections of 20 nanoseconds. A 20 nanosecond pulse is 600 cm long, whereas we are trying to range to a few cm. The question is:

Can we get 10 cm accuracy with pulses 600 cm long?

Once we have developed the necessary position measuring technique , we must ask whether the system is stable. What is the effect of clock synchronization; what is the effect of atmospheric propagation; what is the spreading effect on reflector geometry? Remember that a short pulse is going to come back spread by the reflector and we have to know what the effect of the spacecraft array will be on that pulse.

Under these circumstances, how can we claim something like 10 cm in precision? There are a number of ways we can sense the position of a returned pulse (figure 12). When we started, we used a fixed threshold. We used a very simple circuit and our range precision was ±1½ m. The next improvement was to use a constant fraction trigger threshold. This was something which did

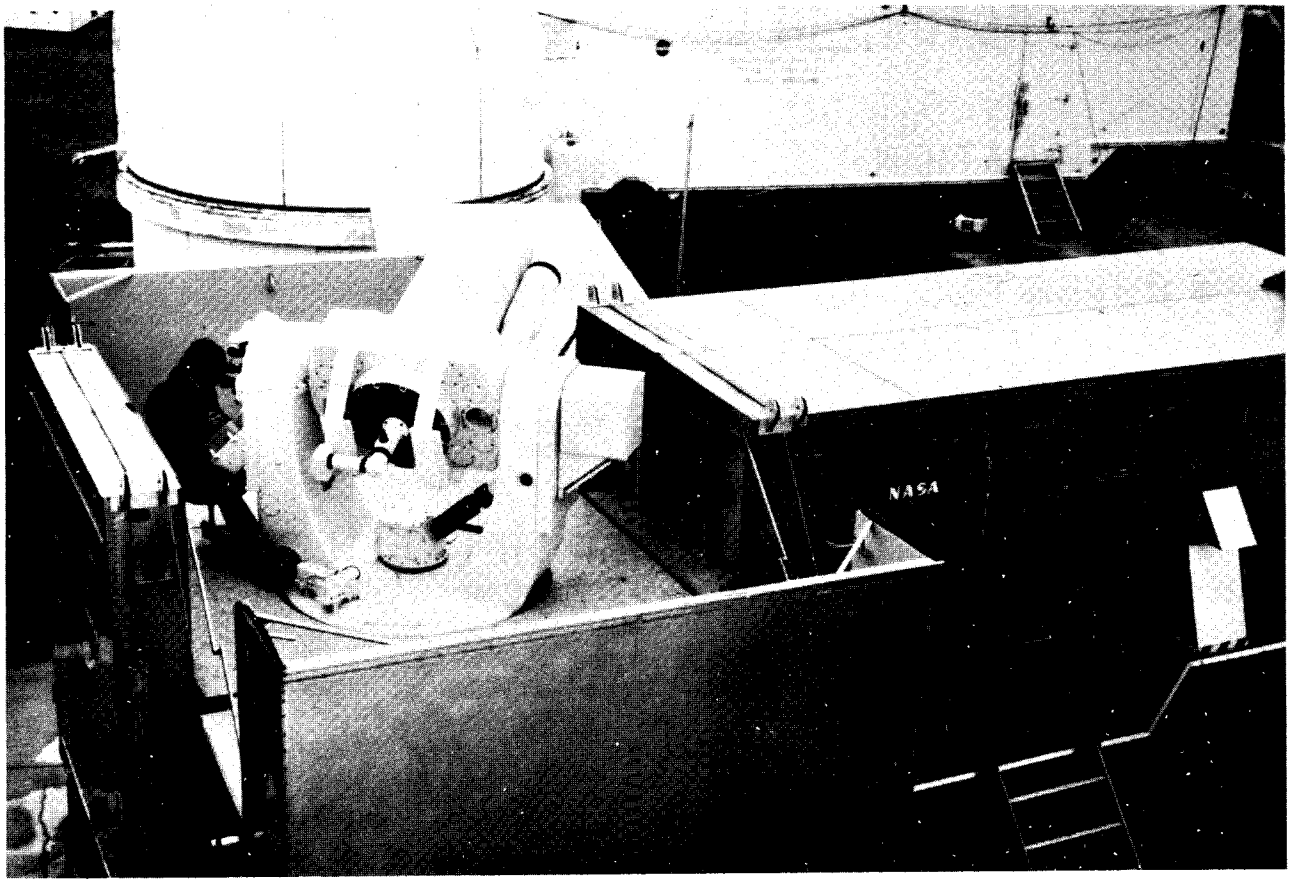

Figure 10. Photograph of MOBLAS 2, NASA Goddard Space Flight Center's Mobile Laser Ranging System

not change much as a function of pulse height but it did depend on pulse shape. The result of using this technique was a precision of ±50 cm.

The next generation will have to do better than the constant fraction trigger. We will measure the centroid of the 600 cm pulse (figure 13). We fire the laser once per second. We pick up a little of the outgoing pulse with a photo diode and use that to start a range interval timing system. At the same time, we also detect the centroid of the transmitted pulse, and record in the computer the position of that centroid with respect to the time at which we actually start timing the range interval. When the received pulse arrives, we use that to stop the range interval timing system. But at the same time, we make a careful analysis of the wave form because now the pulse has changed in both amplitude and shape. It will scintillate a great deal, with wide fluctuations in intensity. It will also be affected by the spreading of the reflector.

In the transmitted pulse, the centroid measuring technique is very simple. We just measure the width of the pulse and add half the width to the time at which the trigger was activated. That represents very well the centroid of the pulse because the pulse is fairly symmetrical and

KEY FACTORS IN LASER RANGING ACCURACY

- CALIBRATION
- PULSE POSITION MEASUREMENT
- SYSTEM STABILITY
- CLOCK SYNCHRONIZATION BETWEEN STATIONS
- ATMOSPHERIC PROPAGATION
- SPACECRAFT RETROREFLECTOR ARRAY GEOMETRY

Figure 11. Key Factors in Laser Ranging Accuracy

reproducible. On the other hand, the pulse which comes back in the returned signal fluctuates over a wide range in amplitude (figure 14) (as much as 1000 or 2000 to 1) and has unpredictable shapes. On the reflected pulse we, therefore, have to use a different technique - we measure the wave form in a digitizer, actually recording the value of the signal amplitudes in a number of channels. As can be seen in figure 15, even though the trigger point would have been the same in the two pulses, the position of the centroid will vary considerably, and must be taken into account.

We now have three such systems in operation:

- A stationary laser at Goddard, and
- Mobile Laser (MOBLAS) systems one and two.

In figure 16 are the results we have been getting in range precision. The rms scatter is about 15 cm on the average. If we assume there are no systematic errors, and that the fluctuations are random, then we can smooth over several measurements. If we do smooth over 10 points, the precision of ranging is about 4.7 cm.

TYPES OF PULSE POSITION SENSING

- FIXED THRESHOLD TRIGGER ON LEADING EDGE OF PULSE.
  - ADVANTAGE: VERY SIMPLE CIRCUIT.
  - DISADVANTAGE: MEASURED POSITION IS A FUNCTION OF PULSE HEIGHT AND PULSE SHAPE.
- CONSTANT FRACTION TRIGGER ON LEADING EDGE OF PULSE.
  - ADVANTAGE: MODERATELY SIMPLE CIRCUIT AND MEASURED POSITION ONLY WEAKLY DEPENDENT ON PULSE HEIGHT.
  - DISADVANTAGE: MEASURED POSITION IS A FUNCTION OF PULSE SHAPE.
- PULSE CENTROID MEASUREMENT.
  - ADVANTAGE: MEASURED POSITION INDEPENDENT OF PULSE HEIGHT AND ONLY WEAKLY DEPENDENT ON PULSE SHAPE.
  - DISADVANTAGE: COMPLICATED CIRCUITRY.

Figure 12. Types of Pulse Position Sensing

What shall we expect for the calibration error ? (See figure 17.) We calibrate by ranging to a tower 3 km away. The surveyors tell us that they trust the survey to 1½ cm. We have propagation errors in measuring the distance to the target and we have the precision with which we can measure the range to that target. Usually, during calibration we fire a hundred shots, with an rms range scatter of ±15 cm for the ensemble.

Having calibrated such a system, how well does the system maintain its calibration with high stability?

Figure 18 shows typical five hour runs on two independent systems. The calibration constant remains stable within an rms of ±4 cm. To accomplish clock synchronization, we have caesium standards at all our stations and we synchronize using LORAN-C.

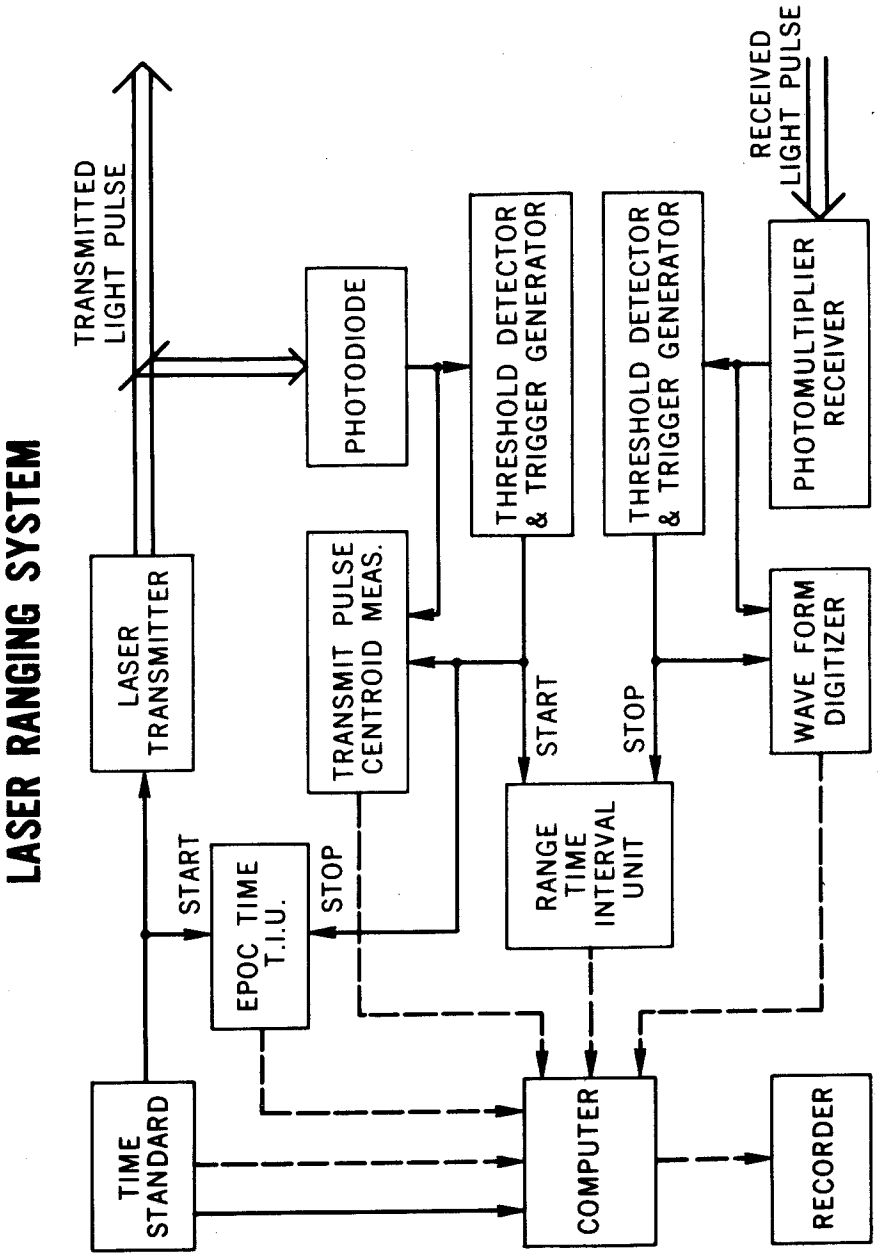

Figure 13. Block Diagram of Laser Ranging System

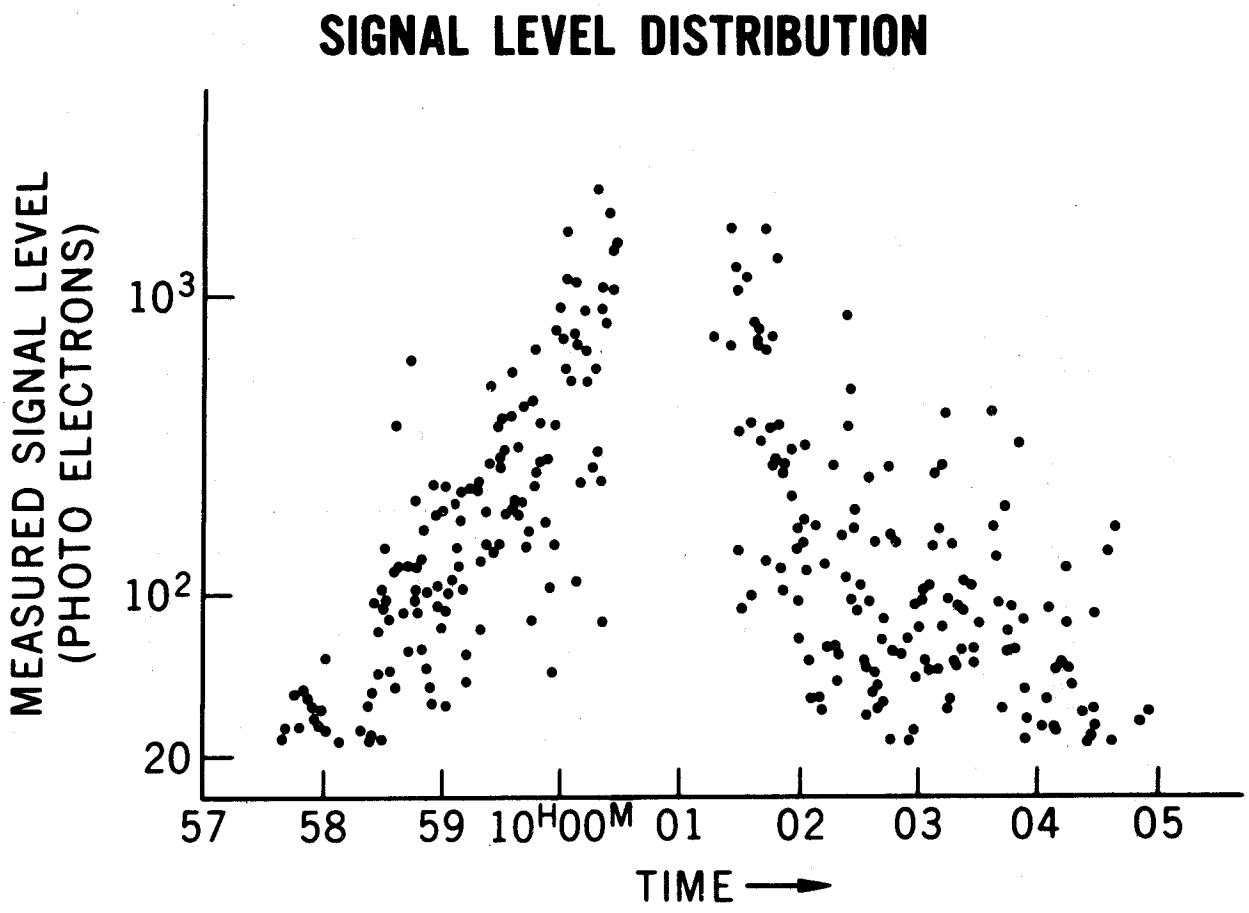

Figure 14. Signal Level Fluctuations from GEOS-B

The kind of performance we get is epoch precision of five microseconds, which is equivalent to space tracking errors of ±3½ cm. The range correction of two metres for the atmospheric refraction delay is known to ±3 cm. The spacecraft array geometry for GEOS-C for a 20 nanosecond pulse, results in an uncertainty in the centroid of the spacecraft's position of about 3 cm. This is because the GEOS-C reflector array is one metre in diameter, the pulse gets spread on its way back, and within that pulse, there is scintillation due to interference between the cube corners of the GEOS-C array. This scintillation gives an uncertainty of ±3 cm. Finally, as summarized in figure 19, the total rms error is about 10 cm, using laser pulses 20 nanoseconds

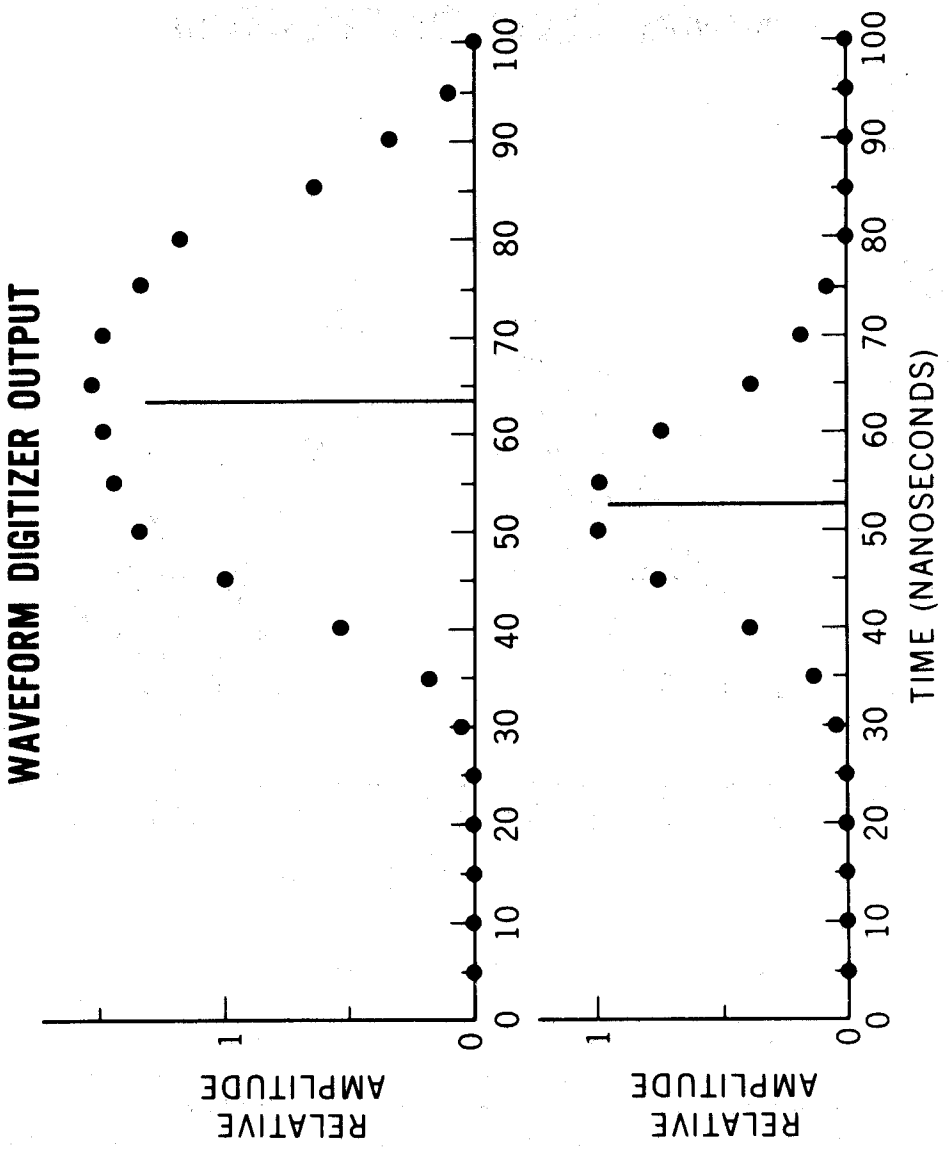

Figure 15. Results from Use of Waveform Digitizer

RANGING DATA RMS

STALAS	9 TO 16 cm	(11 cm AVE.)
MOBLAS 1	11 TO 25 cm	(16 cm AVE.)
MOBLAS 2	10 TO 16 cm	(13 cm AVE.)

PULSE POSITION MEASUREMENT ACCURACY

$$\frac{\text{DATA RMS}}{\sqrt{10}} = \frac{15}{\sqrt{10}} = 4.7 \text{ cm}$$

Figure 16. RMS Ranging Scatter Obtained During Calibration Tests of Goddard Space Flight Center Systems

CALIBRATION ERROR SOURCES

DISTANCE FROM TRACKER AXIS TO CALIBRATION TARGET	± 1.5cm
ATMOSPHERIC PROPAGATION	± 0.6
TIME INTERVAL MEASUREMENT PRECISION	$\frac{\text{RMS MEASUREMENTS}}{\sqrt{\text{NO. OF MEASUREMENTS}}}$

Figure 17. Calibration Error Sources

long.

That is the basis of my confidence. We are now developing a 0.2 nanosecond system. The first of these is being sent to the Haleakala lunar ranging station. As shown in the right hand column of figure 19, if we did very little more than replace a 20 nanosecond system with a 0.2 nanosecond system, we would end up with a 5 cm uncertainty.

This should happen with the NASA mobile stations within the next few years. After the short pulse lasers are introduced, we can further improve the detection systems for measuring the pulse position and we can improve the clock synchronization and get down to about 2 cm. I am confident this can be done.

The above is a slightly edited transcript of a presentation to Session F on Wednesday 28 November 1973.

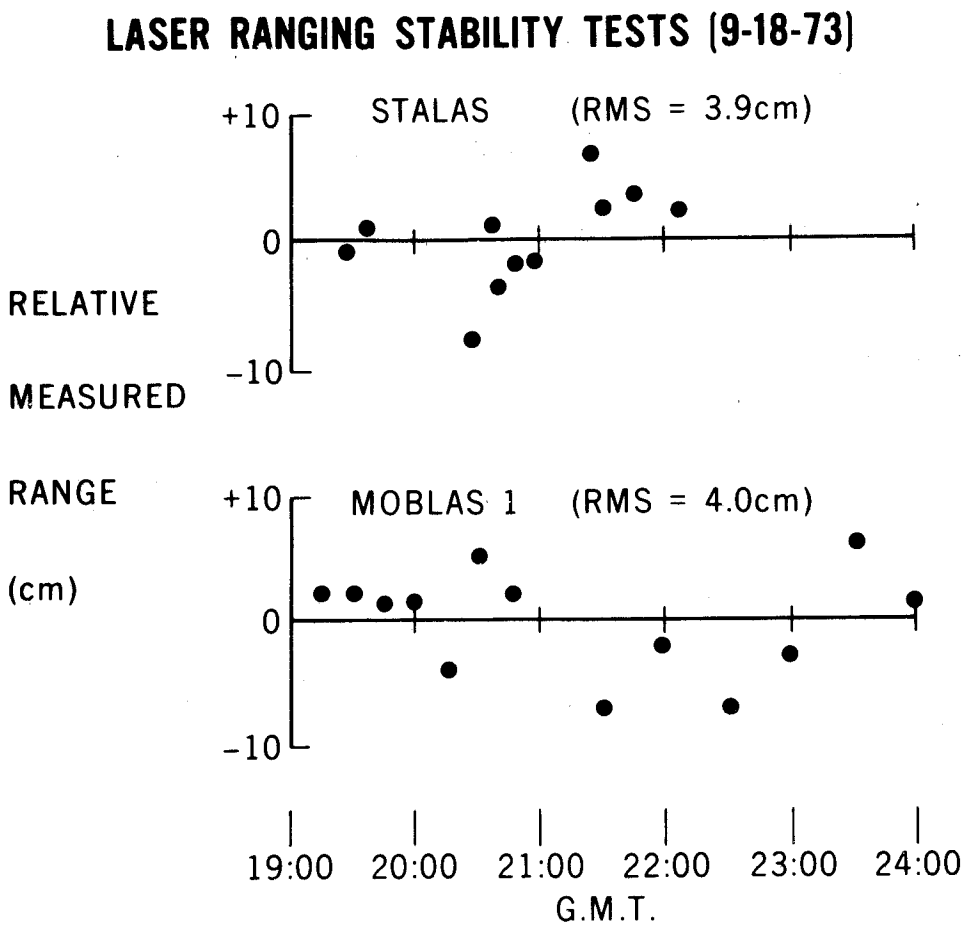

Figure 18. Tests to Monitor the Stability of Calibration on Two of the Goddard Ranging Systems

2. Discussion

ANGUS-LEPPAN: Any special reason why few technical details have been published on the Goddard laser ranging systems?

PLOTKIN: There is no reason for this other than sloth.

WALCOTT: Is there going to be a synchronous satellite with retro-reflectors?

PLOTKIN: There are none now planned. The highest is TIMATION III at 14,000 km. LAGEOS planned for launch in 1976 will be at 6,000 km. Incidentally, these two satellites will satisfy ONG's geometry very well.

ONG: You mentioned an array size of 1 m diameter and a 3 cm accuracy over the range. I am puzzled as to how that can be done.

PLOTKIN: These are figures for GEOS-C. If you have a very short pulse incident on GEOS-C, it would only illuminate a few reflectors facing the incident ray and the returned pulse

LASER RANGING ACCURACY

	20 NS LASER		0.2 NS LASER
• CALIBRATION	2.2cm		1.6cm
• PULSE POSITION MEASUREMENT $(15/\sqrt{10})$	4.7	$(1.5/\sqrt{10})$	0.5
• SYSTEM STABILITY	4.0		0.4
• CLOCK SYNCHRONIZATION (5 μs)	3.5		3.5
• ATMOSPHERIC PROPAGATION	3.0		3.0
• S/C ARRAY GEOMETRY $(9/\sqrt{10})$	2.9	$(2/\sqrt{10})$	0.6
TOTAL RSS	8.5cm		4.9m

Figure 19

would be about 20 cm long. If the signal is very good, as it is for GEOS-C, you should be able to trace the shape of the pulse in a waveform synthesizer and locate the centroid. If the signal strength were infinitely good, this can be done with extreme precision. However, what happens here is that within the pulse there will be scintillations bacause the different reflectors will interfere with one another. Because of those random scintillations we cannot determine the centroid of the 20 cm long pulse with infinite precision; for that geometry and a 20 cm pulse, the uncertainty will be about 20 cm.

PÂQUET, P.
DEJAIFFE, R.
Observatoire Royal de Belgique
Avenue Circulaire 3
B-1180 Bruxelles,
B E L G I U M

Proc. Symposium on Earth's Gravitational Field & Secular Variations in Position (1973), 347-359.

ANALYSIS OF THE FIRST DOPPLER OBERVATIONS PERFORMED AT THE ROYAL OBSERVATORY OF BELGIUM

ABSTRACT

This paper contents a comparative analysis of the results obtained in Brussels by both astronomical and doppler measurements. This study is limited at the internal and external errors distributions. However, the existence of a drift between the NWL and the BIH system is clearly shown. The geodetic coordinates of the station deduced from doppler observations are:

$\lambda = 4^{o}21'31''.113 \pm 0.007, \quad \phi = 50^{o}47'54''.893 \pm 0.003$

1. Introduction

In May 1972 one of the TRANET Doppler Stations was loaned by the US Navy to the Royal Observatory of Belgium, in Brussels. Operational on 23 June, 1972, this station - referred to as TRANET station 021 - is uninterruptedly observing since this date.

Radioelectric observations performed by these Tranet stations permit determinations of the polar motion besides other geodetic goals. Since 1969 the Naval Weapons Laboratory (NWL, Dahlgren, Va.) determines the polar motion generally from the observations of the 1967-92A satellite which is one of the five still in operation Transit satellites.

The deflection of the vertical prevents any direct comparison between astronomical coordinates and results obtained by the Doppler method. However, these two techniques can be compared according to the following points of view:

- global results such as for example, polar motion curves deduced by each of these two techniques;
- evolution of the longitude differences;
- residuals associated with observed elements.

A comparison of the instantaneous astronomical latitude of the Uccle-Brussels station deduced from the BIH (Bureau International de l'Heure, Paris) and the NWL polar motion is presented in figure 1. This figure clearly shows apparently a reduction of the amplitude and a phase of a few days in the NWL observations. These characteristics indicate the existence of a drift in one of these two systems with respect to the other. An homogeneous series extended over some years will probably permit the unification of these two coordinate systems.

In this paper the analysis of the results is limited to the study of the internal and external errors distribution of the doppler method. Also included is a comparison of the same kind of errors tied with the astronomical observations performed at Uccle with a Danjon astrolabe.

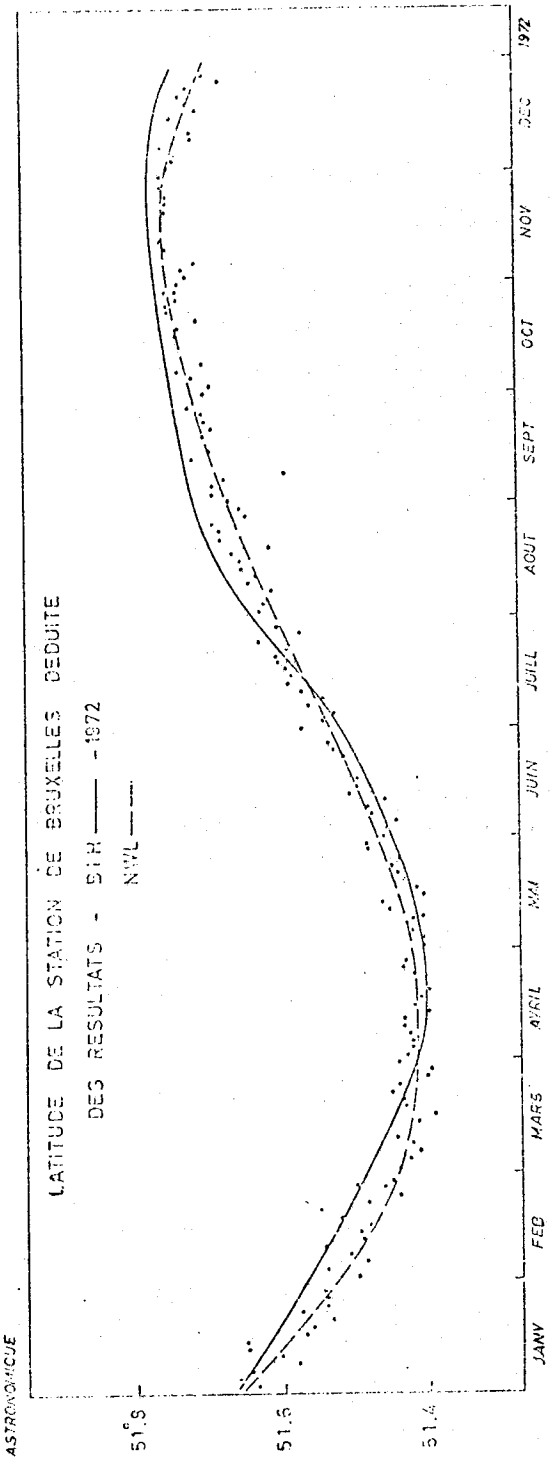

Figure 1. Comparison of the Instantaneous Astronomical Latitude of the Uccle - Bruxelles Station Deduced from the BIH and the NWL Polar Motions

2. Data Reduction

The observed data reduction procedure for the whole Doppler stations has been described by R. J. ANDERLE (1970; 1971). For a better understanding of the elements at our disposal, we indicate that the procedure in use is divided in two steps:

i) On each period of two days and from the complete observational material provided by the whole stations, NWL computes one improved orbit of which the orbital parameters are known in the instantaneous frame of reference;

ii) then this improved orbit and the mean coordinates (λ_M, ϕ_M) of the stations are used for an individual analysis of all the passes considered in the first reduction phase.

The differences between theoretical and experimental values of the frequencies drifts, due to the Doppler effect, lead to the observational equations of which the station coordinates and the frequency of the embarked oscillator in the satellite are the unknowns.

Practically these coordinates of the considered station are indirectly determined by the intermediate of two particular coordinates tied to the orbit.

The origin is located at the point which corresponds to the theoretical minimal distance between the station and the satellite. This origin is then fixed from the station mean coordinates and from the improved orbit. At this particular point there is no Doppler effect. The $\underline{r}$ vector along the origin-station direction and the $\dot{\underline{r}}$ vector directed perpendicular to the $\underline{r}$ vector are two of the coordinate axis system. These two components are respectively defined as slant range and along track components.

For polar orbits, as it is the case for the satellites observed by the Tranet stations, figure 2 shows that the observed along track displacement is nothing else than the Δu difference between the instantaneous and the reference equators. Indeed if the Earth rotation axis did not change the station S would follow the nonperturbed path AA_1; due to the displacement of the pole from CIO (Conventional International Origin) to P the station S really moves along BB_1. During the successive passes above the horizon of station S the along track component (ATC) successively measures the Δu_i displacements.

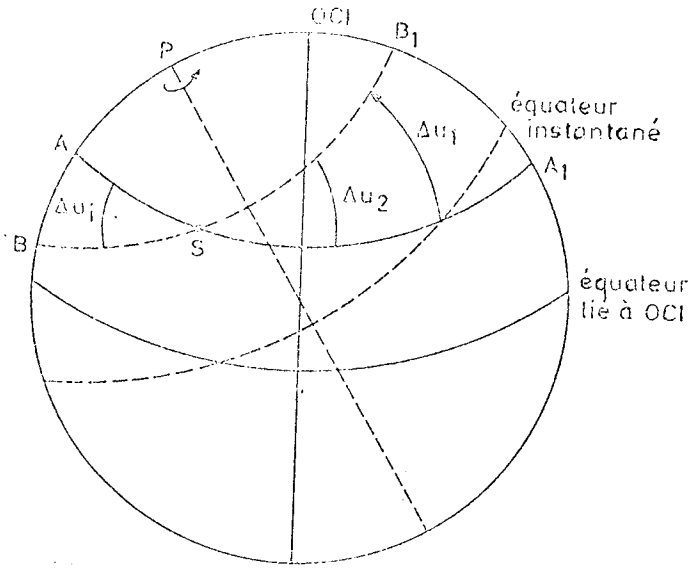

Figure 2. Geometrical Configuration

In each 48 hours time interval the ATC presents two diurnal periods tied with the polar motion. In analysing this component NWL deduces the amplitude and the phase or yet the (x,y) coordinates of the instantaneous pole (ANDERLE 1970).

3. Internal Coherence

From each individually analysed pass one can deduce:

i) the along track and slant range displacements;

ii) the observed ellipsoidal coordinates at which the polar motion corrections have already been applied;

iii) the mean square errors (mse) associated with each of these elements.

As they result from the individual analysis of passes these mse are tied with the *internal errors*.

Table 1 contains the arithmetic mean of these mse computed for the 503 first observed passes in Uccle and the standard deviation σ of their distribution. In (a) all the passes have been considered while the results in (b) have been obtained after elimination of the values greater than 2.57σ. In this same table one can also find the internal errors computed from the results of 343 astronomical observations performed in Uccle with a Danjon astrolabe. These errors are the errors associated with each latitude and longitude determination from the observations of only one group of stars.

T A B L E 1

Internal Coherence

Doppler Measurements				
	Longitude	Latitude	Along Track	Slant Range
N	503	503	503	503
(a) Mean	0''109	0''038	1.27 m	0.93 m
σ	0''248	0''043	1.77 m	1.51 m
N	491	486	491	495
(b) Mean	0''079	0''033	1.07 m	0.78 m
σ	0''081	0''022	0.82 m	0.55 m

Astrolabe Observations		
	Longitude	Latitude
N	343	343
(a) Mean	0''113	0''111
σ	0''101	0''101
N	336	334
(b) Mean	0''104	0''101
σ	0''043	0''043

The distribution in percentage of the internal errors in the four components has been plotted in figures 3 through 6 for the totality of the considered passes. On figures 4 and 5 the same distribution has also been represented for the astrolabe observations. It must be noticed that if the internal coherence may be compared for the longitude, the Doppler measurements are really better than the astrolabe results for latitude determinations. This is due to the fact that the analysis is performed only with polar satellites.

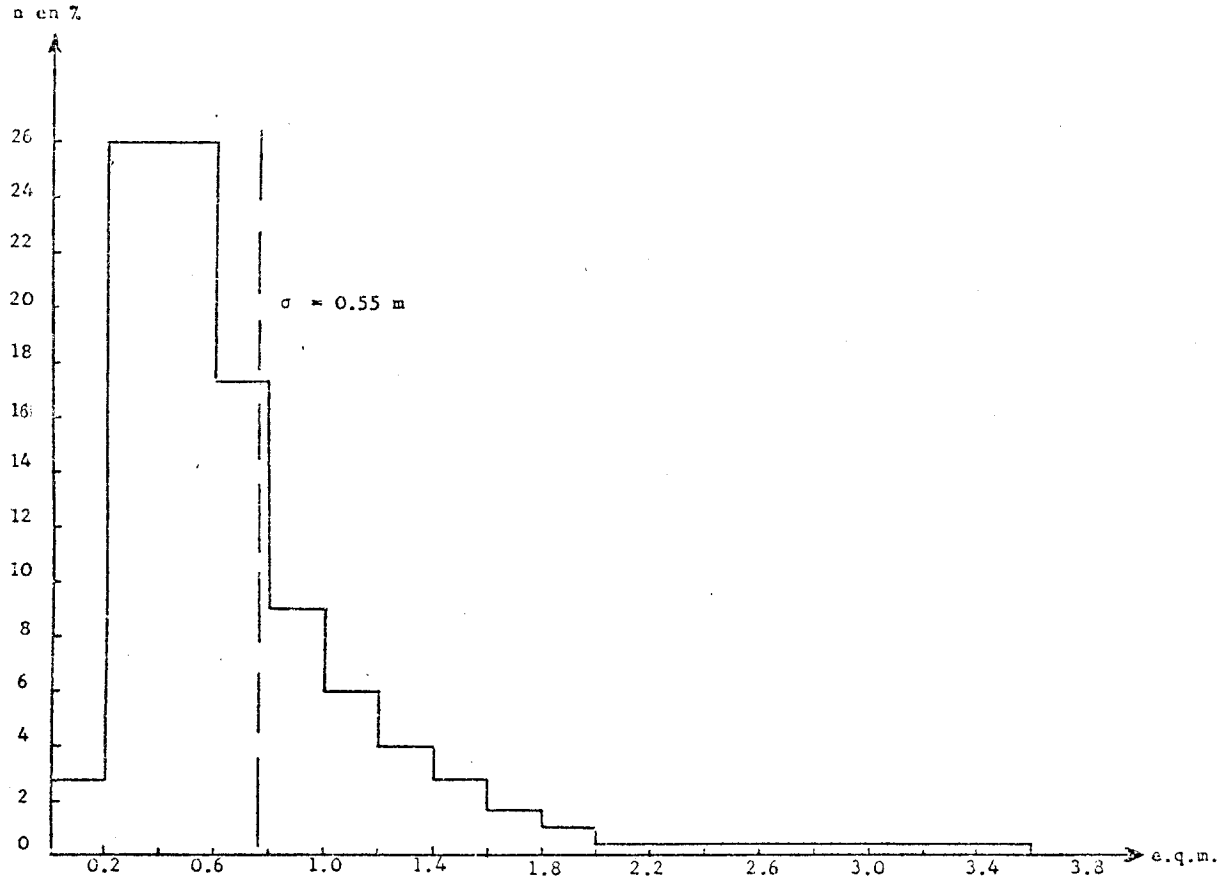

Figure 3. Internal Errors : mse Range Distribution
Mean Value : 0.78 m

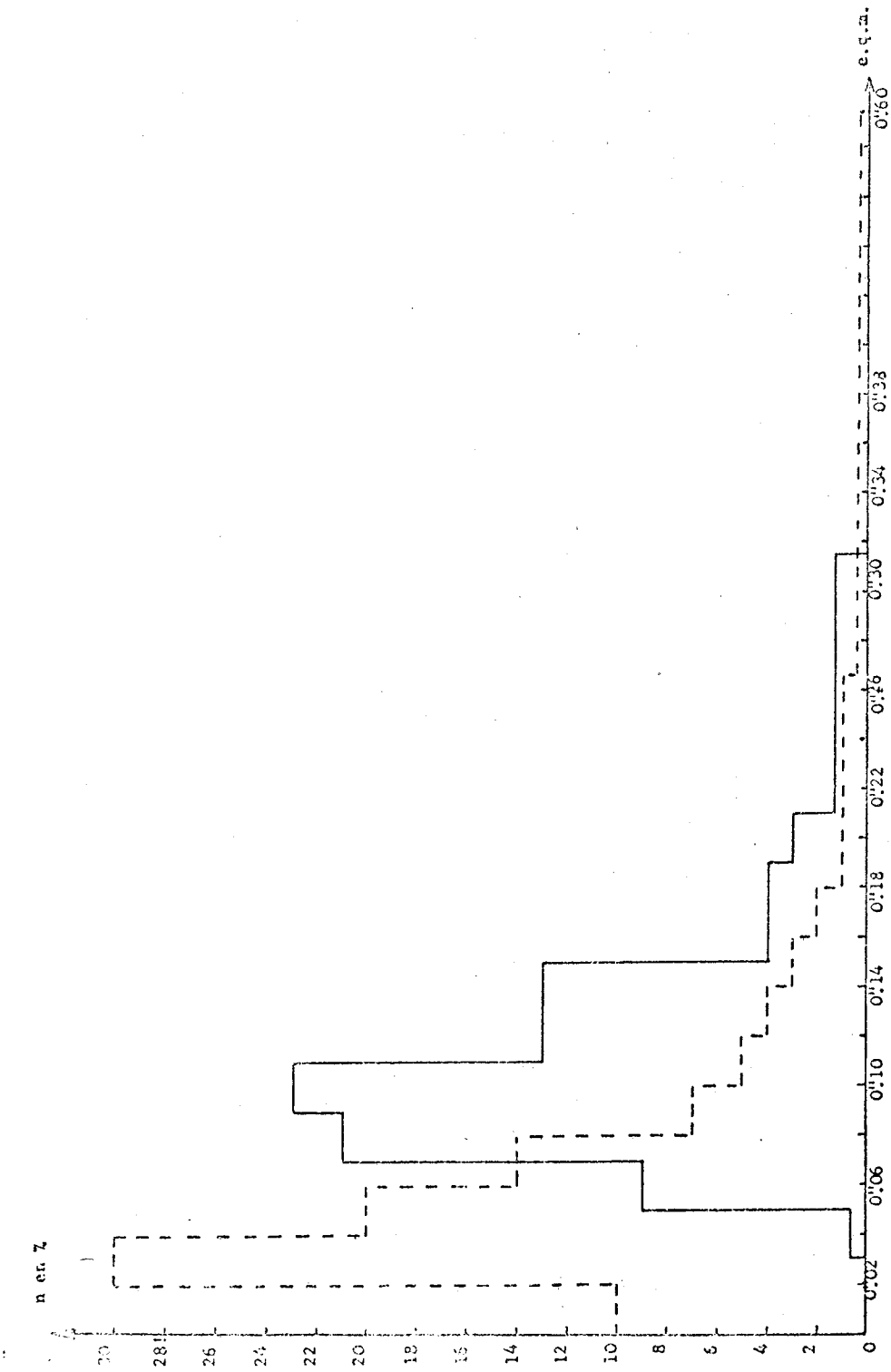

Figure 4. Internal Errors : mse Longitude Distribution -
Mean Values: (D) 0"079; (A) 0"104

——— Astrolabe ---------- Doppler

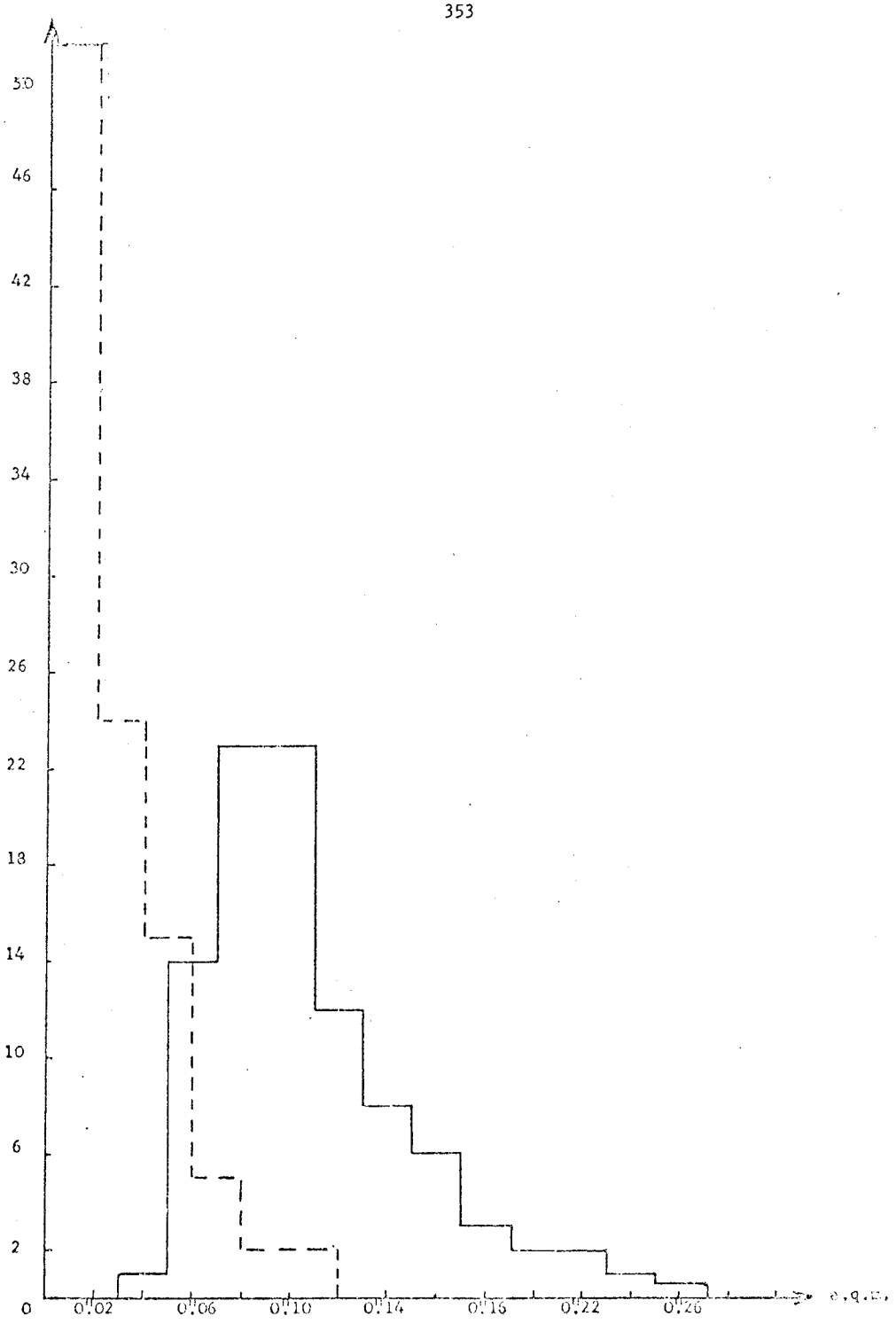

Figure 5. Internal Errors : mse Latitude Distribution -
Mean Values: (D) 0".033; (A) 0".101
——— Astrolabe ---------- Doppler

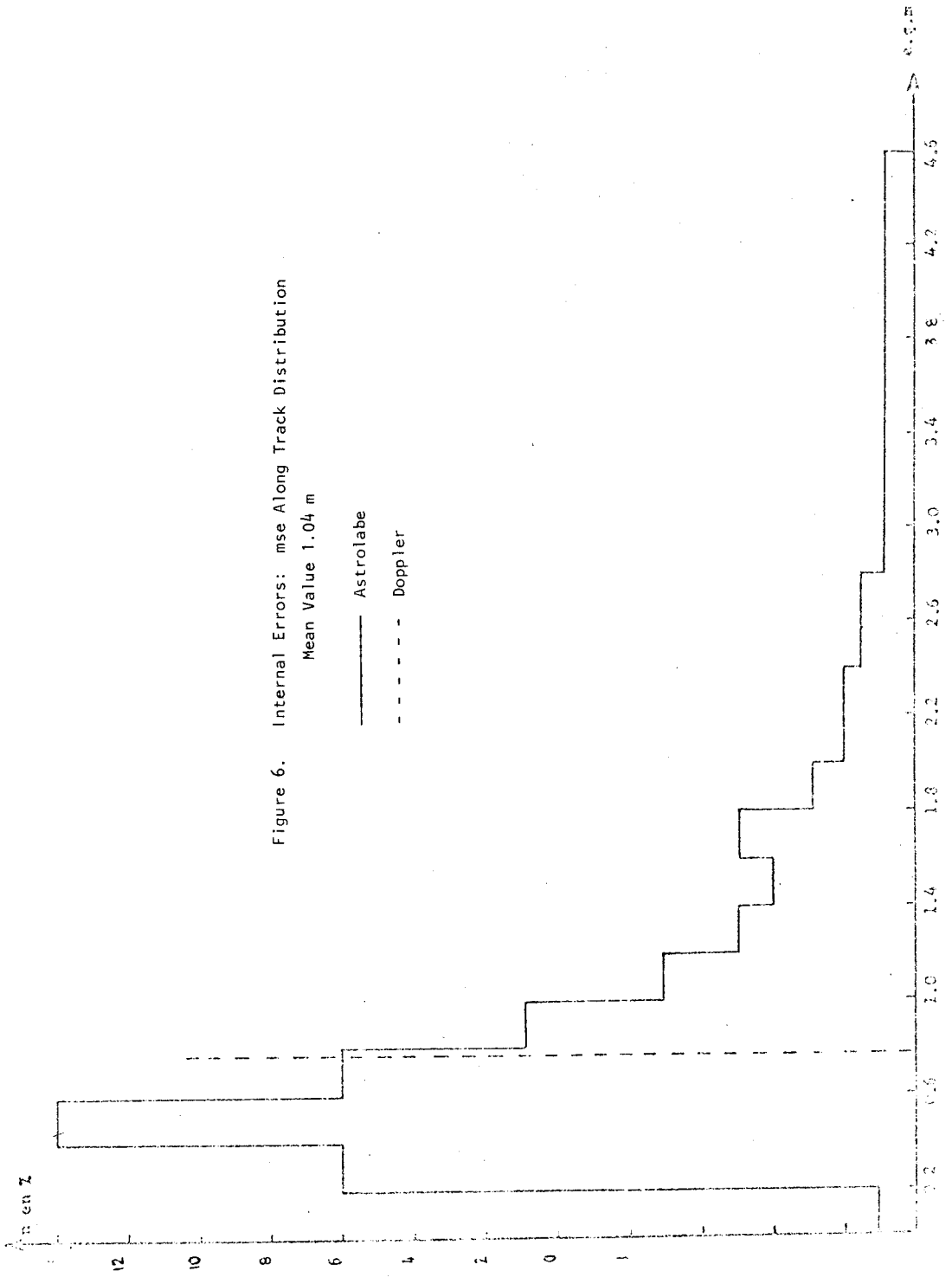

Figure 6. Internal Errors: mse Along Track Distribution
Mean Value 1.04 m

4. External Coherence

If (λ_N, ϕ_N) denote the mean coordinates of a station in the fixed NWL frame of reference, the instantaneous coordinates $(\lambda_{inst}, \phi_{inst})$ deduced from the individual analysis of each pass are brought back in this NWL frame of reference by the relations :

$$\lambda_{obs,N} = \lambda_{inst} + x \tan \phi_N \sin \lambda_N - y \tan \phi_N \cos \lambda_N$$

$$\phi_{obs,N} = \phi_{inst} - x \cos \lambda_N - y \sin \lambda_N.$$

The residuals

$$r_\lambda = \lambda_N - \lambda_{obs,\,N}$$

$$r_\phi = \phi_N - \phi_{obs,\,N}$$

are defined as the *external errors*.

Table 2 gives the standard deviation σ_D of these errors distribution. This table also contains the standard deviations of the distributions of the external longitude and latitude errors obtained with an astrolabe:

$$r'_\lambda = (UT_o - UTC)_{Ucc} - (UT_o - UTC)_{BIH}$$

$$r'_\phi = \phi_{obs} - \phi_{Ucc,BIH}$$

where $\phi_{Ucc,BIH}$ denotes the instantaneous Uccle latitude deduced from the BIH polar motion curve. $(UT_o\text{-}UTC)$ and ϕ_{obs} are deduced from each group of stars. Each line of Table 2 represents the standard deviation of a new distribution obtained in eliminating residuals which are greater than 2.57 the σ value of the precedent line.

The distribution of the random errors of the measurements made by the Doppler and by the astronomical method are shown in figures 7 and 8.

5. Conclusions

In order to obtain a standard deviation value for the longitude which may be compared with the astrolabe one (0".20) about five passes in one hundred have to be abandoned. If one tries to obtain a significant improvement, this percentage rises up to 7.5 . In any case this elimination does not seem excessive in practice.

In the calculation of the astrolabe external errors the annual corrections published by the BIH have not been applied. The latitude internal and external coherences are of the same order of magnitude; that corresponds to the well-known quality of the astrolabe. But in longitude a variation by a factor two occurs. This last remark is a peculiar characteristic of the Uccle astrolabe which has always given less good results in longitude than in latitude (GUINOT et al 1972).

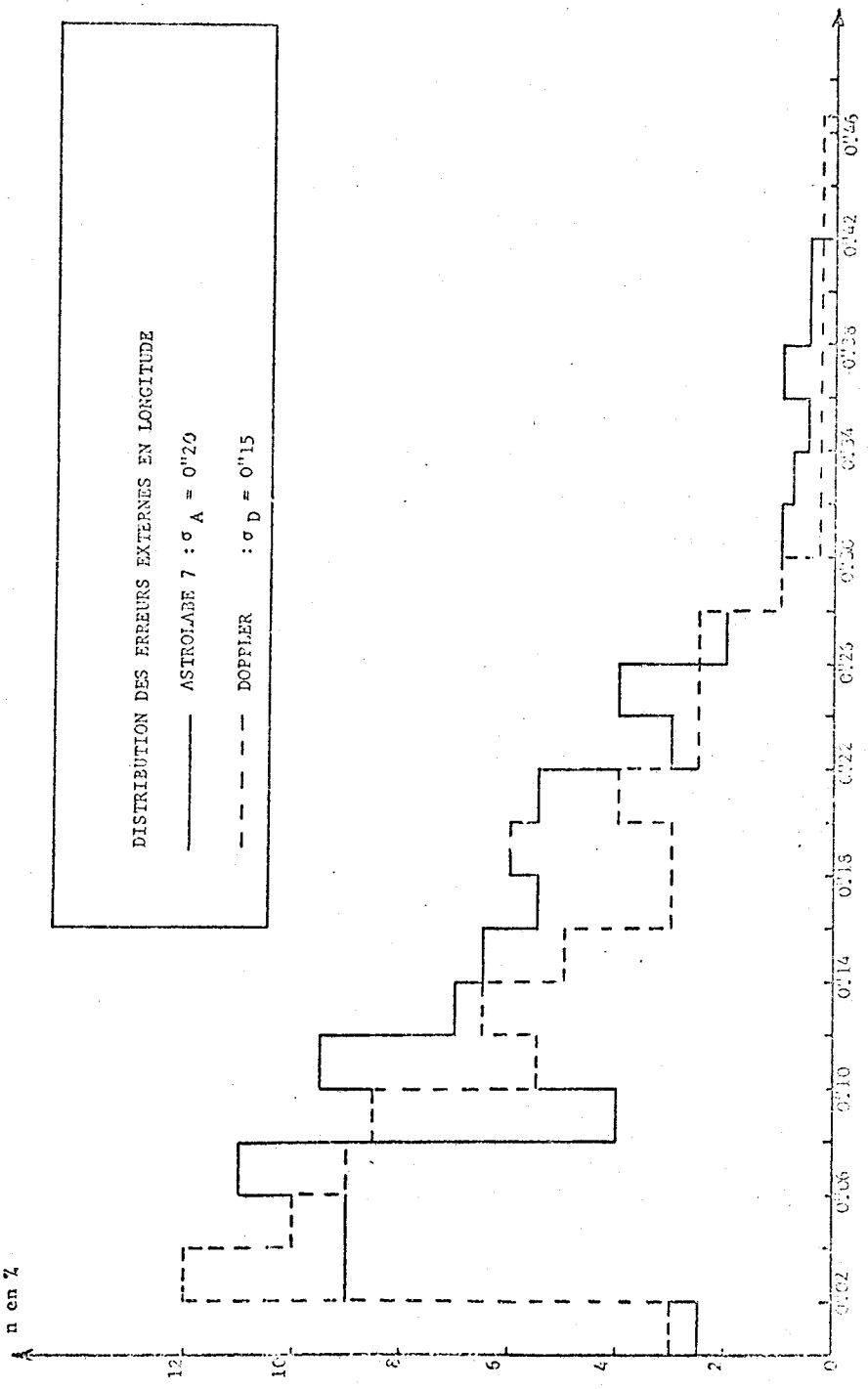

Figure 7. Longitude External Errors Distribution

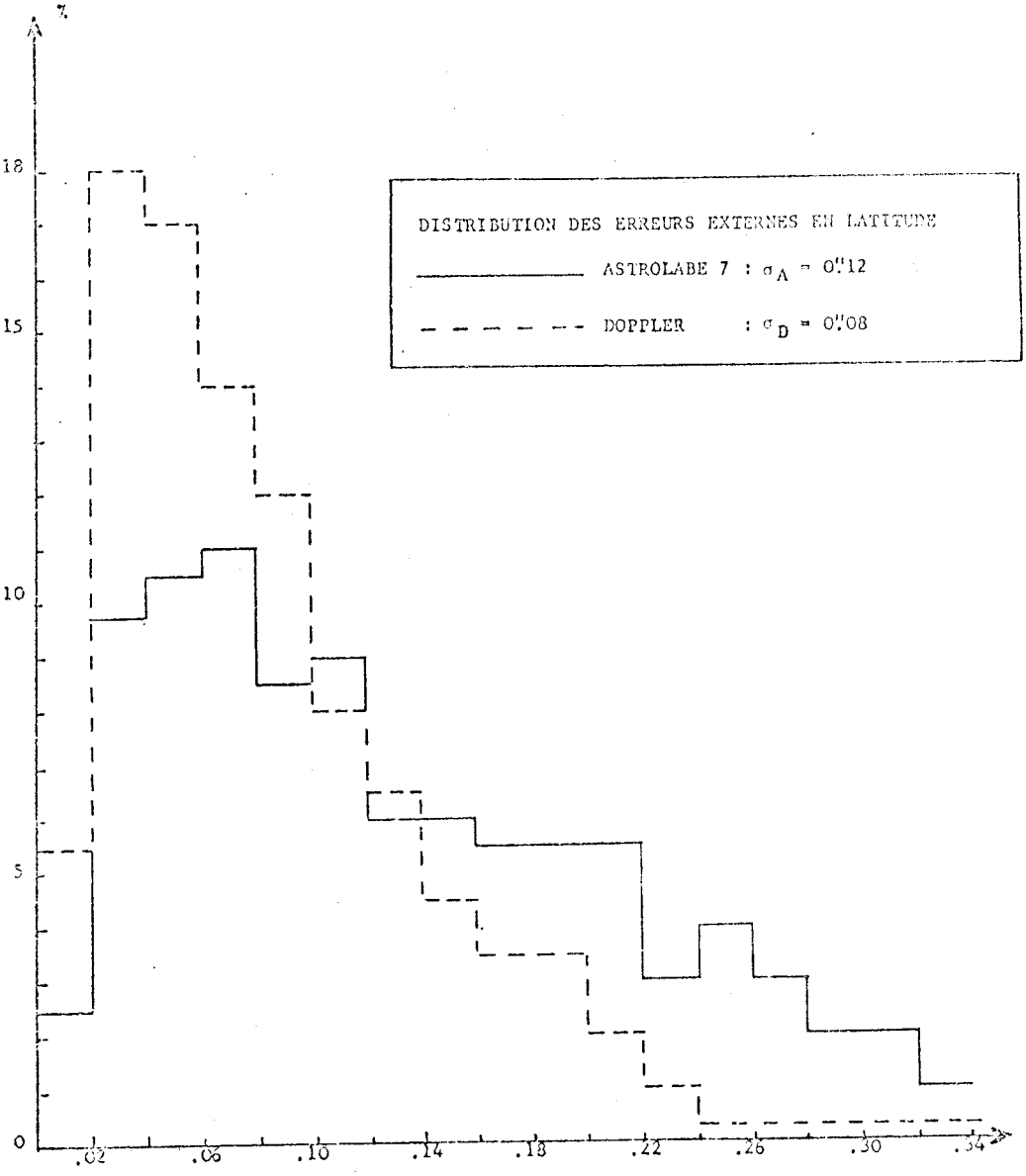

Figure 8. Latitude External Errors Distribution

Finally, in making use of the doppler observations mentioned in the last line of table 2, the coordinates and the corresponding accuracy of the Uccle-Brussels station have been deduced and this important result is given hereafter:

$\lambda = 4^{o}21'31''.113 \pm .007 \qquad \phi = 50^{o}47'54''.893 \pm .003$

TABLE 2

External Coherence

Doppler Measurements			
Longitude		Latitude	
N	σ	N	σ
503	0''667	503	0''116
493	0''279	496	0''091
476	0''189	486	0''084
465	0''154	484	0''083
Astrolabe Observations			
Longitude		Latitude	
N	σ	N	σ
274	0''222	274	0''141
270	0''207	268	0''131
268	0''202	266	0''128

6. References

ANDERLE, R.J. 1971. Refined geodetic results based on Doppler satellite observations. *NWL Technical Report TR-2889.*

ANDERLE, R.J. 1970. Polar motion determinations by US Navy Doppler satellites observations. *NWL Technical Report TR-2432.*

GUINOT, B., FEISSEL, M. & GRANVEAUD, M. 1972. Rapport annuel pour 1971. *Bureau International de l'Heure.* Paris.

7. Discussion *

LLOYD: What method is used to correct for refraction, especially for ionospheric effects and secondly for lower atmosphere effects?

MELCHIOR: Corrections for atmospheric effects are made by NWL. There are two frequencies 400 MHz and 150 MHz. By using that you can eliminate the ionospheric effect because the Doppler effect is proportional to the frequency, while the ionospheric effect is inversely proportional to the frequency. A better precision could be obtained if we had a third frequency in GHz. I don't believe the lower atmosphere has any effect on Doppler. As regards the tropospheric effect, ten years ago when they developed the Doppler system, they made meteorological

measurements to try and correct the Doppler. But it was not successful and finally they just adopted a model and this seems to be the best way.

WALCOTT: In addition to your operation, there will also be satellite Doppler alongside the two PZT's in Canada. It will be interesting to compare the results.

MUELLER: As the computations were done by NWL (US Naval Weapons Laboratory, Dahlgren Virginia), I presume the NWL ephemeris was used in these calculations.

MELCHIOR: Yes.

* The paper was presented on behalf of the authors by P. MELCHIOR.

SIRY, J.W.
National Aeronautics & Space Adminsitration
Washington, DC 20546
United States of America

Proc.Symposium on Earth's Gravitational Field & Secular Variations in Position (1973),360-379.

SATELLITE TECHNIQUES FOR THE STUDY OF SECULAR VARIATIONS IN POSITION

ABSTRACT

Secular variations in position are associated with seismic activity on a number of occasions. Crustal motions of the order of several centimetres, for example, have been observed to precede earthquakes. SCHOLZ, SYKES & AGGARWAL (1973) propose a model which relates these and other precursory phenomena to dilatancy. They present evidence linking the precursor time interval with the earthquake magnitude and the length of the aftershock zone. Dilatant regions of the order of a few tens of kilometres in scale and precursor time intervals ranging from roughly half a year to a year and a half are expected to be of interest in connection with earthquakes of magnitude six, for example. The dilatancy mechanism seems to be operative in the case of thrust faults and probably also in the case of some strike-slip events. A system for sensing precursory crustal motions should thus have the capability for determining site positions with an accuracy of the order of a couple of centimetres in a time interval of approximately a quarter of a year at spacings of roughly ten kilometres in a region of interest such as a fault zone. Several hundred such locations are needed to cover the fault systems in the California area.

A system for monitoring such precursory crustal motions is presented. It involves a set of automated corner reflector stations tracked by means of a laser operating in the Geopause satellite. It should be possible to range some three times during every Geopause pass to each of the sites in such an ensemble, weather permitting. One centimentre range data gathered during a quarter of a year should yield position component accuracies of the order of a couple of centimetres. A laser beam of a tenth of a milliradian in diameter would, in general, illuminate a single station in such an array. A broader beam would generate reflections from several sites, yielding overlapping data. A chain or pattern of such overlapping regions can strengthen the solution for site positions. Pressure, temperature and humidity gauges can provide refraction correction data. Turnaround transponders interrogated by the Geopause radio tracking system can furnish corresponding data in excessively cloudy regions.

This concept based on satellite techniques offers the prospect of a practical approach to the problem of monitoring secular variations in position such as precursory crustal motions.

1. Introduction

Secular variations in position of more than one kind are associated with seismic activity on a number of occasions. Some are viewed in terms of strain in regions near earthquake fault zones. Others associated with dilatancy are thought to have a more specific precursory nature.

2. Crustal Motions which are Precursory to Earthquakes

Precursory phenomena of several types have been observed to precede earthquakes. Among these are crustal motions, variations in the ratio of the seismic compressional velocity, V_p, to the seismic shear velocity, V_s, and changes in the electric resistivity, magnetic fields, radon emission, and

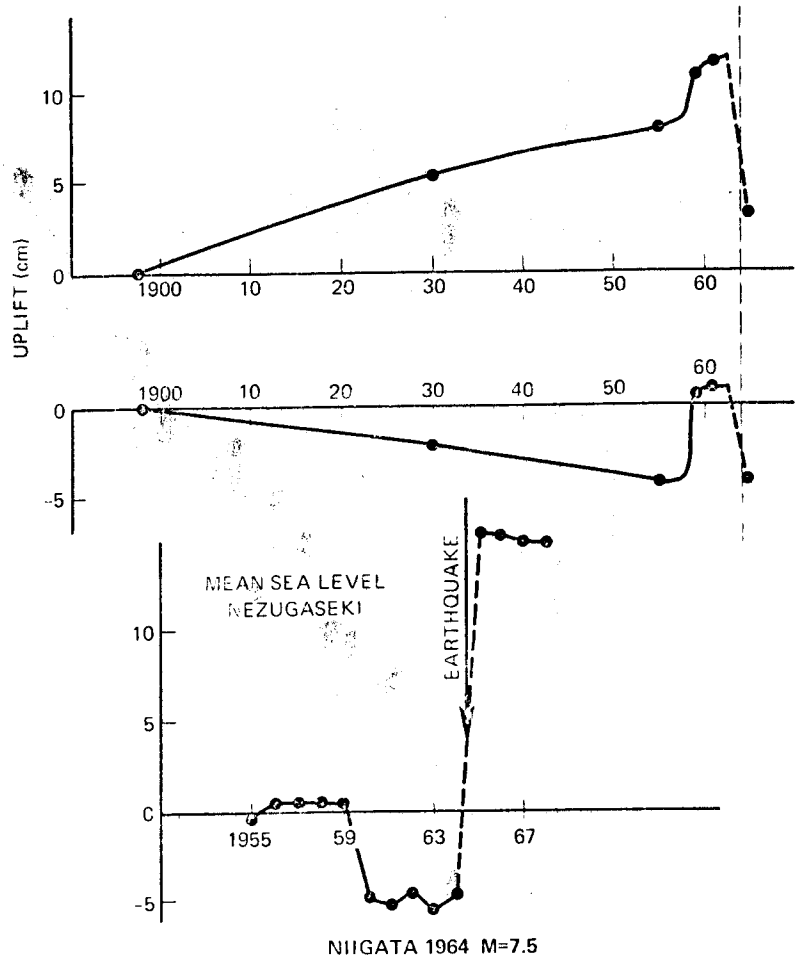

Figure 1. Earthquake Related Secular Variations in Position in Japan (SCHOLZ ET AL 1973). Sea Level Data corrected for oceanographic and meteorological conditions (YAMAGUTI 1968); Levelling data from (TSUBOKAWA ET AL 1968)

the relative numbers of large and small seismic shocks (SCHOLZ ET AL 1973; WHITCOMB ET AL 1972; KELLEHER ET AL 1973). An example of vertical crustal motion occurring before a large earthquake is seen in figure 1.

A model which relates these various premonitory effects to dilatancy has been proposed by SCHOLZ, SYKES & AGGARWAL (1973). They present evidence linking the precursor time interval with the magnitude of the subsequent earthquake. This is seen in figure 2. The long term precursory effects occur months and even years prior to large earthquakes. They also find a connection between the precursory time interval and the length of the aftershock zone, which is taken as a characteristic dimension. This is exhibited in figure 3. These data relating a variety of different phenomena are in good agreement with the diffusion relation. This circumstance lends further support to the dilatancy theory as an explanation of the array of effects.

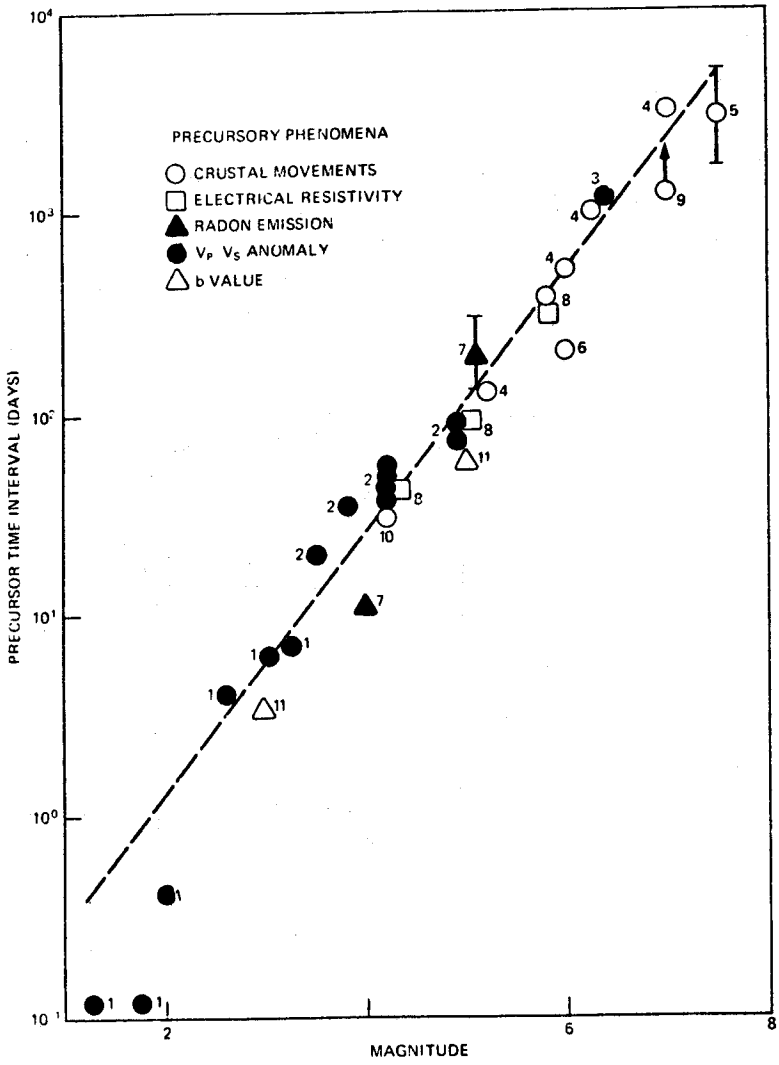

Figure 2. Precursor Time Interval as a Function of Earthquake Magnitude (SCHOLZ ET AL 1973)

The scale of the dilatant region is thus an indicator both of the magnitude of the subsequent earthquake and of the time interval between the earthquake and the precursory phenomena such as crustal motion. The dilatant region itself is about twice the length of the fault or the aftershock zone.

At thrusting faults the vertical precursory crustal motions are of the order of several centimetres. There is also some evidence in connection with the Danville, California earthquake which indicates that it is appropriate to view at least some strike-slip events in terms of the dilatancy mechanism. The vertical components of the motion will be approximately a third of the horizontal strain for shallow earthquakes, i.e., ones for which the depth is small relative to the dimension of the source. This is true for the moderate and large California earthquakes. Scholz, Sykes & Aggarwal point out

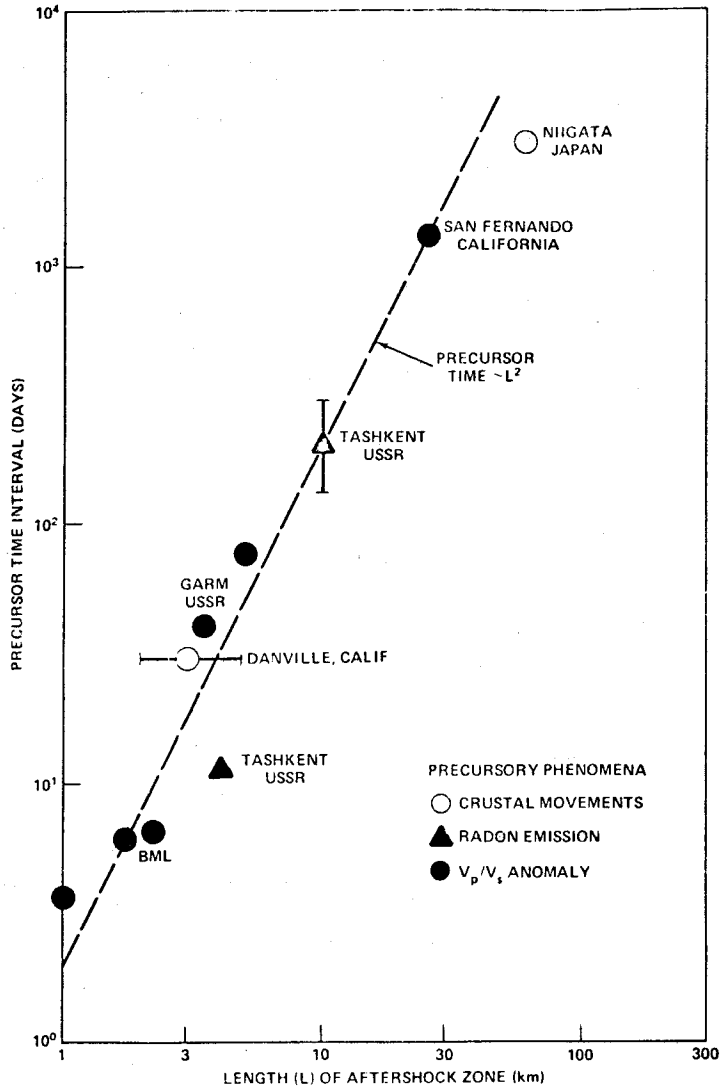

Figure 3. Precursor Time Interval as a Function of the Length of the Aftershock Zone (SCHOLZ ET AL 1973)

that, although they cannot demonstrate that premonitory effects occur before shocks deeper than about 10 to 15 km, the depth range where the effect is observed includes virtually all earthquakes on or near the San Andreas fault system in California and most of the world's damaging earthquakes (SCHOLZ ET AL 1973).

Earthquakes of magnitude six or larger can cause significant damage as is pointed out, for example in figure 4 which is presented in the NASA Earth and Ocean Physics Applications Program (EOPAP) Plan (NASA 1972).

Earthquake	Magnitude	Estimated Property Damage ($ × 10^6) Contemporary $	1966 $*	Estimated Loss of Life
San Fransisco, Calif. April 18, 1906	8.3	400	2600	700
Alaska March 27, 1964	8.5	311		114
Long Beach, Calif. March 10, 1933	6.3	50	170	120
Kern County, Calif. July 21, 1952	7.7	50		12
Aleutian Islands April 1, 1946	7.4	25**		173**
Puget Sound, Wash. April 13, 1949	7.0	25		8
Puget Sound, Wash. April 29, 1965	6.5	12		6
Hegben Lake, Mont. August 17, 1959	7.1	11		28
Santa Barbara, Calif. June 29, 1925	6.3	8	26	13
Imperial Valley, Calif. May 18, 1940	7.1	5		9
Montana Series October & November 1935	up to 6.2	4		4
San Fernando, Calif.† February 9, 1971	6.6	553		64

Figure 4. Property Damage and Loss of Life from Major Earthquakes in the United States in the Present Century

* Based on *Engineering News Record* Building Cost Index

** Most of the damage and loss of life resulted from the tsunami that hit the Hawaiian Islands

† The San Fernando, California Earthquake of February 9, 1971. *Professional Paper* 733, U.S. Geological Survey, U.S. Government Printing Office, Washington DC.

3. Preliminary Design Parameters for a Precursory Crustal Motion and Regional Strain Field Monitoring Network

3.1 Crustal Motion Characteristics of the Dilatancy Model with Particular Reference to Major Earthquakes

A magnitude six earthquake can be characterized in an order of magnitude way in terms of the preceding discussion as one associated with a dilatancy which precedes the earthquake by a time interval of the order of half a year to a year and a half, and a dilatant region some 20 to 30 km long, which is marked by crustal motions having a scale of several cm in the case of thrusting faults and at least some strike-slip faults (figure 5).

A system for monitoring such precursory crustal motions can be an important element of an earthquake prediction capability. Such a system would involve an array of stations about 5 to 10 km apart along the fault deployed in two lines symmetrically placed on each side of it and separated by a distance

A Magnitude 6 Earthquake can be Characterized in an Order of Magnitude Way as Follows:

Precursor Time Interval:	0.5 - 1.5 yr
Fault Length:	10 - 15 km
Dilatant Region Length:	20 - 30 km

Crustal Motion in Dilatant Region:
At Thrusting Fault - Several cm Vertical Motion
At Strike-Slip Fault -
Vertical Motion ∿ 1/3 Horizontal Motion

Scale of Dilatant Region is an Indicator of Time and Magnitude of Subsequent Earthquake

Figure 5

comparable to the interval between the sites in each line. This arrangement is indicated in figure 6. This means an average of one site for roughly every four km of fault line. Position components should be measured to the order of a centimetre or two in times of approximately a quarter of a year or less.

3.2 The California Region Viewed from the Standpoint of Possible Criteria for Predicting Earthquake Locations

An extensive study of possible criteria for predicting earthquake locations has been conducted by KELLEHER, SYKES & OLIVER (1973). They have categorized segments of the circum-Pacific belt in terms of the following initial set of criteria:

1. The segment is a part of a major shallow seismic belt characterized predominantly by strike-slip or thrust faulting (plate boundaries other than spreading ridges according to plate tectonic theory).

2. The segment has not ruptured for at least 30 years .

The shallow seismic belts which they studied here, i.e., those which satisfy the first of these criteria, are indicated in figure 7a. The segments which meet both of the initial criteria and hence

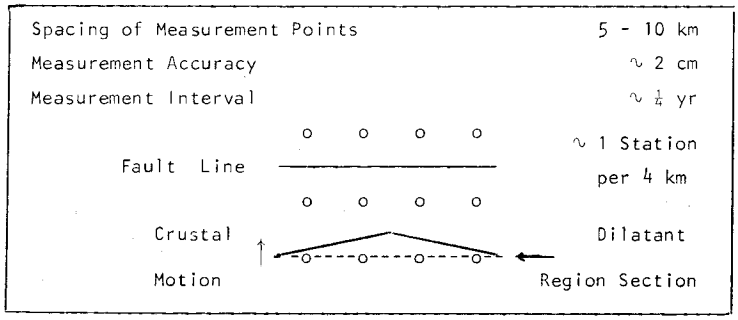

Figure 6. Precursor Crustal Motion Monitoring Network for Major Earthquakes, i.e., M ≥ 6. Preliminary Design Parameters

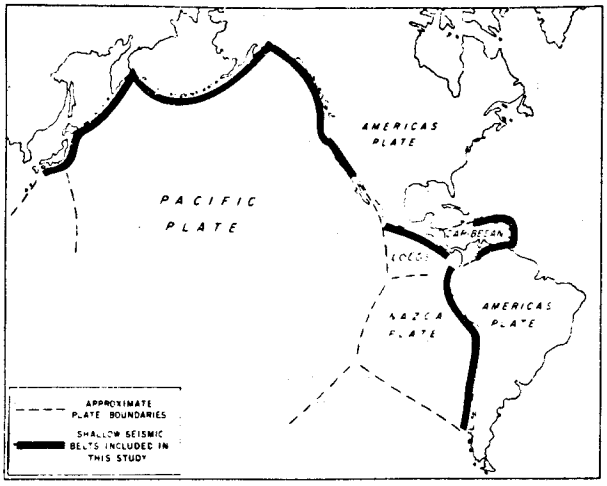

Figure 7a. Major Shallow Seismic Belts Examined by KELLEHER, SYKES & OLIVER (1973)

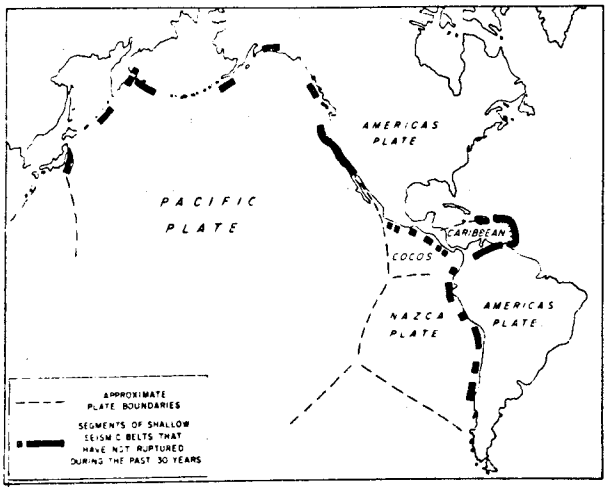

Figure 7b. Shallow Seismic Zones of Figure 7a with Rupture Zones of the past 30 years removed. Zones of Sea Floor Spreading also removed (IBID)

are designated by them as areas of "special seismic potential" are indicated in figure 7b.

Interest in certain of these latter segments of special seismic potential is further heightened if at least one of the following three criteria is fulfilled.

1. A historic record of one or more large earthquakes along a segment is taken as evidence that large earthquakes can again occur along that segment. This criterion is not trivial since several segments along the major plate boundaries examined in this study are not known to have experienced large earthquakes during historic times

2. Evidence based on historical data and relative plate motions suggests that the recurrence interval for large earthquakes is near the duration of the time interval since the most recent large earthquake of that segment.

3. The segment appears to be the site for the next event of a series of earthquakes progressing regularly in space and time.

(IBID)

Areas of special seismic potential which meet at least one of three criteria are shaded doubly in figure 8. Looking more closely at a small part of this region, they find a picture of the San Andreas fault system which is seen in figure 9, where the shading conventions are the same as in the previous figure. Added in figure 9 are indications of the zones of the great earthquakes of 1857 and 1906 (IBID).

Allen views the San Andreas fault system as being composed of five segments for the purpose of estimating the potential for future great earthquakes (ALLEN 1968). He proposed that the 1857 and 1906 earthquake zones are probable locations for infrequent great earthquakes and that the three other segments of the San Andreas system release strain energy by means of creep and small - and moderate- magnitude earthquakes more or less continuously and hence are not likely locales for great earthquakes (KELLEHER ET AL 1973; ALLEN 1968). Significantly, however, SCHOLZ, MOLNAR & JOHNSON (1972) found in the laboratory that a small amount of stable slip always precedes stick slip. It is of interest to note in this connection that the Imperial Valley neighbourhood south east of the 1857 break is an area where strain may be accumulating even though the region is active, as is indicated in figure 10. Similarly, fault creep slippage along the San Andreas is widespread between the 1857 and 1906 earthquake zones, yet the question as to whether strain is accumulating or is already high there is a controversial one (SAVAGE & BURFORD 1970; 1971; SCHOLZ & FITCH 1969; 1970; 1971; NASON 1971; KELLEHER ET AL 1973). KELLEHER, SYKES & OLIVER (1973) point out that special interest must be attached to creeping segments of the San Andreas if creep at active faults indicates high stress. They point, too, to the region southeast of the 1857 earthquake zone as also being of special interest since it has not broken during historic time. Conspicuously high apparent stresses

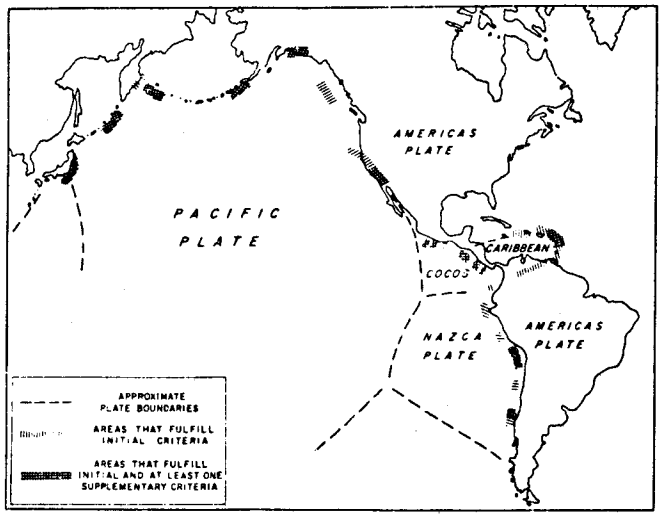

Figure 8. A Summary of Segments and Plate Boundaries that Fulfill the criteria of KELLEHER ET AL (1973) for Identifying Likely Locations for Large Earthquakes of the near future. *All areas that meet these criteria are designated regions of special seismic potential. Because of the scale, the areas indicated are approximate. See reference for detailed description and qualifications.*

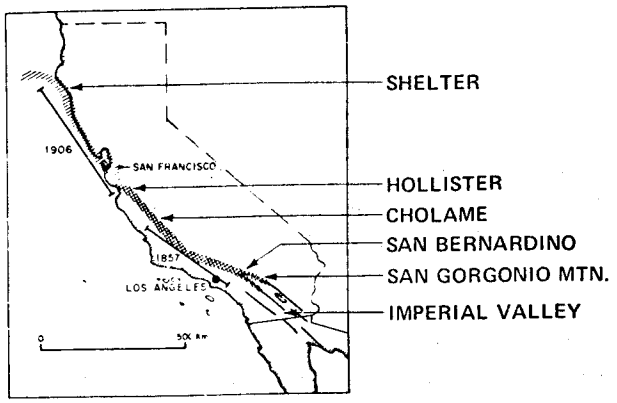

Figure 9. Segments of the San Andreas System that Fulfill Initial or Supplementary Criteria of KELLEHER ET AL (1973)

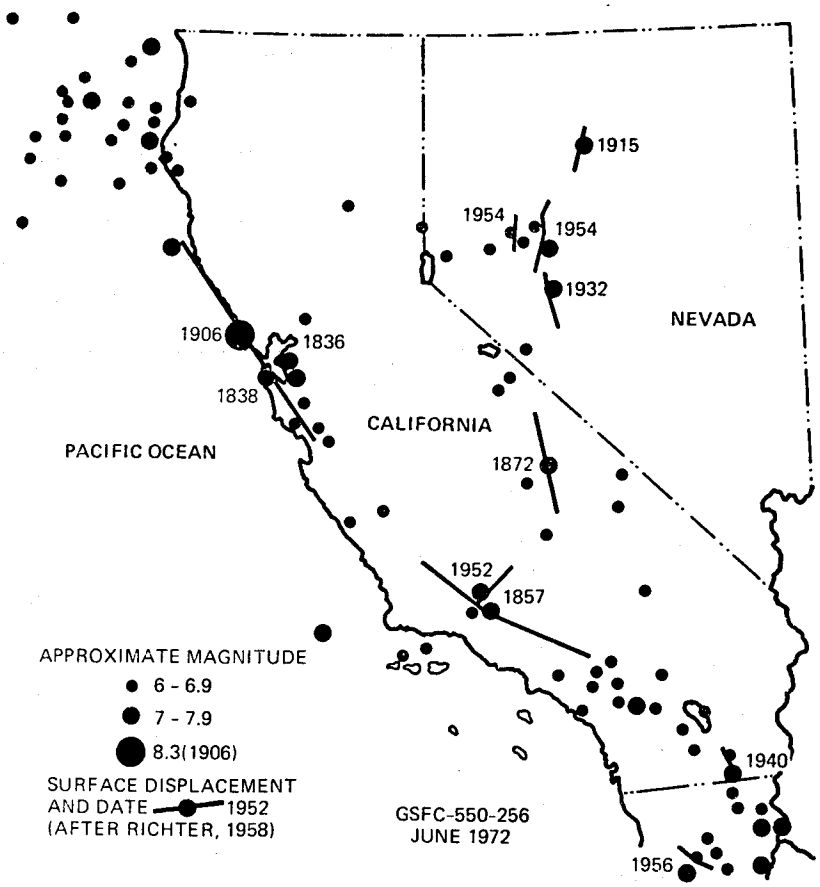

Figure 10. Major Earthquakes Along the San Andreas Fault and in Neighbouring Regions of California and Nevada.

from earthquakes in the area between San Bernardino and the San Gorgonio mountain were observed by WYSS & BRUNE (1971). The location of major earthquakes occurring in eastern California and western Nevada including, for example, the Owens Valley earthquake of 1872 are also seen in figure 10. The segment of the San Andreas fault system having special seismic potential is some 1100 km long, as can be seen in figure 9. The zones of the 1857 and 1906 earthquakes, which are probable locations for future great earthquakes, and hence are of particular interest from the standpoint of the present discussion, are together nearly 800 km long. The San Andreas fault system as a whole is some 1400 km long.

3.3 A Regional Strain Field Monitoring Network

KELLEHER, SYKES & OLIVER (1973) call attention to the clear need for surveys across faults which are paralliel to the Cholame-Hollister fault zone but many tens of km from it. The measurement of regional strain fields is contenplated in the NASA EOPAP Plan (NASA 1972). In California, some of the arrays for this purpose would be roughly normal to the San Andreas fault at spacings of, e.g., 10, 30, 100, 300, and perhaps 1000 km, say. There would be at least several such lines on each side of the fault, to the extent that land and island geography permits. Techniques for determining positions of ocean floor points such as those described by MOURAD ET AL (1972) may be applicable here. Selection of sites to the eastward would take due account of the complex structure and patterns of activity extending at least as far as the Wasatch region.

As the preceding discussion indicated, it will probably be of interest to locate such lines near the ends and centres of the 1857 and 1906 earthquake zones, and also north of Shelter Cove, between Cholame and Hollister, and one or more south east of San Bernardino, e.g., in the Imperial Valley region, and perhaps south of it. Such locations are indicated schematically in figure 11.

The San Andreas Fault Experiment (SAFE) constitutes the first step in the NASA EOPAP regional strain field measurement program (NASA 1972; VONBUN 1972; SMITH ET AL 1972; PLOTKIN ET AL 1973). The SAFE project is aimed at determining the changing distance between mobile laser stations near Quincy and San Diego in California. The locations of these two sites are also indicated in figure 11.

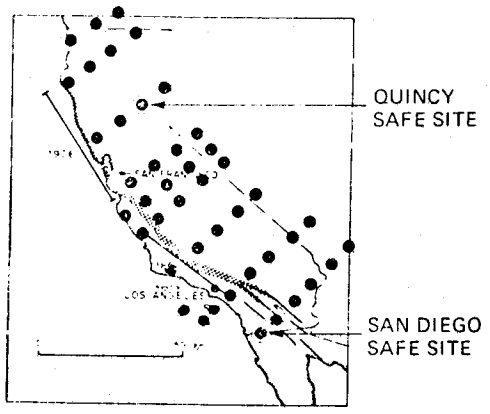

Figure 11. The San Andreas Fault System as depicted by KELLEHER ET AL ET AL (1973)
Added are schematic possible locations for regional strain field measurement sites. The locations of the present SAFE sites near Quincy and San Diego are also shown.

Data obtained through laser tracking of existing satellites such as Beacon Explorer-C will be used for the initial intersite distance determinations.

3.4 The Precursory Crustal Motion and Regional Strain Field Monitoring Network

The regions of interest in figures 9 and 10, in all, have a linear extent of the order of a quarter to a half on Earth's radius. This corresponds to some 400 to 800 stations.

The preliminary design parameters for a premonitory crustal motion and regional strain field measurement network system presented in this section do indeed pose formidable problems which arise chiefly due to the stringent accuracy requirements associated with station location determination and the extremely large number of sites involved.

4. A Precursory Crustal Motion and Regional Strain Field Monitoring System

4.1 General Characteristics

An alternative approach to the problem of monitoring precursory crustal motions and regional strain fields can be based on the use of corner reflectors at the sites indicated in the preceding discussion which are tracked by means of a laser system operating in the Geopause satellite (SIRY 1971). Each of the automated ground stations would also be equipped with simple apparatus for measuring atmospheric pressures, temperatures and humidities, and telemetering them via Geopause. Sites troubled by excessive cloudiness would also be equipped with turnaround transponders operating in conjunction with the Geopause radio tracking system. Such a Precursory Crustal Motion and Regional Strain Field Monitoring System is indicated schematically in figure 12.

In this approach, the problems associated with the site location accuracies are attacked by means of the Geopause spacecraft equipped with accurate laser and radio range tracking systems, and the challenge posed by the very large number of sites is met by means of the relatively simple and inexpensive ground stations.

4.2 The Geopause spacecraft

The state of the art orbit analysis and station position determination is roughly an order of magnitude away from the accuracy levels required for this precursory crustal motion application. The realization of the required accuracies awaits the solution of four kinds of problems, namely, those involving orbit determination and the lack of sufficient knowledge of tracking station biases, the gravity field and tracking station locations.

The Geopasue satellite system concept offers promising approaches in connection with all of these areas (IBID). A typical Geopause satellite orbit has a fourteen hour period, a mean height of about 4.6 Earth radii, and is nearly circular, polar, and normal to the ecliptic. At this height only a relatively few gravity terms have uncertainties corresponding to orbital perturbations above the decimetre level. Refer to figure 13. The orbit is, in this sense, at the geopotential boundary, i.e., the "geopause". The few remaining environmental quantities which may be significant can be handled by means of orbit analyses and surface force compensation systems or accelerometers.

The Geopause satellite system also provides the tracking geometry and coverage needed for determining the orbit, the tracking system biases and the station locations. This is indicated in figures

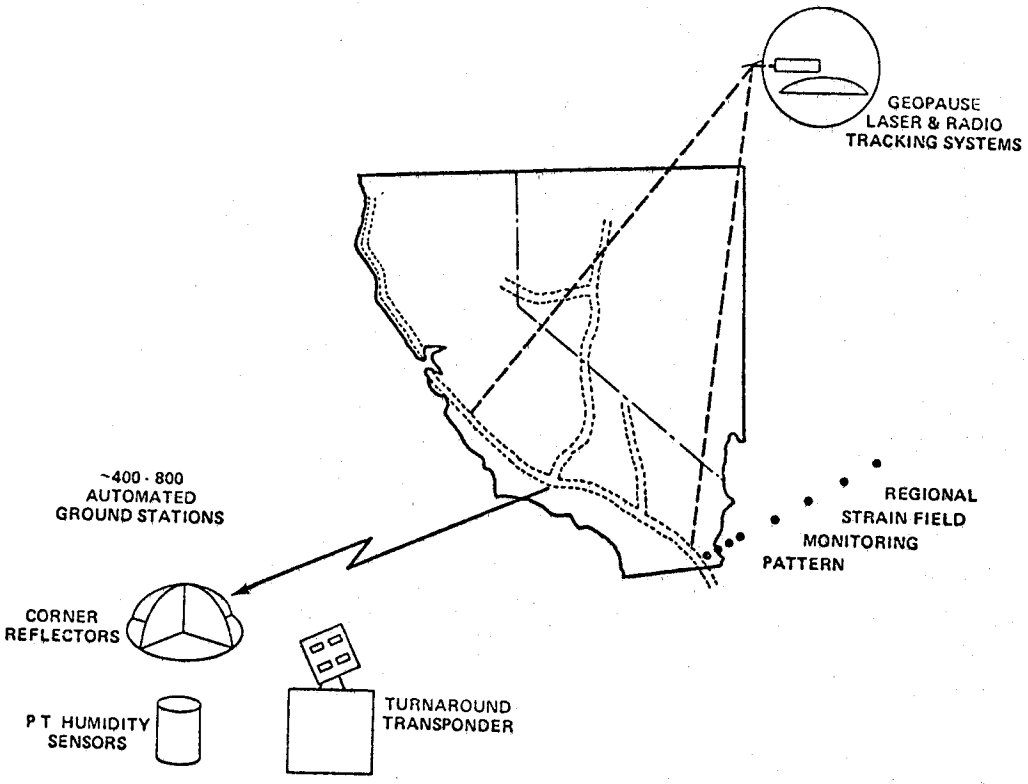

Figure 12. Precursory Crustal Motion and Regional Strain Field Monitoring System Based on the Geopause Satellite

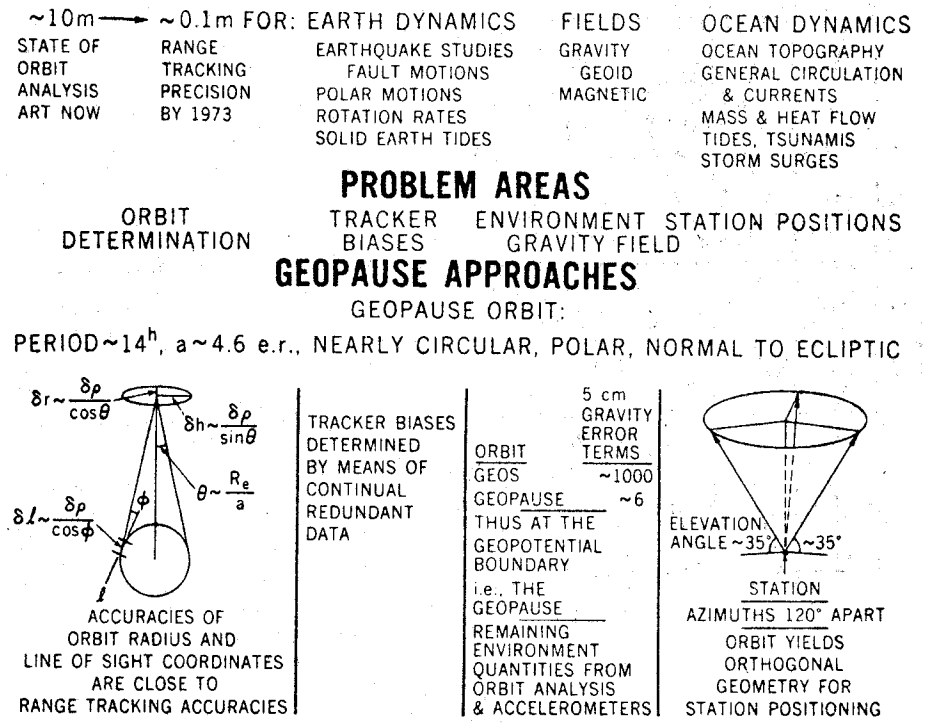

Figure 13. Geopause Approaches to the Meeting of Earth and Ocean Physics Applications Program Goals

13 and 14.

Results of an analysis based on a week of simulated observations from ten NASA affiliated sites are shown in figure 15. It was assumed that range data having a two cm bias were taken at intervals of a quarter of a minute. The uncertainties in the geopotential coefficients were taken to be a quarter of the difference between the SAO 1969 Standard Earth Model and the APL 3.5 Model (LUNDQUIST & VEIS 1966; GUIER & NEWTON 1965; MARTIN & ROY 1971). This assumption has been found to be consistent with some observational experience (IBID). The quantities solved for were the station position co-ordinates, GM and the sets of geopotential coefficients listed in figure 15. The resulting uncertainties in these quantities are also shown there. The designation "Rosman L" denotes a site whose longitude was effectively fixed and taken to be 90°W for reasons of convenience associated with the program. The study was carried out using the program system employed in connection with the analyses of SIRY (1971) and MARTIN & ROY (1971). The uncertainties in the station co-ordinates obtained in this case are listed in figure 15. The largest is 4.8 cm. The root mean square value and the mean value of the magnitudes are 3.1 cm and 2.7 cm respectively.

Since the Geopause spacecraft will be simultaneously visible from four or more sites in several parts of its orbit, it will become practical to determine tracking instrument biases on a continuing basis.

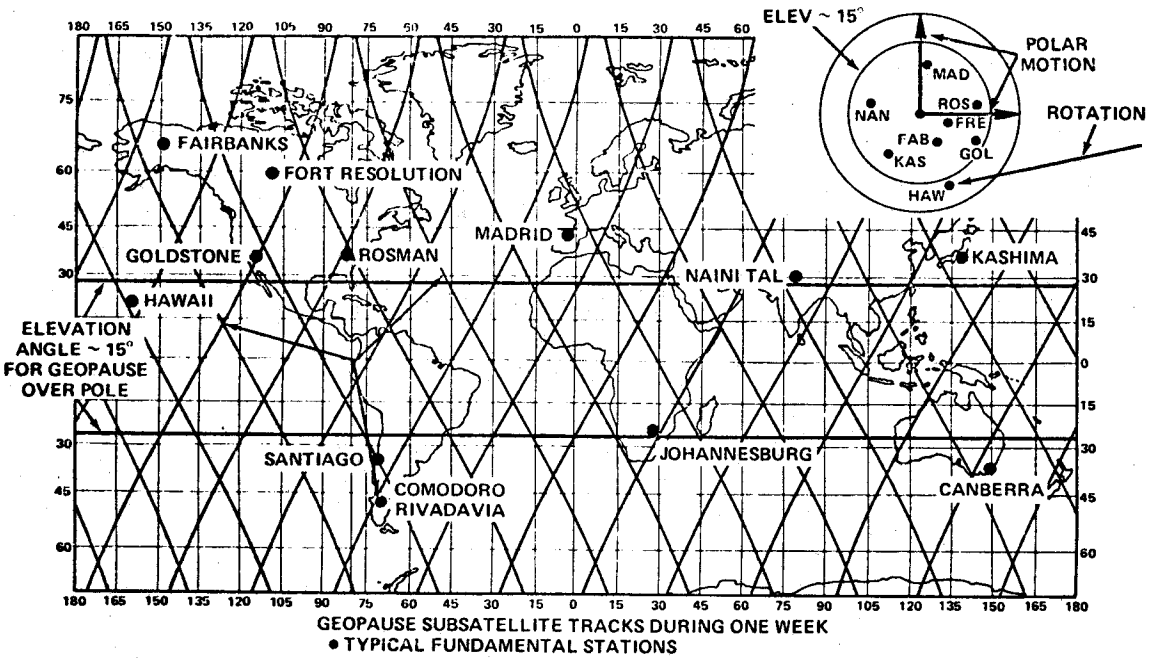

Figure 14. Geopause Orbit Yields the Geometry for Determination of Orbit, Tracker Biases, GM, Station Locations, Fault Motions, Polar Motions, Rotation Rates, Tides

For example, when Geopause is over the North Pole, it is visible at elevation angles above about 10° not only from the Arctic zone but also from the entire temperate zone, i.e., from all stations north of the Tropic of Cancer. This includes most of the Northern Hemisphere stations affiliated with NASA. Similar remarks apply to the visibility of Geopause when it is over the South Pole or near the equatorial plane. This visibility of Geopause over very wide zones of the Earth not only means that tracking system biases can be determined on a regular continuing basis, but also that the effects of the Earth's polar motions and rotational rate variations can also be observed frequently. Accordingly, it will be possible to decrease correspondingly the adverse effects of these factors on the accuracy of site position determinations.

It is anticipated that it will also be helpful to include as fundamental stations some locations in regions of relative crustal stability such as a Canadian shield site at Fort Resolution, for example.

The analysis summarized in figure 15 was based on tracking data obtained during a single week, which is the basic time interval during which a geometrically strong set of data can be obtained with Geopause for all stations over the globe. Much of the geometrical strength of the result is obtained from the three normal place observations during each pass which occur on the rising and setting branches and near culmination.

The Geopause satellite will be visible from a point or a region such as California for about 5 hours during a nearly overhead pass. If, say, 5 seconds are allowed for both the ranging to a ground site and the pointing motion to the next site, there would be enough time during a nearly overhead pass to

Adjusted Parameter	Standard Deviation ($\times 10^{10}$)	Adjusted Parameter	Standard Deviation (mm)	Adjusted Parameter	Standard Deviation (mm)
GM	9	ROSMAN X	5	JOHANNESBURG X	31
C(2, 2)	2	ROSMAN Y	34	JOHANNESBURG Y	40
S(2, 2)	35	ROSMAN Z	39	JOHANNESBURG Z	35
C(3, 1)	270	SANTIAGO X	3	KASHIMA X	26
S(3, 1)	140	SANTIAGO Y	37	KASHIMA Y	33
C(3, 2)	5	SANTIAGO Z	40	KASHIMA Z	41
S(3, 2)	5	ROSMAN-L Y	33	CANBERRA X	7
C(3, 3)	7	ROSMAN-L Z	39	CANBERRA Y	45
S(3, 3)	1	GOLDSTONE X	20	CANBERRA Z	38
C(4, 2)	21	GOLDSTONE Y	33	FAIRBANKS X	4
S(4, 2)	160	GOLDSTONE Z	39	FAIRBANKS Y	20
C(4, 3)	1	COMODORO RIVADAVIA X	5	FAIRBANKS Z	48
S(4, 3)	3	COMODORO RIVADAVIA Y	30	HAWAII X	9
C(4, 4)	0.1	COMODORO RIVADAVIA Z	45	HAWAII Y	37
S(4, 4)	2	MADRID X	19	HAWAII Z	38
		MADRID Y	32		
		MADRID Z	41		

Assumptions: Range bias, 2 cm. Range rate bias, 0.05 mm/s. Geopotential Harmonic Coefficient Uncertainties, 0.25 (SAO M1-APL 3.5). Tracking Interval, 1 week. Rms and mean of magnitudes of station coordinate standard deviations are 3.1 and 2.7 cm, respectively.

Figure 15. Geopause Satellite Orbit Properties
Determination of Gravitational Parameters and Co-ordinates for Stations of a Typical Fundamental Network

make a total of some 3000 site observations, or 3 or more observations per site.

Laser beams having a diameter of some 20 arc seconds corresponding to a spot size at the ground of 3 to 6 km are practical. Such a beam would, in general, illuminate a single site. Somewhat broader beams of 15 or 20 km spot size would generate reflections from several sites, yielding overlapping data. A chain or pattern of such overlapping data sets would strengthen the solution for the site positions in general, and the relative site positions in particular.

The different returns could, in general, be easily distinguished on the basis of prior knowledge of the ranges. The latter would usually differ by km, while knowledge of the positions of the sites and of the Geopause satellite would be orders of magnitude smaller than this, i.e., of the order of less than 1 m. The information which could be generated on the basis of the range predictions could be used, say, to program range gates.

It also appears that it will be feasible to maintain knowledge of the Geopause attitude with adequate adequacy, i.e., of the order of 5 to 10 arc seconds, and hence to control or point the laser mirror beam correspondingly (see, for example TRW 1972).

Programs for pointing the laser to the numerous targets could be generated in a ground-based computer and transmitted to the Geopause control system computer. The laser system might alternately range to a site and then move to the next one. On the other hand, it might simply move continuously at a slowly varying or infrequently changing rate, ranging to the sites in a linear array at the appropriate

times as it passes them (KANT 1973). In either case, the pointing motions and rates involved are reasonable. Thus it appears that during nearly overhead Geopause passes, it will be technically feasible from the standpoint of controls and pointing to obtain three normal places, each based on several individual measures, for each of the hundreds of sites in a regional network such as the California-Nevada one contemplated in figure 12. Power resources of a specific Geopause design will govern the rate at which data would be gathered. It appears that this point will probably not be a critical one, however, since it is estimated that the time available for determining the site positions is an order of magnitude or more longer than the basic one week interval during which Geopause affords the opportunity for complete geometrical coverage.

Experience indicates that the data set actually required to achieve a given result may be larger than that implied by an analysis such as the one described above in connection with figure 15. This may be due, in part at least, to the fact that weather and other practical factors tend to increase the amount of time which is needed to achieve a geometrically strong data set. Even so, it seems that a reasonable margin is available here.

The Geopause radio tracking system will, in general, interrogate more than one transponder if several neighbouring sites are equipped with them. The remarks made above in connection with laser ranging concerning the ability to distinguish between the various returns apply here too. Control and pointing capabilities needed for the laser system are more than adequate for the radio system.

4.3 The Automated Ground Stations

The automated ground stations would include laser retro-reflector arrays, meteorological sensors and, as appropriate, radio turnaround transponders. Four corner reflectors in a Cartesian array would provide the hemispherical coverage. These would be suitably mounted on rock formations or occasionally on concrete piers. A transparent cover could be hemispherical, or consist simply of four face planes perhaps at a fairly steep angle forming a spire. It could be kept sufficiently clear by wipers and/or a blower. Power could be furnished by batteries which might be powered by solar cells if experience indicates such an approach to be cost effective. Servicing of non-responding sites and periodic maintenance, battery replacement, etc. could be accomplished by truck and helicopter patrols. Fencing may be useful in some cases to discourage souvenir hunters. Additional meteorological ground stations forming a larger linear array with roughly 20 km separations straddling the basic sites would provide a two-dimensional data base for refraction corrections. Laser corner reflectors and turnaround transponders at such outlying sites could provide additional data concerning fault motions having a corresponding scale. The dilatant regions may not extend out to these distances very often (SCHOLZ 1973). Accordingly, if reflectors and transponders were placed at such sites, they would serve primarily to provide some additional information about regional strain fields.

The turnaround transponders would be, in general, of the type which are already being readied in connection with the ATS-Nimbus satellite-to-satellite tracking (SST) experiment and the SMS tracking system. The antenna, for example, could be of moderate size and gain, comparable to the Nimbus SST transponder antenna, for example. This would provide the necessary link margins, and yet not place excessively stringent requirements on the pointing control system. Antennas with a beam width of the order of 0.1 radian or so would need to be re-pointed only every minute or even only once every several minutes in order to follow the relatively slow motion of Geopause as it is seen from a ground

Geopause Range Tracking Systems	*Automated Ground Stations*
Laser System	*Laser Corner Reflector Stations*
0.1 - 0.2 mrad beam; 2 - 8 km spot size	4 large open corner reflectors in Cartesian array
6 arc seconds attitude control	Rock mounting or concrete pier
Range to: ~ 720 sites/hr	Hemispherical or spire transparent cover-wipers/blowers
~ 3000 sites/overhead pass ~ 3 ranges/site/overhead pass ~ 2 cm position component accuracy in $\frac{1}{4}$ yr	Pressure, temperature & humidity gauges at corner reflector sites and at peripheral sites for 2-dimensional data measures relayed through Geopause
	Truck & Helicopter maintenance patrols servicing non-responding sites and for periodic maintenance, battery replacement, etc.
Radio System	*Radio Turnaround Transponder Stations*
Multiple return discrimination via programmed range gates	Added at low visibility sites, e.g., under persistent dog or clouds, etc.
~ 2 cm position component accuracy in $\frac{1}{4}$ yr	Commands from Geopause for antenna pointing, etc.
Laser & radio systems also track low-altitude spacecraft yeilding oceanographic and gravity data	Radiometer for water vapour refraction correction

Figure 16. Precursory Crustal Motion Monitoring System

station. Commands to point the turnaround transponder antennas would come from Geopause. The turnaround transponder sites would also be equipped with radiometers for gauging the water vapour contribution to the refraction correction where this is necessary. The Geopause laser and radio tracking systems should be able to provide ranging data with an accuracy of the order of 1 cm once the refraction correction data are applied (see, for example HOPFIELD 1972).

Characteristics of the Precursory Crustal Motion and Regional Strain Field Monitoring System are summarized in figure 16.

Once the warning is given and the dilatant region has been located with this system, other equipment can be brought to bear on the problem. For example, seismic velocity measurements can be used to trace out the history of the V_p/V_s curve. Resistivity measurements might also be made. Data gathered by means of various additional techniques would generate further confidence in the earthquake predictions.

The cost of an automated ground station may turn out to be of a lower order than the cost of preparing a site for a mobile ground station.

The Geopause laser and radio tracking systems would also be used to track the low-altitude Earth and Ocean Physics Applications Program spacecraft yielding oceanographic and gravity data (e.g., NASA 1972;

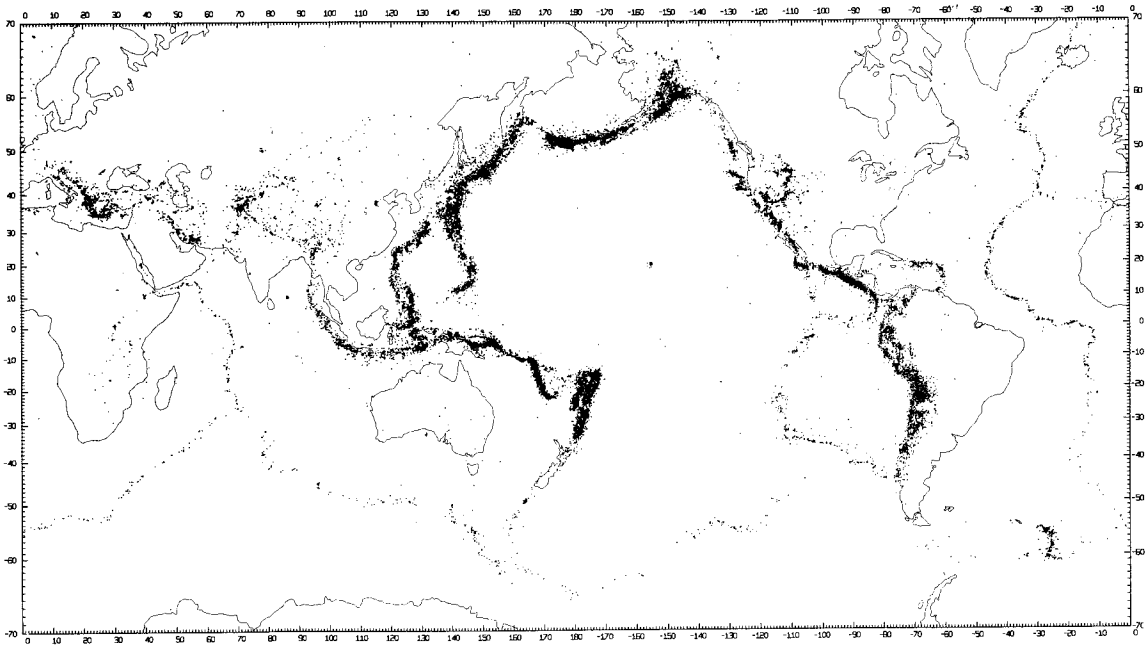

Figure 17. Seismicity of the Earth, 1961-1967. Depths to 700 km (KELLEHER ET AL 1973; BARAZANGI & DORMAN 1969)

SIRY 1971; VONBUN 1972). Some conventional laser. VLBI, and radio ground stations of the type already planned will still be needed as part of the overall Geopause system in connection, for example, with the determination of its orbit and the validation and calibration of the Geopause tracking systems (see figure 14, for example).

The concept outlined here based on Geopause satellite techniques offers the prospect of a practical approach to the problem of monitoring secular variations in position such as precursory crustal motions and regional strains, and providing data potentially useful for earthquake predictions.

The above discussion is in terms of the California region. Similar approaches might be applied in some of the other areas shown in figures 7 and 8, and in other parts of the world indicated in figure 17 which are troubled by seismicity, such as the Middle East, to the extent that geography and other factors allow.

Areas of high seismic risk in central and eastern North America indicated in figure 18 may also be of interest from the standpoint of crustal motion measurement. Crustal motions which may occur in the region between the Rocky Mountains and the eastern United States could also be monitored by this approach (DRAKE 1973).

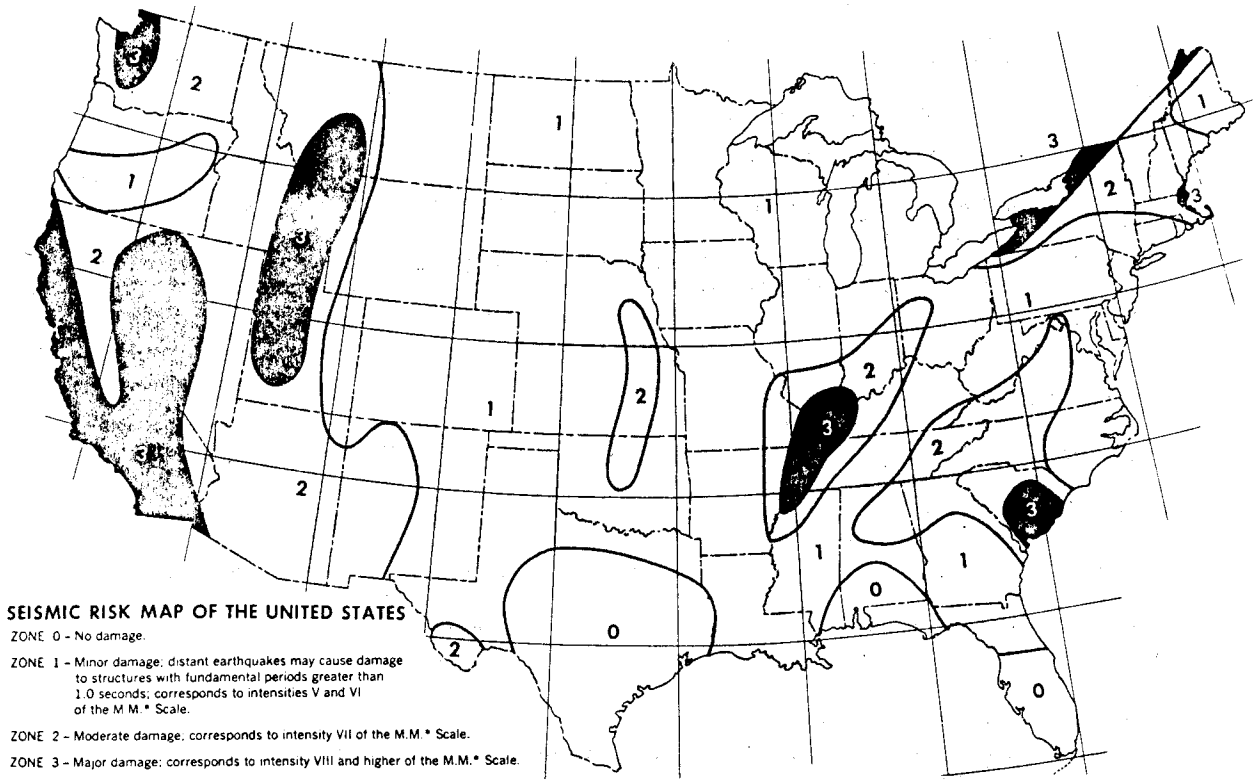

Figure 18. Seismic Risk Map of the United States. (From ALGERMISSEN 1969) (NASA 1972)

5. Acknowledgments

It is a pleasure to achnowledge helpful discussions with Drs. C. Scholz, C. Drake, C. Allen, F. Vonbun, H. Plotkin and D. Smith, and Messrs H. Hoffman, S. Kant, P. Minott, P. Schmid and S. Stevens.

6. References

ALGERMISSEN, S.T. 1969. Seismic Risk Studies in the United States. *Fourth World Conference on Earthquake Engineering*, Vol 1,26.

ALLEN, C. 1968. The Tectonic Environments of Seismically Active and Inactive Areas along the San Andreas Fault System. *Publ.Geol.Sci.* 11,Stanford University, Stanford Calif.,70.

BARAZANGI, M. & DORMAN, J. 1969. World Seismicity Maps of ESSA, Coast and Geodetic Survey Epicenter Data for 1961-1967. *Bull.seismol.Soc.Amer.* 59,369.

DRAKE, C. 1973. Private communication.

GUIER, W.H. & NEWTON, R.R. 1965. The Earth's Gravitational Field as Deduced from the Doppler Tracking of Five Satellites. *J.geophys.Res.* 70,4613-4626.

HOPFIELD, H.S. 1972. Tropospheric Range Error Parameters: Further Studies. *Rep.* CP 015,Applied Physics Laboratory,Johns Hopkins University,Silver Spring Md.

KANT, S. 1973. Private Communication.

KELLEHER, J., SYKES, L.R. & OLIVER, J. 1973. Possible Criteria for Predicting Earthquake Locations and Their Applications to Major Plate Boundaries of the Pacific and the Carribean. *J.geophys.Res.* 78(14).

LUNDQUIST, C.A. & VEIS, G. 1966. Geodetic Parameters for a 1966 Smithsonian Institution Standard Earth. *Spec.Rep.* 200,Smithsonian Astrophysical Observatory,Cambridge Mass.

MARTIN, C.F. & ROY, N.A. 1971. An Error Model for the SAO 1969 Standard Earth. *Third International Symposium, Use of Artificial Satellites for Geodesy.* American Geophysical Union,Washington DC.

MOURAD, A.G., FUBARA, D.M., HOPPER, A.T. & RUCK, G.T. 1972. Geodetic Location of Acoustic Ocean-Bottom Transponders from Surface Positions. *EOS Trans.Amer.geophys.U.* 53,644-649.

NASA 1972. *NASA Earth and Ocean Physics Applications Program.* National Aeronautics & Space Administration,Washington DC.

NASON, R. 1971. *Investigation of Fault Creep Slippage in Northern and Central California.* Ph.D. Thesis,University of California, San Diego Calif.,250 pp.

PLOTKIN, H., JOHNSON, T. & MINOTT, P. 1973. Progress in Laser Ranging to Satellites: Achievements and Plans. *COSPAR,IAG Symposium*, Technical University,Athens.

SAVAGE, J. & BURFORD, R. 1970. Strain Accumulation in California. *Bull.seismol.Soc.Amer.* 60,1877.

SAVAGE, J. & BURFORD, R. 1971. Discussion of paper by C.H. Scholz & T.J. Fitch "Strain Accumulation along the San Andreas Fault". *J.geophys.Res.* 76,6469.

SCHOLZ, C. 1973. Private Communication.

SCHOLZ, C. & FITCH, T.J. 1969. Strain Accumulation Along the San Andreas Fault. *J.geophys.Res.* 74,6649.

SCHOLZ, C.H. & FITCH, T.J. 1970. Strain and Creep in Central California. *J.geophys.Res.* 75,4447.

SCHOLZ, C.H. & FITCH, T.J. 1971. Reply to "Discussion of Paper by C.H. Scholz & T.J. Fitch, 'Strain Accumulation along the San Andreas Fault' by J.C. Savage & R.O. Burford". *J.geophys.Res.* 76,6480.

SCHOLZ, C., MOLNAR, P. & JOHNSON, T. 1972. Detailed Studies of Frictional Sliding of Granite and Implications for the Earthquake Mechanism. *J.geophys.Res.* 77,6392.

SCHOLZ, C.H., SYKES, L.R. & AGGARWAL, Y.P. 1973. The Physical Basis for Earthquake Prediction. *54th Annual Meeting,American Geophysical Union*,Washington DC; and Earthquake Prediction: A Physical Basis. *Science* 181,803-810.

SIRY, J.W. 1971. A Geopause Satellite System Concept. *Space Science Reviews* 14(2),314-341; and *Third Internationa Symposium, Use of Artificial Satellites for Geodesy*,Washington DC.

SMITH, D., SAVAGE, J., TOCHER, D. & SCHOLZ, C. 1972. The San Andreas Fault Experiment. *EOS Trans. Amer.geophys.U.* 53(4).

TRW 1973. Precision Pointing Control System Design and Analysis. *Rep.* 13900-6012-R0-01,TRW Systems Group,Redondo Beach Calif.

TSUBOKAWA, V., DAMBARA, T & OKADA, A. 1968. In KAWASUMI, H. (ed.) *General Report on the Niigata Earthquake.* Tokyo Electical Engineering College Press,p.129.

VONBUN, F.O. 1972. Earth and Ocean Physics Applications Program (EOPAP). *XXIII International Astronautical Congress*,Vienna.

WHITCOMB, J.H., GARMANY, J.D. & ANDERSON, D.L. 1972. Earthquake Prediction: Variation of Seismic Velocities Before the San Fransisco Earthquake. *Science* 180,632-635.

WYSS, M. & BRUNE, J. 1971. Regional Variations of Source Properties in Southern California Estimated from the Ratio of Short-to-Long-Period Amplitudes. *Bull.seismol.Soc.Amer.* **61**,1153.

YAMAGUTI, S. 1968. *Bull.Earthquake Res.Inst.* **46**,1269.

7. Discussion

ANGUS-LEPPAN: Can you give us some idea of the cost of such a system?

SIRY: I refer the question to Plotkin.

PLOTKIN: This is a difficult question to answer. We are developing laser systems to go into spacecraft for communications and, more recently, for tracking spacecraft-to-spacecraft. These developments are at a very early stage. We certainly can think in terms of space-borne laser systems. To say what such a system would cost is not possible at the present time.

MUELLER: What is a reasonable estimate of the weight of a satellite which could carry a system like that described?

PLOTKIN: The collecting area need not have to be so large because the reflectors on ground are not limited in size as the spacecraft reflectors are. The difference is going to be in carrying a laser and power supply on board, as well as (systems for) pointing. 1/10th mrad is quite feasible from ground because we have reference directions. Your are talking about doing this from space with very high accuracy but with essentially no beacons, and pointing to a passive reflector. This could be difficult. It is a concept we will have to study.